1283

SOLAR CENTRAL RECEIVER PROTOTYPE HELIOSTAT

PHASE I

Contract:

ET-78-C-03-1745

TECHNICAL PROGRESS

FINAL REPORT

SEPTEMBER 1978

VOLUME I

DESIGN, PRODUCTION, TEST

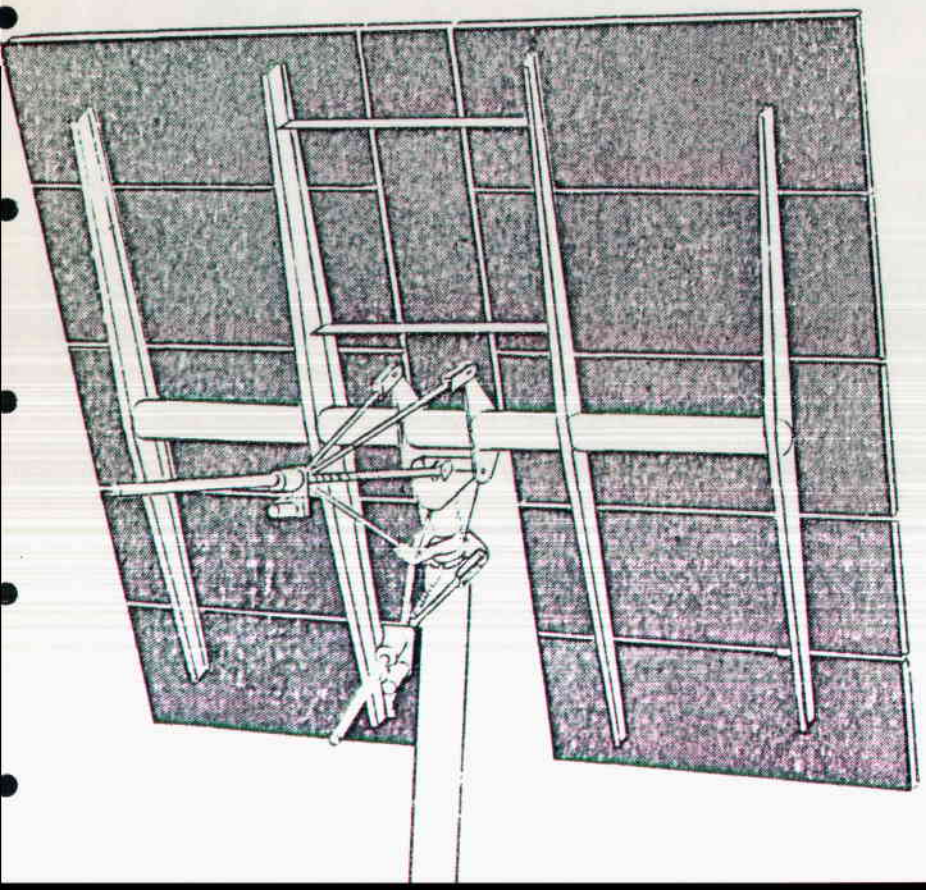

SOLARAMICS

1301 EL SEGUNDO BLVD.
EL SEGUNDO, CA 90245

CONTENTS

ILLUSTRATIONS

VOLUME I

1.0 SUMMARY & RECOMMENDATIONS

The objective of this study & analysis was to optimize the structural design & performance of the heliostat so that satisfactory performance would be achieved over a system life of 30 years at minimum cost. Briefly, the design constraints can be broken into two categories; those of a transient nature & those of a steady-state nature. Transients include wind loading, local ambient vibrations, earthquakes, rain and hail loading, & temperature changes. The steady-state parameters include gravity, ice loading, and long-term weathering effects.

Furthermore, there are design parameters which are pertinent to normal operation & to abnormal operation. During normal operation the reflective surface, the support structure, the drive & control system, and the foundation must be sufficiently rigid so that 95% of the reflected beam is received in the target area during daylight hours. Factors which will influence heliostat design during normal operation include flutter & vortex shedding due to normal wind conditions, ambient ground vibration, gravity loads, & temperature transients. During abnormal operation, the heliostat must be capable of withstanding loads imposed by maximum postulated winds both in operating orientation, & in stowed orientation; it must be capable of withstanding loads due to dust devils, rain, snow, hail & earthquakes. Structural integrity must not be threatened and realignment of the reflective surfaces is allowed only after occurence of earthquakes.

For this study the reflective component of the SOLARAMICS heliostat consists of a foamed waste glass panel to which a thin glass reflector will be permanently bonded. Ten 4 ft. X 10 ft. panels

and one 10 ft X 2 ft panel arrayed for 420 sq ft of reflecting surface are proposed in this design. The total heliostat array and controls are mounted on a vertical implanted hollow column (pedestal) made of a rigid ceramic material.

Several innovative designs were achieved during the preliminary design phase. One was the tilted azimuth axis to eliminate control singularity that could exist in certain field positions. By tilting the azimuth axis 23° away from the tower, it is possible to achieve the required vector motion for all site locations. With this concept only 180° of azimuth control is required if oriented such that 90° is provided to each side of a radial line from the tower to the heliostat. This allows a simplified actuator mechanism requiring only one motor and actuator for each motion function. Another innovative design was the elimination of the Heliostat Field Controller in the Control System by utilizing the capability of the microprocessor to accomplish two functions simultaneously. Also an environment-free local controller was developed using fibre optics through a translucent window in the controller to provide the commands for local control. An additional innovative function was the selection of a high density urethane foam, called "Poleset", to implant the heliostat pedestal. This allows a low-cost, rapid installation of pedestals to reduce cost & expedite deployment. Development of foamed glass as the substrate support structure for the mirror has progressed, including fabrication of 4'X 10' panels, characterization tests substantiating the

design characteristics of foam glass, and the conceptual design of a continuous production process of foam glass that can accomplish high output with low cost.

Design analysis shows that the desired stiffness of the drive mechanism requires a pedestal diameter of 15" rather than the twelve(12") inches developed in the preliminary design. It is recommended that this design change be made, thus improving the stiffness qualities. Along with that, trade-off studies (see section 8.0) show that with larger diameter, it is more cost effective to use the Centrecon reinforced concrete pole and weld or bolt the kingpin to the Centrecon end plate. Use of the larger diameter pedestal also assures proper foundation dynamic support for the 9-10 ft. depth presently planned.

The mechanism tests showed that design improvements in the trunnion and kingpin will resolve stiffness problems. A change to a 460 volt 3 phase motor is recommended to improve the cost effectiveness of the power distribution network. Magnetic position encoders for benchwork encoding should be thoroughly investigated and developed and then applied to the motor shaft for heliostat position encoding.

2.0 PRELIMINARY DESIGN

2.1 Heliostat Configuration

The heliostat consists of ten(10) panels each 48" X 120" supported in an array 22'6" wide X 20'4" high, with a total reflective area of approximately 420 sq ft(Fig.1.1). The reflective panels consist of second surface silvered microglass adhesively bonded to a structural foam glass substrate. Each panel is attached at three(3) points to a conventional steel rack fabricated from formed steel zees welded to a steel tube cross member. The tubular cross member is attached to a pedestal trunnion by means of a two axes modified azimuth-elevation drive mechanism.

The azimuth-elevation drive mechanism provides 180° azimuth motion and 203° of elevation. The azimuth axis is tilted 23° from the vertical in a radial direction from the tower center line. This modification to a conventional azimuth-elevation system permits full field coverage with only 180° of azimuth thereby allowing significant simplification of the azimuth drive. The 203° of elevation travel provides 23° over the shoulder orientation, plus 180° face down night and high wind stowage position. By utilization of a unique bell crank mechanism, this 203° of rotational motion is accomplished by a single linear actuator.

The drive mechanisms are powered by a conventional 3 phase induction motor which is pulsed with a triac solid state switching control device. This permits incremental motion of less than 1 milliradian per pulse or con-

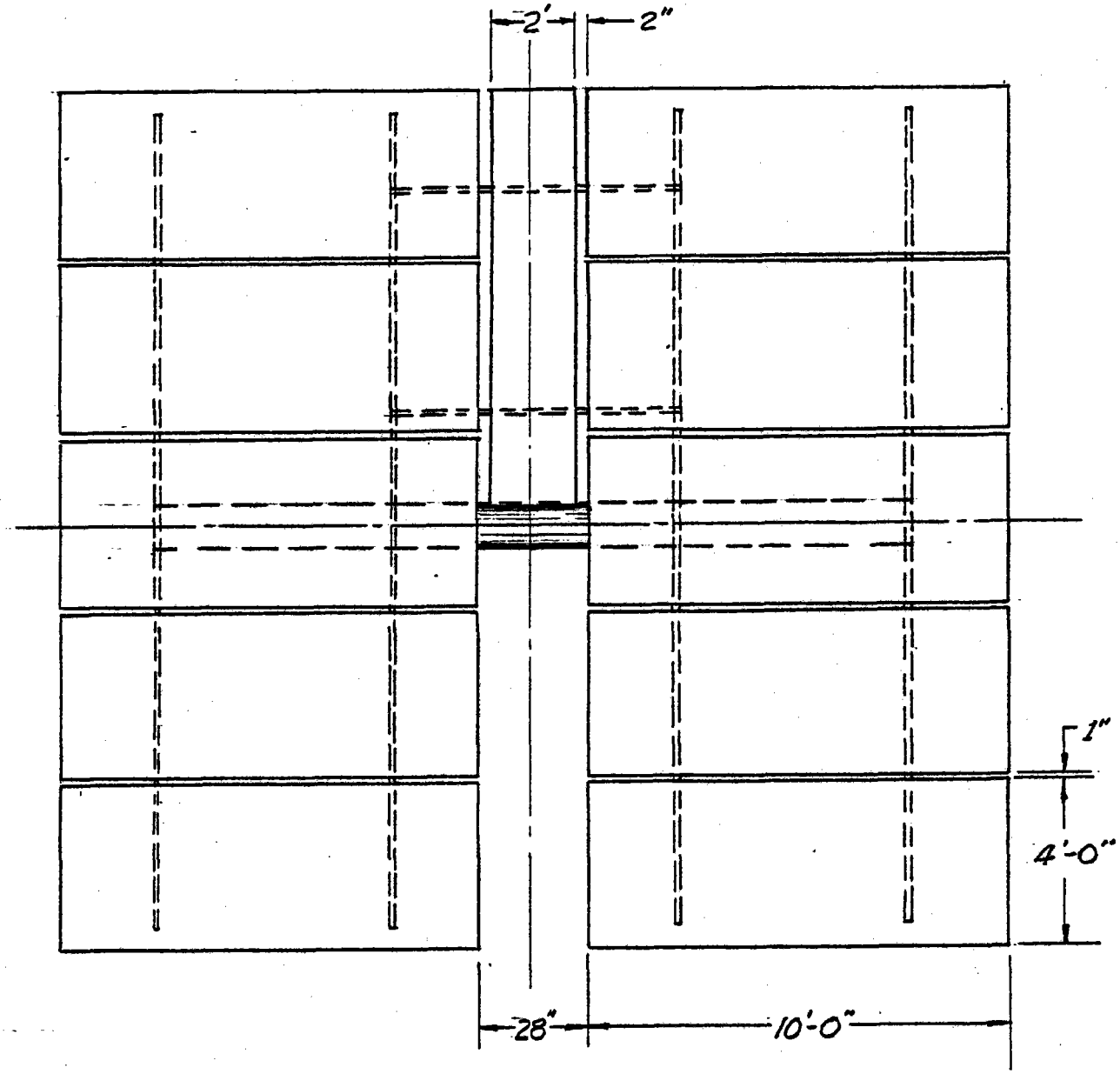

FIG. 1-1

HELIOSTAT ARRAY CONFIGURATION

2.1 Heliostat Configuration(cont'd)

tinuous drive for high speed acquisition, shut down, or storage actions.

Each heliostat control will contain single chip microprocessors to provide the control command and integrate the encoder output to provide open loop control. A 'bench mark' encoder will also be provided on each of the gimbal axes, and a one bit encoder on each drive motor shaft.

The heliostat array and trunnion are mounted on a tilted axis king pin atop a pier/pedestal. The pier or pedestal is installed 10 ft. deep in a bored hole in much the same manner as utility poles are set.

PROTOTYPE HELIOSTAT
WEIGHT DISTRIBUTION

SUPPORT STRUCTURE:	
TORQUE TUBE	392
FRAMES	512
INTERCOSTALS	20
DRIVE AND PIVOT CRANKS	49
	973
ROTATING MECHANISM	
JACKS(ELEVATION & AZIMUTH)	137
MOTOR/ENCODER	40
TRUNNION	145
GIMBAL AXIS ENCODERS & MOUNTING EST.	5
KING PIN	173
LINK TUBES (5)	141
LINK END FITTINGS (10)	43
AZIMUTH COLLAR	13
ELEVATION JACK ADAPTER	47
AZIMUTH JACK BRACKET	14
BALL BEARINGS (3)	8
BOLT HEADS AND NUTS (11)	4
	770
MIRROR MODULES	
FOAM GLASS PANELS	1,731
MIRROR (.09) AND ADHESIVE	80
ATTACH TEES, ADHESIVE, AND FASTENINGS	28
	1,839
PEDESTAL	
CERAMIC POLE (with 6" dia. core) 2.15 DENSITY	2,218
CAP AND FASTENERS	119
	2,337

TOTAL = 5,919#

2.0 PRELIMINARY DESIGN

2.1.1 Mirror Module

2.1.1.1 Microglass Reflective Surface

Second surface silvered very thin (.010) microglass is selected as the reflective system. This concept provides the superior environmental resistance of glass second surface mirrors with very low absorption in the glass resulting from thinness of the sheet. Specular reflective efficiency of .94 to.95 is projected. The silvered microglass is laminated to a thin support material to achieve handling advantages and to improve impact resistance. The silvered microglass laminate is bonded to the mirror module in a two 24-inch wide X 120-inch long sheets.

2.1.1.2 Mirror Module Substrate

A foamed glass structural substrate for the microglass reflector provides a continuous support which is thermally compatible with the soda lime glass mirror. The foamed glass material to be used is a material specially developed by SOLARAMICS for solar applications. The material is produced to higher densities than customary for the insulation grade "foam glass" to develop physical properties for structural application. It is produced from waste soda-lime window glass. Specific properties of the foamed glass are presented in Section 4.0. A material with density of .4 gms/cc. has been selected for this application for a panel of 50 mm(2 in.) thickness.

2.1.1.2 Mirror Module Substrate(contd)

The assembly is bonded with a room temperature curing polyurethane adhesive by vacuum chucking the mirror face down on a surface table and bonding the substrate to the back of the mirror so as to replicate the flatness of the surface table. The adhesive selected is a two-part, catalytically cured material of 100% solids which provides positive curing at room temperature in a minimum period of lapsed time. A number of attach fittings are installed in cored holes in the foamed glass for attachment of an intermediate rib to the back side of the foamed glass. These intermediate ribs provide three attach points for support of the panel on the structural frame. These attach points are utilized to achieve the desired focal position during assembly.

2.1.2 Structure

2.1.2.1 Mirror Support Structure

A conventional fabricated steel support is constructed of four(4) vertical zee elements welded to a cross tube. The reflector panels are supported at a pad support in the zee web such that the reaction is positioned at the zee shear centroid. The zee sections are 13" web height with "C" flange width of 3-1/2", roll formed from 10 ga. steel, and tapered to 6 in. web height at the tip.

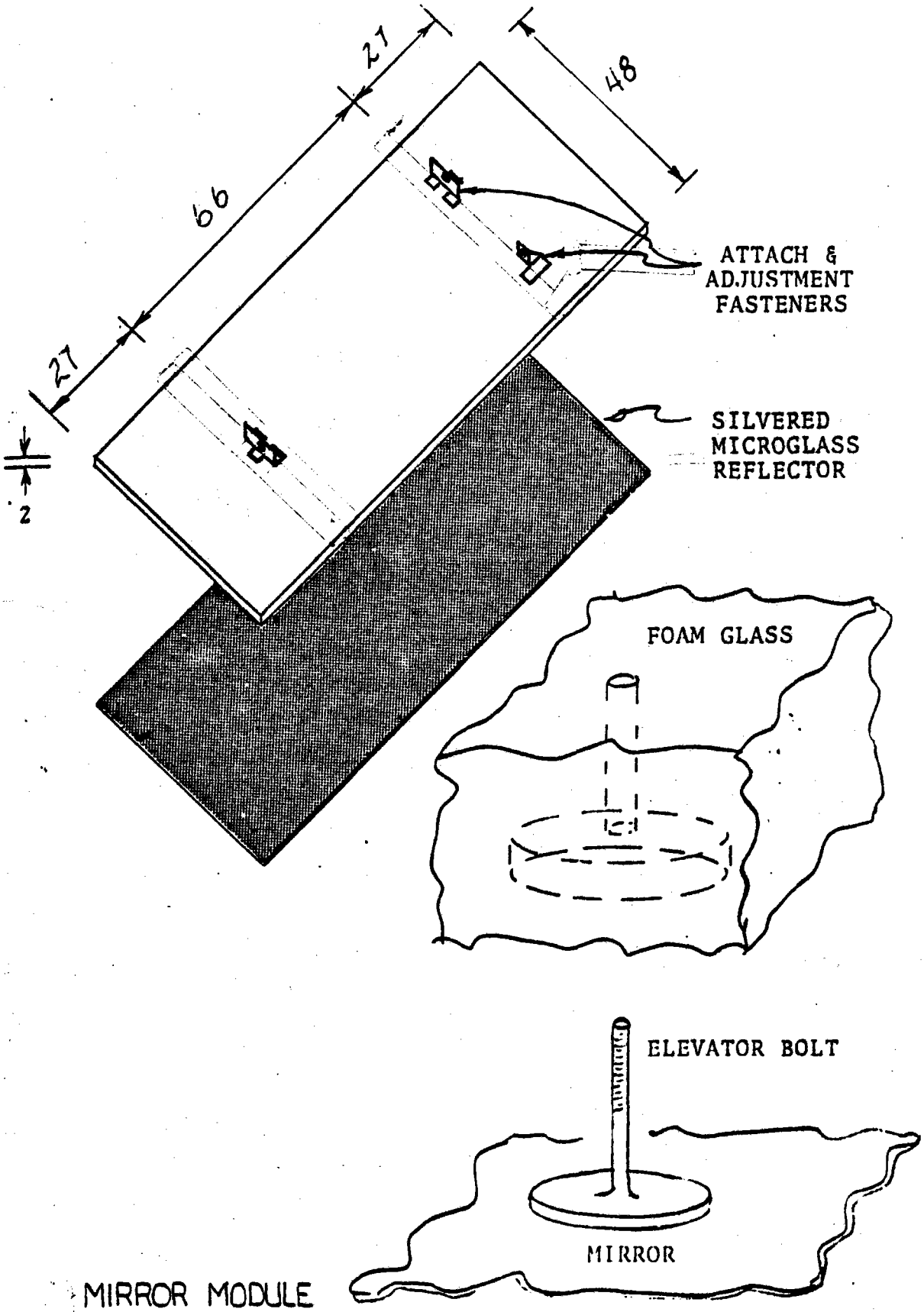

MIRROR MODULE

FIGURE 2-0

2.1.2.1 Mirror Support Structure(cont'd)

The cross beam consists of a 12.75" dia. welded steel pipe with a wall thickness of .165". The cross beam is supported at the center trunnion at lugs welded to the cross tube. The lugs are widely positioned laterally to provide rigidity in the attachment to the trunnion. Similar lugs are located at the cross tube for attachment of the elevation control linkage.

The cross tube assembly is fabricated in two(2) halves, being cut at the center section so that a shippable configuration can be achieved while maintaining as much of the fabrication at the factory as possible. The joint is designed so that the attach and control lugs are entirely on one half of the structure to permit precision dimensional control by factory tooling. The two(2) sections are positioned in a holding fixture and welded with an automatic pipe welder at the site assembly area.

2.1.2.2 King Pin and Trunnion

The reflector panel array is supported at the center of the cross tube by the trunnion at two lugs. The trunnion is a ductile iron casting which rotates on the King Pin Assembly and provides the primary structural support for the elevation drive system. The trunnion is supported on the King Pin by two tapered roller bearings, preloaded to minimize tolerances and initial slack. The trunnion provides the pivot point for the elevation drive actuator as well as the fixed position attachment for the elevation drive linkage. The function of the

2.1.2.2 King Pin & Trunnion(cont'd) elevation drive mechanism is discussed in Section 2.1.3.3. The trunnion also provides the movable position of the azimuth drive linkage.

The King Pin Assembly is attached to the top of the pedestal, inclined at a tilt angle of 23° from the vertical. It is mounted on a ring of studs to the top plate of the pedestal. The King Pin Assembly also contains the bearing journal for the azimuth actuator pivot as well as the fixed link pivot lug. (Ref. Fig. 2-1)

2.1.2.3 Pedestal

The pedestal consists of a vertical column made from a glass-flyash ceramic material being developed by ECP,INC., for EPRI. The material, produced entirely from waste products, is reclaimed glass and fly-ash from coal fired utilities. An extruded mix (50/50) is dried and fired to form a dense ceramic material with good strength characteristics and environmental resistance.

The pedestal is extruded in a square (with edges beveled) shape to facilitate processing, which also produces an efficient shape to improve torsional stability at the top cap encapsulation, and at the pedestal/soil interface. The pedestal is also hollow, with a center hole diameter approximately one half the square dimension to reduce weight and increase section properties per unit cost. The ceramic pedestal is in-

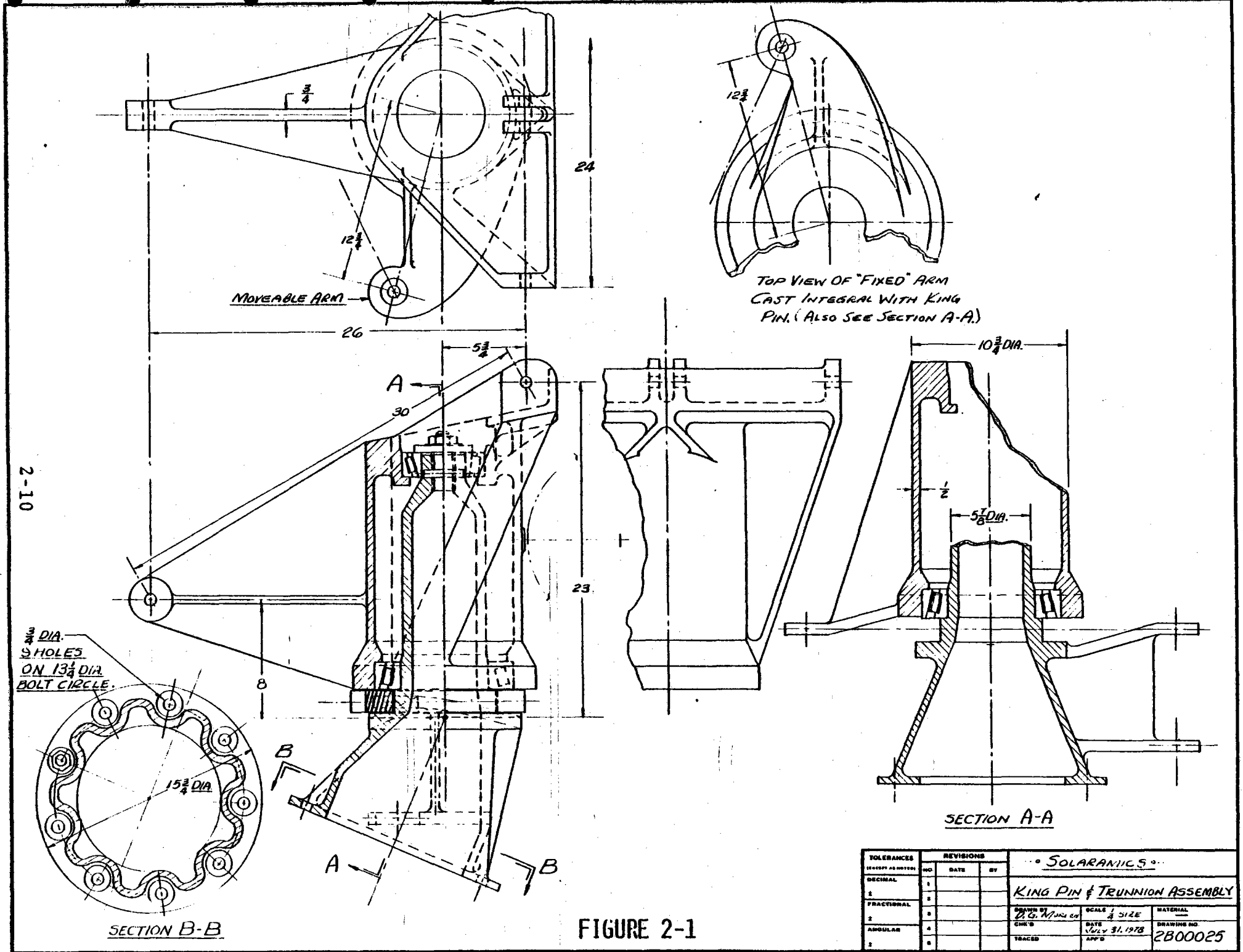

FIGURE 2-1

2-10

TOLERANCES (EXCEPT AS NOTED)	REVISIONS NO.	DATE	BY	° SOLARAMICS °
DECIMAL ±	1			KING PIN & TRUNNION ASSEMBLY
FRACTIONAL ±	2			
ANGULAR ±	3			
	4			
	5			
	6			

DRAWN BY D. G. MANN | SCALE 1/4 SIZE | MATERIAL —
CHK'D | DATE JULY 31, 1978 | DRAWING NO. 2B00025
TRACED | APP'D

2.1.2.3 Pedestal(cont'd)
stalled in a bored hole, and set with a dense polyurethane foam called "Pole Set", much the same as utility poles. The corresponding design moment at the ground line of a 40 ft. class four utility distribution pole is 76,000 ft. lbs. compared to a heliostat design maximum moment of 30,600 ft. lbs. The 40 ft. utility pole is normally installed in 6 feet of soil. The heliostat pedestal is planned to be installed to a 10 ft. depth to provide assurance of installation stability. The results of an analysis of the pier/foundation/soil as determined from a computer program developed at the University of Colorado is presented in Section 2.2.2.1.

The top cap assembly of welded steel is bonded, (encapsulated) on the top of the ceramic pedestal. The cap assembly provides the tilted plane for mounting the King Pin at a 23^{o} angle.

In the installation sequence, the pedestal is held in position while the bored hole is filled with "pole set", a dense polyurethane foam, which cures in 15 minutes. The alignment fixture uses a transit type line of sight to the tower centerline for establishing the tower vector and two bubble levels for proper vertical orientation.

Precise alignment is not essential, variations in orientation are compensated in the computer software for computation

2.1.2.3 Pedestal(cont'd)

of tracking coefficients. An alternate pedestal design utilizing a 15 in. dia. Spin Cast, hollow, prestressed concrete member has also been developed which is cost competitive with the above design. The method of installation would also utilize insertion into a bored hole and setting with "pole set". The top mounting plate with studs becomes an integral part of the pedestal. The spin cast concrete members are presently produced by Centrecon of Everett, Washington for pier and transmission pole applications.

2.1.3 Drive Mechanism

2.1.3.1 Concepts

An analysis of control and tracking vector motions required for the specific field geometry and latitude range discloses that 180° of azimuth drive is more than adequate to provide all tracking functions if the azimuth axis is inclined 20° from normal. The inclination is specifically advantageous in the south field & for the inner circle of heliostats at the tower base. Inclination is not required in the north field; however, it is provided to achieve interchangeability objectives and does not introduce any undesirable performance. It is significant to note that with the inclined axis system, no control singularities occur. An additional 3° of axis inclination (to 23°) is provided to reduce the azimuth drive rate

2.1.3.1. Concepts(cont'd)

requirements.

A unique scheme is proposed to achieve 180^{o} and 203^{o} motion with linear actuators. By attaching the actuator base to the functional rotation centerline with one link to a fixed point and the other to the movable element, a two to one amplification of the rotational action is achieved. Thus large angles are achieved with a bell crank system which is normally limited to angles only slightly greater than 90^{o}.

The advantages of linear acutators for this application include irreversible motion (i.e., self-locking),zero backlash (with adjustment capability for wear), & availability as a commercially developed high volume low cost product. The actuator chosen is a 5-ton capacity actuator produced by Duff Norton.

2.1.3.2 Azimuth Drive

180^{o} of azimuth control, 90^{o} to each side of a vector from the heliostat to the tower is provided by the actuator drive mechanism. The general configuration and motion of the linkage mechanism is shown in Fig. 2.2 . The stroke and moment characteristics are shown in Fig.2-3 . The reactive moment capability utilizing the overload capability of the actuator increases from 86,120 in lbs. at the extreme positions to 136,000 in lbs. at center. This achieves a minimum factor of 1.19 over survival requirement of 72,106 in

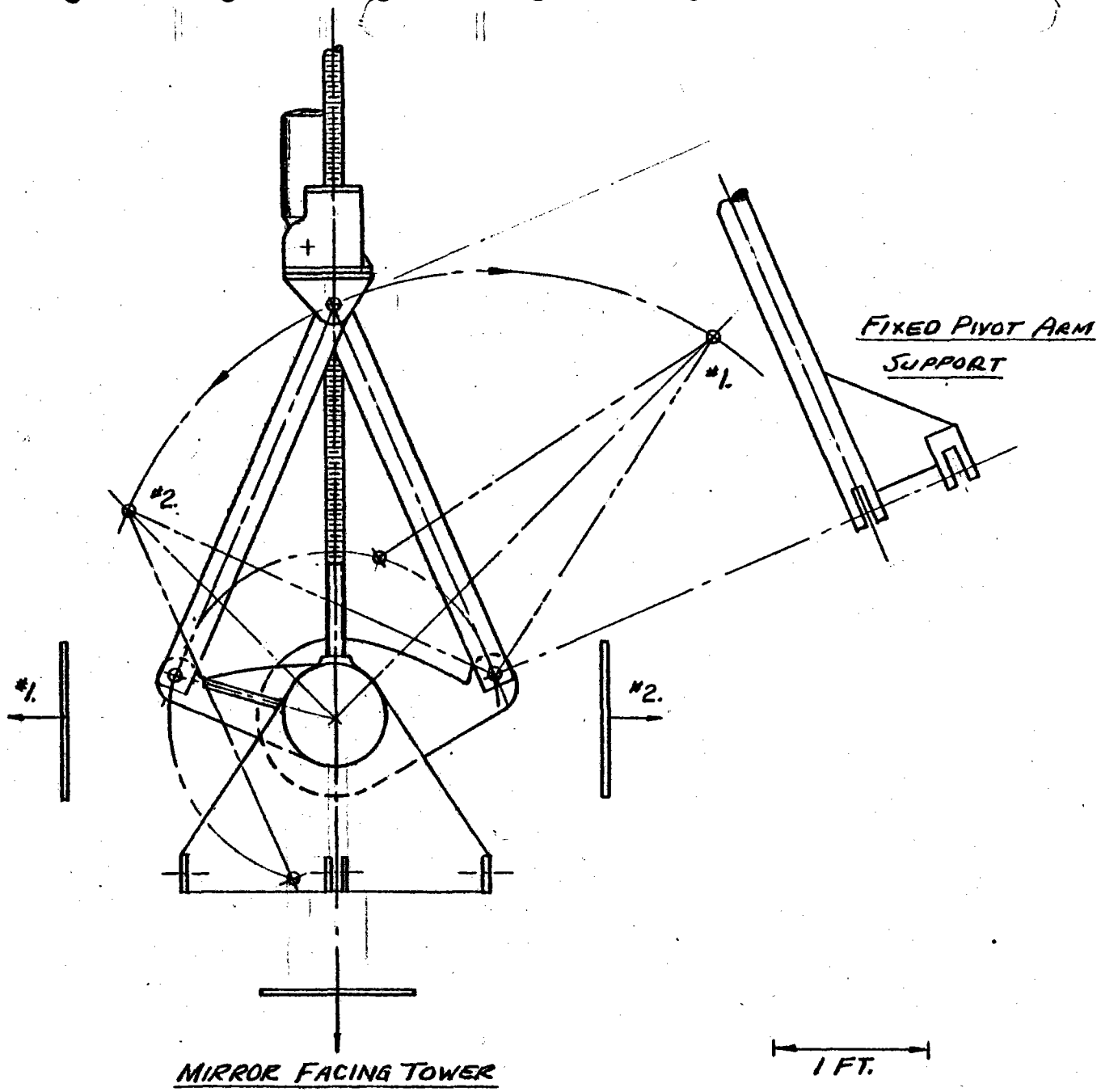

FIGURE 2-2

AZIMUTH DRIVE MECHANISM

LOOKING DOWN

2.1.3.2 Azimuth Drive(cont')

lbs. at 22 m/sec. wind velocity. An ave. mechanism stiffness of 235,000 in lbs. per degree and total backlash of 1.1 mr has been analytically determined. The actuator is fitted with a backlash adjustment system to minimize backlash and compensate for wear. High azimuthal moments occur only with the panel array near parallel with the King Pin axis. Review of the normal tracking action reveals that the high azimuth angles ($>45^{o}$) are only exercised at high elevation (i.e. heliostat near horizontal). Therefore high azimuthal moments and stiffness are predominately of interest in the -45^{o} to $+45^{o}$ azimuth orientation and 45^{o} to 90^{o} elevation angles. (from zenith)

Sealed ball bearings are employed at all of the rotating link pivots except at the large journal for the actuator shaft pivot, (for this pivot, a fibre-filled teflon bearing is used). The actuator shaft is threaded only for the length of the required stroke, providing a smooth shaft over which an environmental protection sleeve rides. The protection sleeve is fixed to the actuator body. The outboard extension of the actuator shaft is protected by a closed tube attached to the actuator body. Slew, from the extreme position, $\pm 90^{o}$, to center 0^{o} requiring a stroke of the actuator of 9.5 in., is achieved

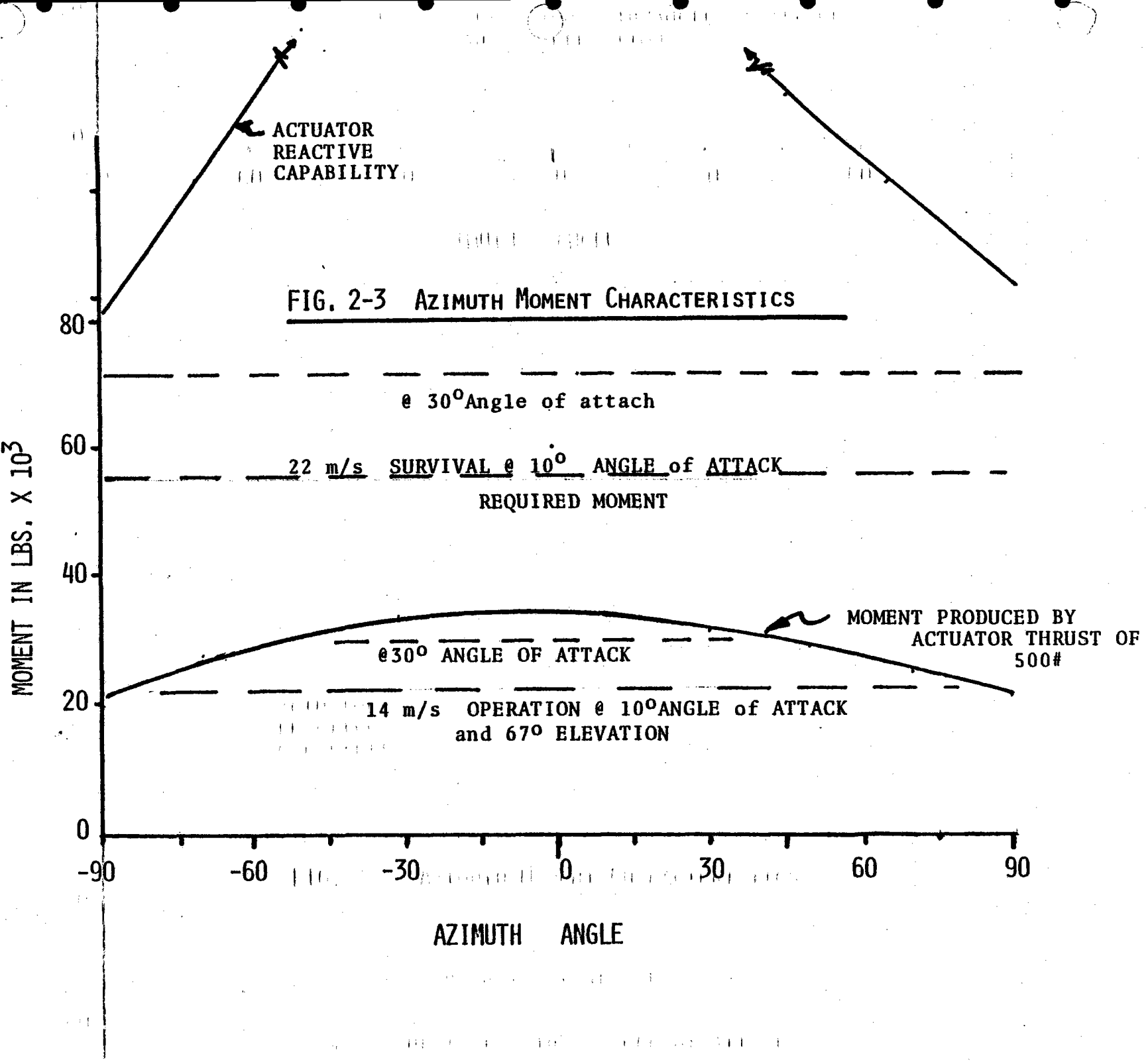

FIG. 2-3 AZIMUTH MOMENT CHARACTERISTICS

FIG. 2-4 AZIMUTH ACTUATOR STROKE

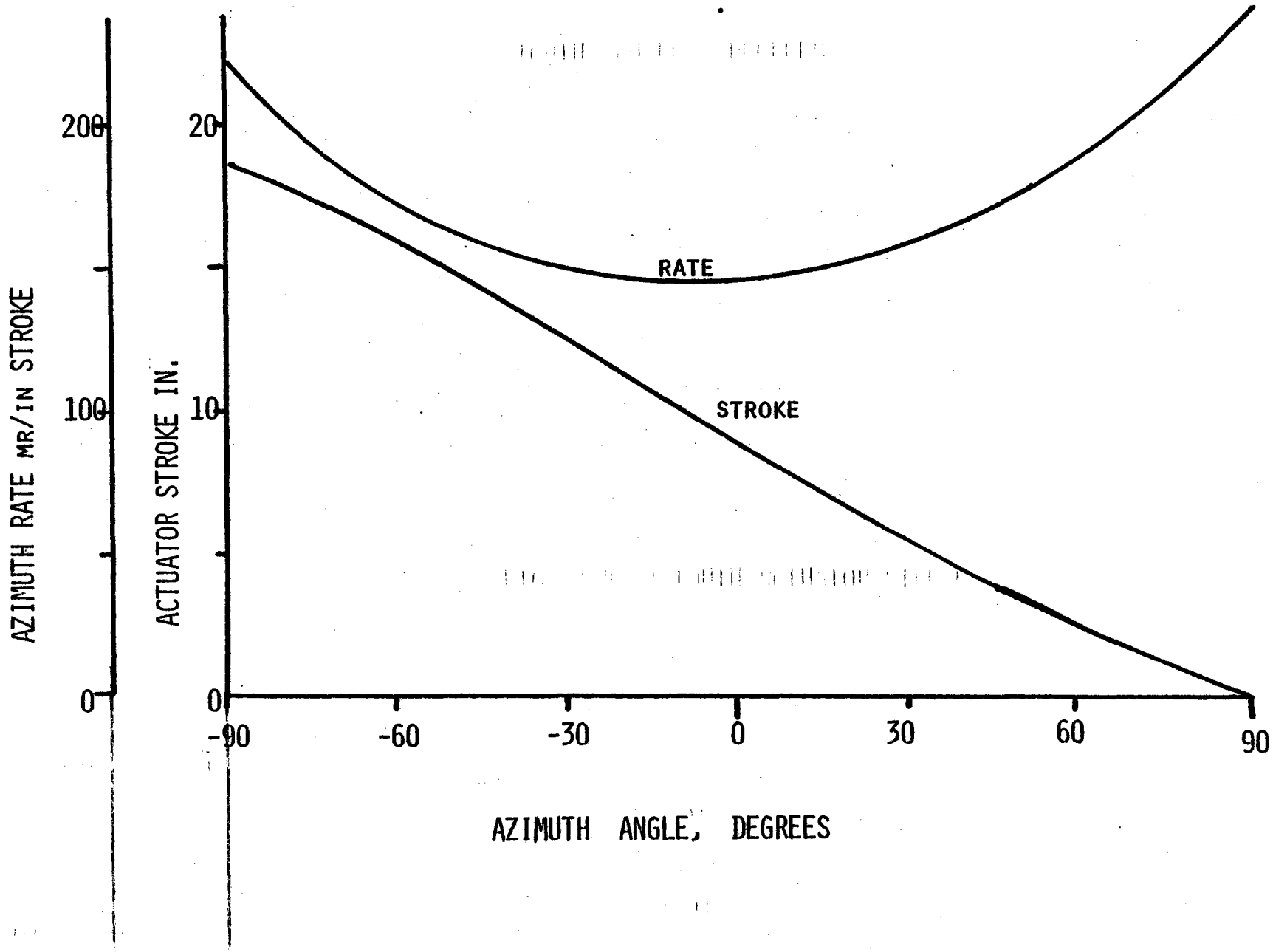

2.1.3.2 Azimuth Drive(cont'd)
in 3.5 minutes. The actuator ratio is 64 turns per inch of travel. Drive is accomplished by a 1/3 HP, 1750 rpm motor through a 10:1 gear reducer producing 90" pounds of torque and actuator thrust of 5000 lbs.

2.1.3.3 Elevation Drive

The elevation drive mechanism utilizing the linear actuator is shown in Fig. 2-5 . The moment and stroke characteristics are presented in Fig. 2-6& 2-6a. The reactive moment capability, 160,000 in lbs. for the stowed position is the primary design criteria, together with the 22 m/sec survival at the other extreme, -23° orientation.

Backlash of the mechanism is 0.8 mr at the most adverse orientation, i.e. -23°, decreasing significantly at other positions. The stiffness of the elevation drive mechanism varies with the position, increasing from 170,000 in lbs/degree at -23° to 850,000 in lbs/degree at 67°, then decreasing to 230,000 in lb per degree at storage. At the critical vortex shedding angle of 30° the stiffness is 555,000 in lbs/degree.

The elevation drive is constrained in the storage drive quadrant to azimuth position of 0° (centered). This constraint is required with the canted

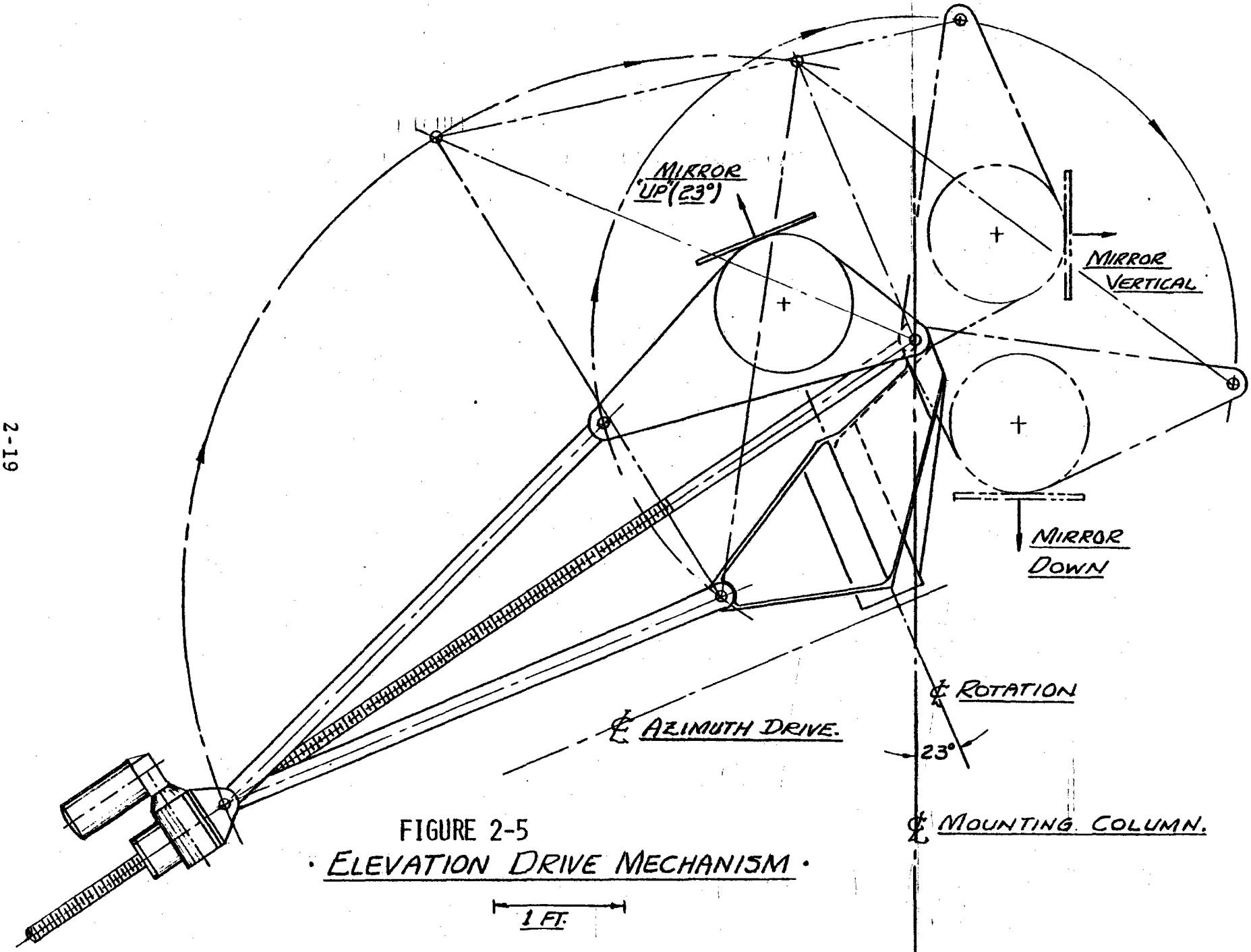

FIGURE 2-5

· ELEVATION DRIVE MECHANISM ·

FIGURE 2-6 ELEVATION MECHANISM

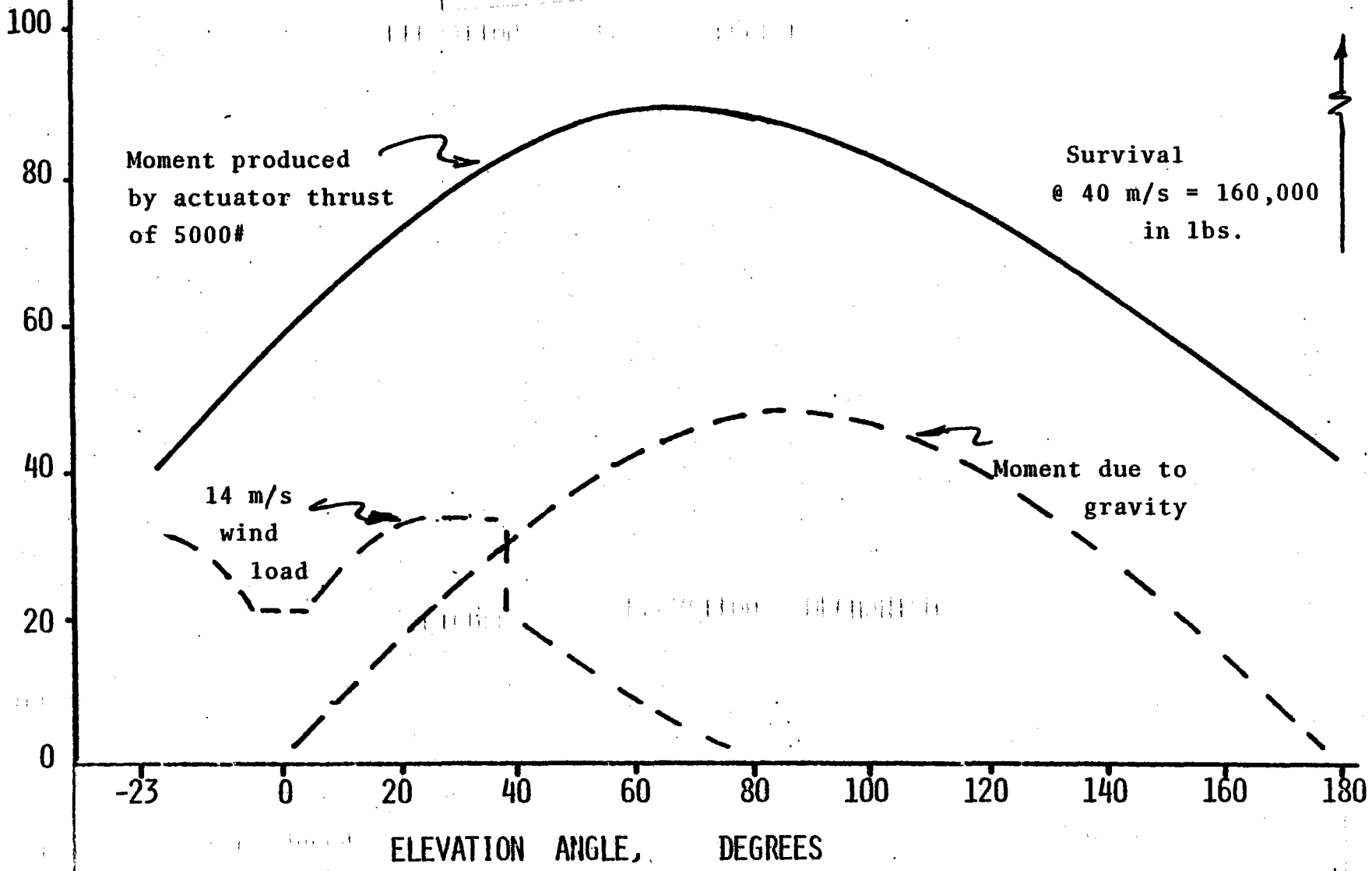

FIG. 2-6A ELEVATION ACTUATOR STROKE

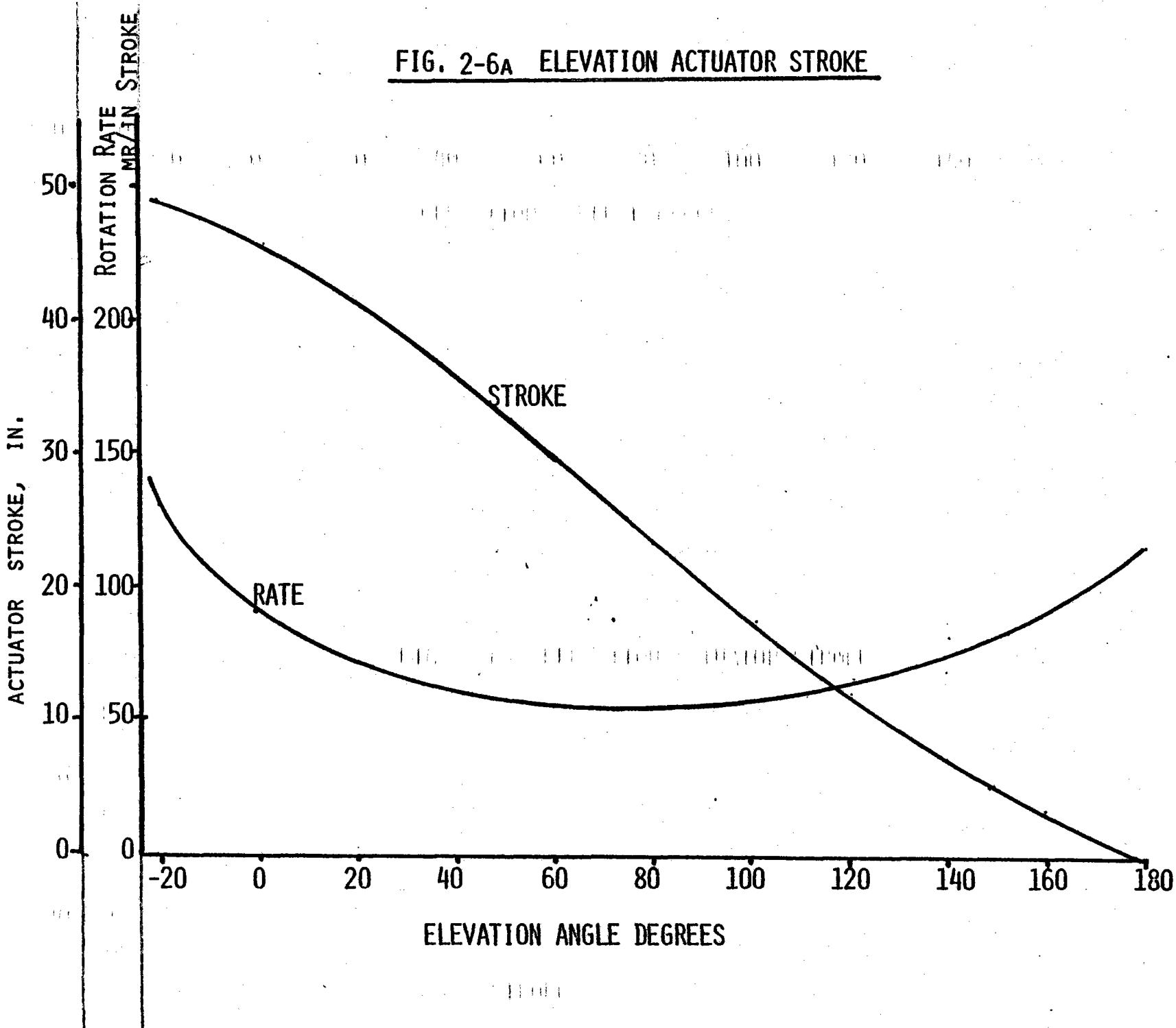

2.1.3.3 Elevation Drive(cont'd)
azimuth axis, and is provided within the microprocessor controller. Redundant protection is provided by limit switches which if triggered prevent further elevation drive.

The full stroke of the elevation actuator is 49 in. which is accomplished in 18.2 min. The actuator ratio is 64 turns per inch of travel. Drive is accomplished by a 1/3 HP, 1750 rpm motor through a 10:1 gear reducer producing 90 in. lbs. of torque and actuator thrust of 5,000 lbs.

The actuator is protected by a telescoping shield between the base and the trunnion, and by a solid tubular cover on the aft extension. Sealed ball bearings are installed at all rotating points.

2.1.3.4 Motors and Controller

The motor selected for the drive mechanisms is a 1750 rpm, 1/3 HP, 1Ø, 240V Ten V motor. An inline gear reducer with 10:1 ratio provides 90 in lbs. of torque at 172 RPM to the actuator shaft.

The motor is controlled by a solid state switching device for forward and reverse drive of both motors. The motors can be operated independently or simultaneously. The input signal from the HC is 4 signal TTL compatible and employs negative logic switching, i.e.

2.1.3.4 Motors and Controller(cont'd)

current sinking. The controller employs an optical-isolated zero voltage gate trigger circuit to energize the load voltage at the zero crossing of the line voltage. The line voltage is also terminated at zero voltage.
A protection circuit is utilized to prevent energizing both forward and reverse Triacs simultaneously. Should such an erroneous signal be received, no motor excitation occurs.

The motor revolutions are counted by a magnetic reed switch, tripped by a permanent magnet on the extension of the motor shaft. The encoder circuit is continuously monitored during heliostat operation. The encoder is enclosed by a separate cover on the back of the motor.

2.1.3.5 Manual Control

The motor shaft extends one inch out the back of the motor and encoder housing and contains a square section. This permits coupling with a hand-held drive motor or a hand crank for emergency operation. The QC auxiliary drive motor is powered by batteries carried with the service vehicle.

2.1.3.6 Gimble Axis Encoder

It is necessary to establish a 'bench mark' from which to start the count of drive motor rotation, upon starting each

2.1.3.6 Gimble Axis Encoder(cont'd)
morning. The design provides for this function in elevation by use of a collimated light, which is mounted near the base of the pedestal, reflected off a mirror on the cross tube back to a photo diode housed adjacent to the light source. The light path is 240 inches long as shown in Figure 2-7.

To achieve the objective of 0.2 mr reproducible indication, discrimination of .048 inches is required which is readily achievable. A similar technique is utilized to obtain the azimuth bench mark by mounting the optical unit on the end of the cross tube and the mirror on the pedestal cap. Reference Fig. 2-8.

Upon start up in the morning, the light source will be energized and as the heliostat is activated from storage, the Gimbal axis encoders will trigger, first, the elevation, upon which the elevation drive will be interupted and azimuth drive energized to sweep the azimuth encoder. After both axis encoders are read, the optical units are de-energized and the microprocessor counts all motor shaft rotations for tracking feed back. Acquisition is accomplished according to individual microprocessor instructions.

Initial alignment is performed during installation and can be verified or readjusted with the aid of the special equipment fixture which attaches to the trunnion.

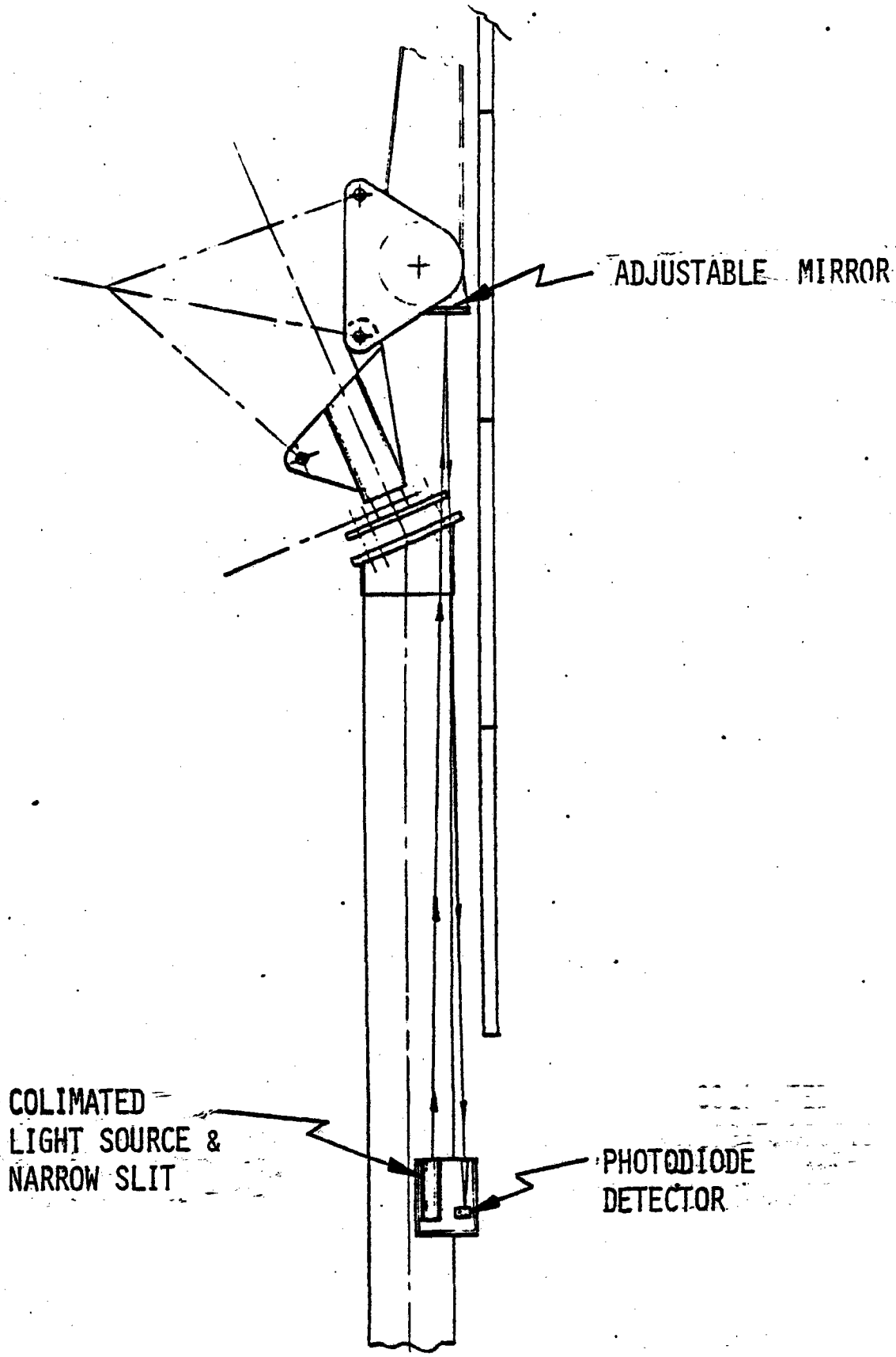

FIG. 2-7 ELEVATION GIMBAL AXIS ENCODER

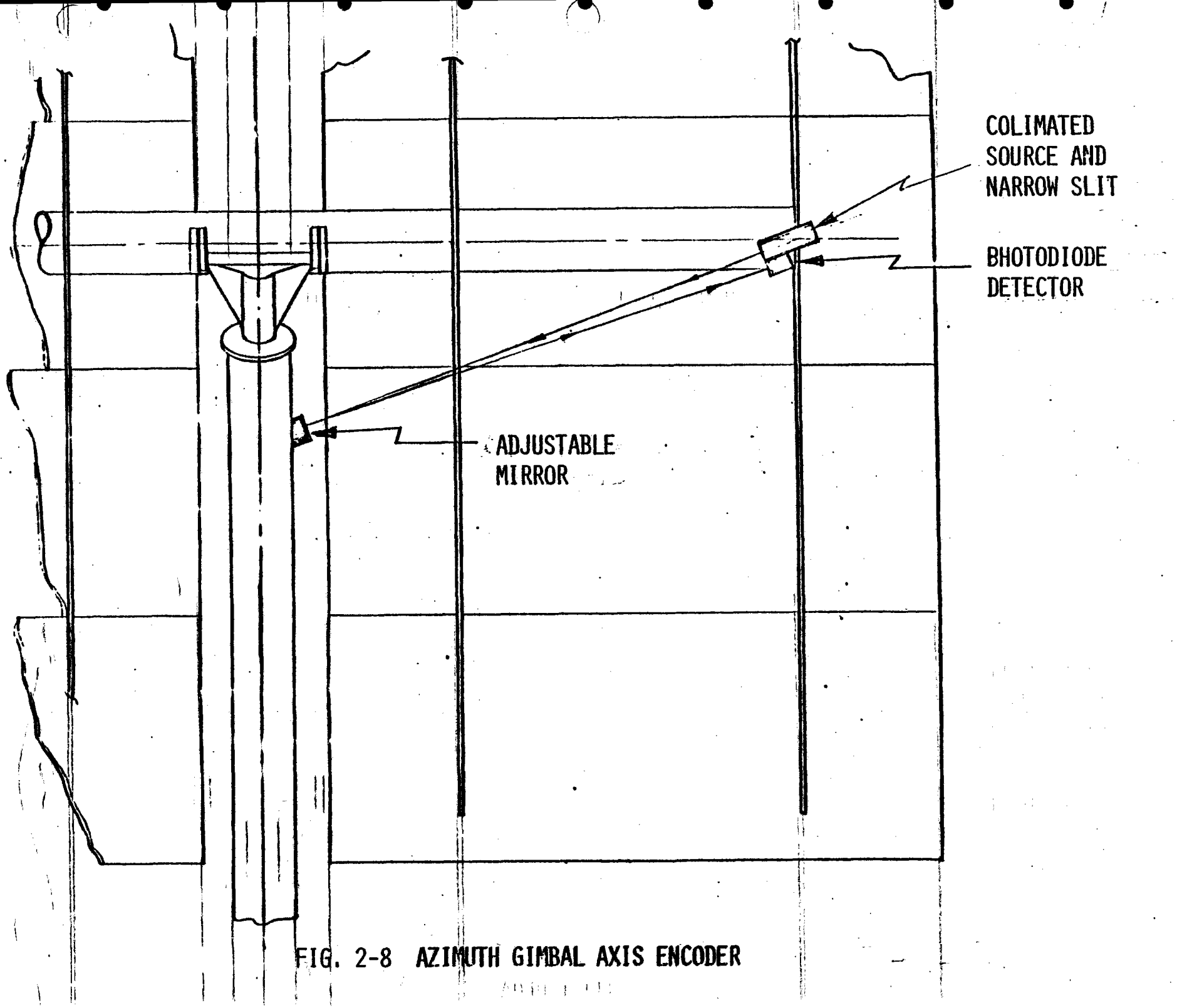

FIG. 2-8 AZIMUTH GIMBAL AXIS ENCODER

2.1.4 Heliostat Control System

The control system orients each heliostat so as to continuously reflect solar insolation at the target. The heliostat array controller (HAC) provides control commands to the entire field of heliostats and also communicates with the Master Control System.

Communications between the HAC and individual heliostat controllers (HCs) take place over a three tier communications bus.

Each HC contains a microprocessor programmed for tracking and control functions plus communications and manual control. Positional (axis) information is also sensed by the HC and commands are issued to the motor drive for heliostat movement.

A unique, cost effective tracking algorithm simplifies the tracking and control functions of the HC.

2.1.4.1 Heliostat Array Controller(HAC) Subsystem

General--The HAC subsystem provides support data and network control for the microprocessor heliostat controllers(HC). This includes such functions as MCS interface communications, operator command & display, HC calibration, and data collection as well as the primary tasks of tracking computations and HC network communication management.

The HAC responds to commands from the Master Control System for general field

2.1.4.1 Heliostat Array Controller (HAC) Subsystem (cont.)

control functions. The HAC also communicates with each HC or groups of HC's, and interfaces directly with the Sensor Array Controller (SAC) used for calibration.

The HAC is comprised of a standard minicomputer with an accurate time base with battery backup included. Communications with the heliostat field is effected by 64 serial input-output ports buffered with differential bus drivers and receivers.

A primary design objective for the HAC computer is a low expected failure rate with minimal dependence on electromechanical peripherals since there is a relatively high cost for system down-time. To that end, the configuration does not use any disk peripheral as a system device and the interface to the MCS is a binary communication port rather than shared memory, shared disk or inter-processor bus. The disk will only be used as an initial program loading and off-line data storage device but the basic HAC operating system will continue to function independently of the disk and the port to the MCS. This configuration results in more inherent reliability for the primary HAC function than a complex, interdependent network of back-up computers and alternate control system. All basic processing and control functions operate in internal core memory with no reliance on disk overlays or data files. The communication port to the MCS computer is easily protected from failure conditions in the MCS.

2.1.4.1 Heliostat Array Controller (cont.)

The configuration for the HAC computer is as follows:

1) Data General Eclipse S/230 with 128 K (K=1024) 16 bit words core memory. 11 additional interface slots are available for expansion to 256K words and a wide variety of peripherals. System includes Memory protection, power fail/auto restart, automatic program load and hardware multiply.

2) Eclipse floating point processor.

3) Dual Diskette subsystem - 2 drive floppy disk subsystem for program loading and data storage.

4) Digital interface 16 bit general purpose I/O for Sensor Array Controller.

5) Data General 30 CPS terminal printer for hardcopy of system control operations.

6) Intelligent Systems Corp. - Intecolor Color Graphics display terminal for operator interaction and control.

7) Data General Communications Subsystem. Provides special 4 interface slots for communications parts - both synchronous and asynchronous and allows expansion with communications preprocessor computer for high data rates.

8) Asynchronous line multiplexor - 64 lines available to provide two-way serial data streams with the Heliostat controllers at 9600 BPS.

2.1.4.1 Heliostat Array Controller (cont.)

9) 2 line synchronous line multiplexor - Binary communication port (Bisync) to the MCS and dial-up access to the engineering development computer for remote data collection and program update. Line data rates are 9600 BPS for the dial-up port.

10) Real time clock based on external time standard to ± 0.1 ppm.

Software Systems - The proposed configuration will support the following standard software products offered by Data General Corp.

Real time operating system (RTOS) a multi-tasking core resident system which supports all of the devices in the configuration and is a true subset of the Real Time Disk Operating System (RDOS) used for software development.

Communications Access Manager (CAM) provides complete communications support for both synchronous and asynchronous ports. Allows the expansion with a communications pre-processor computer with no change in the application software. The synchronous support provides complete protocol for IBM compatible binary synchronous communication and will also operate in 2780, 3780, and HASP emulation.

The languages supported in the configuration include Fortran IV, Fortran V, and a special Algol based system programming language called DG/L. Fortran V and DG/L can be intermixed in the same program and are optimizing, re-entrant,

2.1.4.1 Heliostat Array Controller(cont'd)

real time languages. They are easily interfaced with special devices and assembly language subroutines.

Development Support System -- A similarly configured Eclipse computer with the addition of development support peripherals is required to implement the real-time software on both the HAC and the HC microprocessor (using a cross assembler). These additional peripherals would include a 20 M Byte cartridge disk subsystem, a 300 LPM line printer and a 75 IPS, 800 BPI magnetic tape unit.

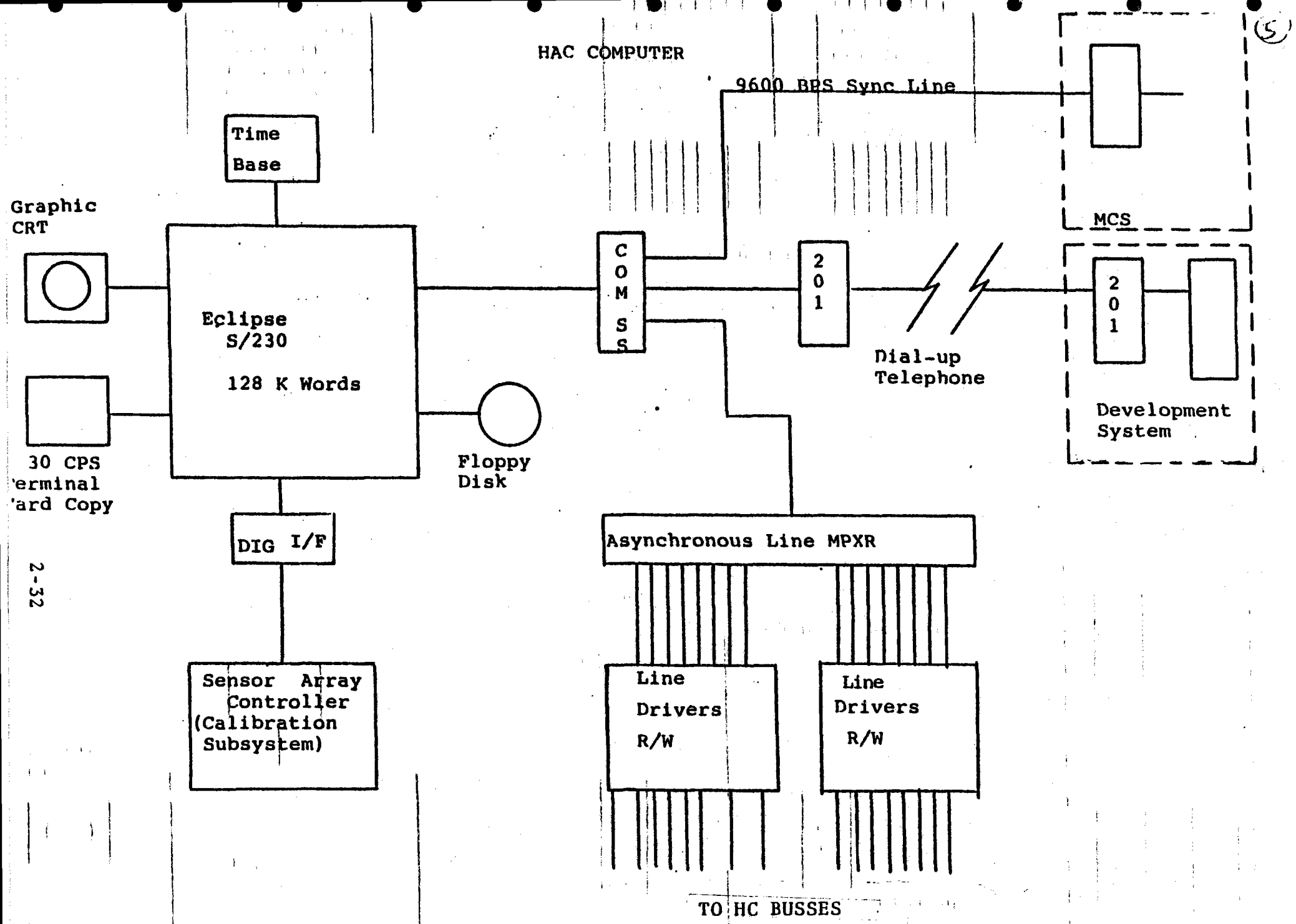

Figure 2-9 HAC Computer

2.1.4.2 Communications Bus

The communications bus is a three level digital interface between the HAC and all the HCs. All bus lines use a twisted-shielded pair driven at 5 volts and operated at a 9600 band data rate.

Figure 2-10 shows the first level "A" bus field partitioning which connects each of the 64 HAC ports to eight A-level HCs. Each A-Level HC connects to seven B-Level HCs and each B-Level HC connects to seven C-Level HCs as shown in Figure 2-11. Total field capacity is 29,184 heliostats.

Level A cables are installed in groups of eight along radial lines from the target to minimize installation costs.

Each HC has three (3) ID bits which define eight distinct ID codes. Each bus level has a maximum of eight HCs, and therefore any individual HC on a given bus can be identified. Bus levels are assigned by means of a simple software routine. This technique uses a brief initialization procedure in which the HAC assigns Level A to all HCs on the A-Level bus. All A-Level HCs then assign B-Level to their lower level bus HCs and so forth.

Bus protocol uses immediate answer-back except for modes requiring large amounts of data transfer in which case a summary echo-back is sent after each data block load.

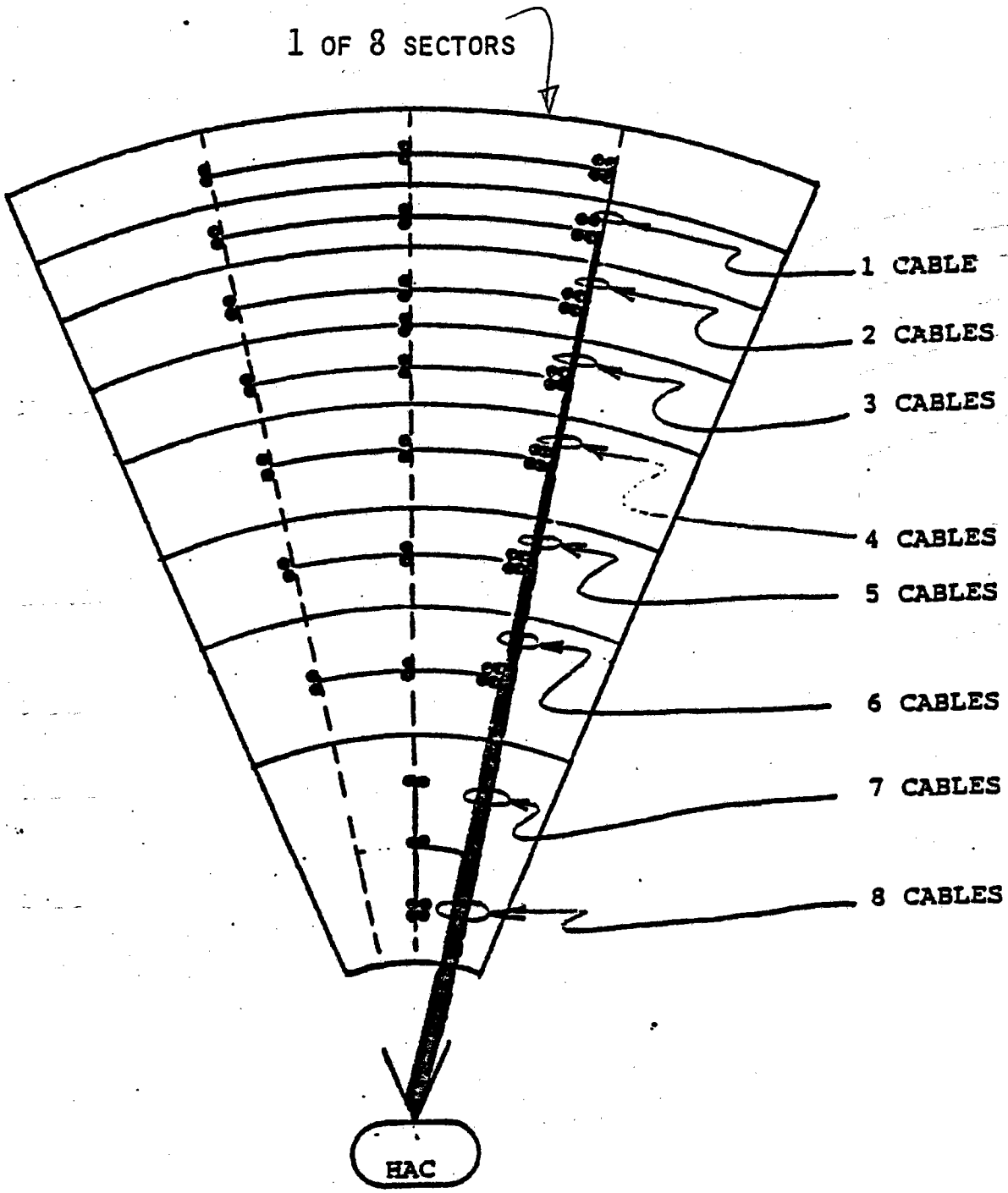

@ = A LEVEL HELIOSTAT CONTROLLER

FIGURE 2-10 FIRST LEVEL ("A") FIELD WIRING

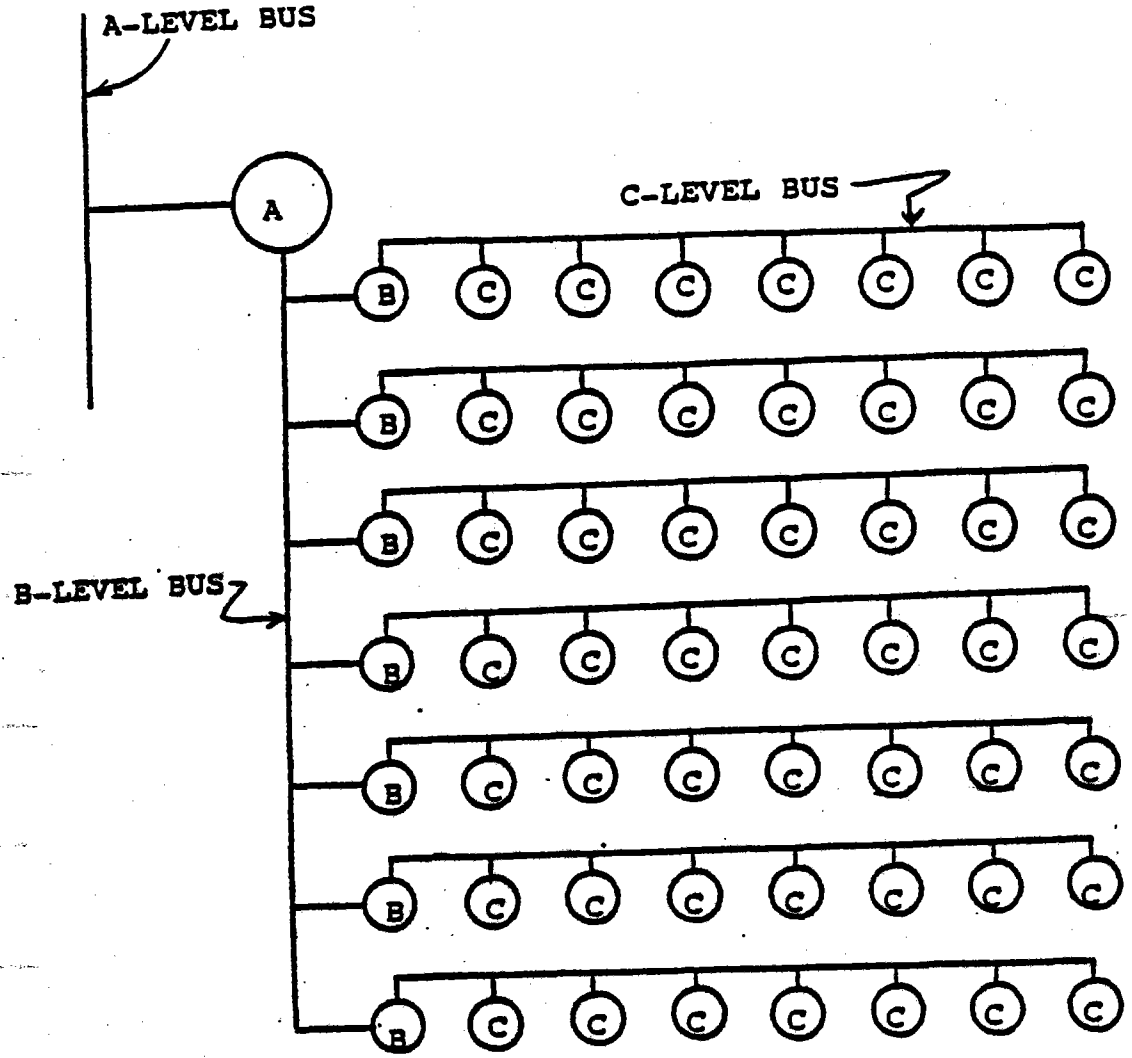

57 HELIOSTATS PER GROUP

FIGURE 2-11 LOWER LEVEL ("B" & "C") FIELD WIRING

2.1.4.2 Communications Bus(cont'd)

The chosen field wiring system plus three ID bits per HC define each HC with a unique address.

The field wiring also simplifies the driver/receiver electronics since the maximum number of HC loads on each bus is eight (8).

Board IDs are set during manufacture during board drilling where computer control is convenient and economical. For field replacements, a universal board is punched to the appropriate code.

The communications system is structured for efficient detection of failures. HCs which detect faults report directly to the HAC as described below. An HC which fails & cannot report or which captures a bus would inhibit control of a group of HCs. However, each HC expects a message from its Master HC at least every 20 seconds during Normal operation. If none is received, the HC goes to Automatic Emergency Shutdown.

The HAC "Status" Command is used to detect failure conditons. This command generates automatic polling by Master HCs every 5 seconds. This communication is brief and in this mode only go/no-go conditions are reported. The five (5) seconds interval is chosen so that a power outage or interruption can be detected within $\pm$ 2.5 seconds, which corresponds to a fraction of the tracking accuracy. Power loss is detected by a low voltage detector in the HC. This detector

2.1.4.2 Communications Bus (cont'd)

serves to reset the HC circuitry during voltage ramp-down to prevent erroneous outputs. Furthermore, the microprocessor is reset to indicate that data in volatile memory has been lost or is suspect.

Since the HAC records this time (within 2.5 sec) it can calculate the position of the heliostat at the time of power loss or dropout and can re-establish all values of position, time and coefficients when the power returns. Furthermore, a calibration is initiated for the heliostat to check accuracy of re-established parameters.

Table I shows a summary of the details of communications between the HAC and HCs. Paragraphs I and II of the table delineate data rate and group sizing.

Four types of data blocks are shown in paragraph III along with details of data communications overhead and time.

While all HCs do not require the same number of coefficients, the HAC calculates and assigns the same to all HCs. This approach simplifies the data structure both on the communication lines and within the HC microprocessor. Echo-back is used for communication of data blocks shown in paragraph III. Echo-back occurs after all data have

2.1.4.2 Communications Bus (cont'd)

been loaded. This approach tests the retention of random-access memory (RAM) in the HC microprocessor, and is a more reliable test than immediate answer-back.

TABLE I - SUMMARY OF HAC/HC COMMUNICATIONS SYSTEM

I. Data Rate:
9600 Baud or 1.15 ms. per byte

II. Field Size
64 parallel A bus outputs from HAC

8 "A" HCs per bus
7 "B" HCs per bus
7 "C" HCs per bus

512 Total "A" HCs
57 HCs per "A" HC group

29,184 Total HCs (maximum)

III. Coefficient Loading

DATA TYPE	ACCURACY (mRdn)	# of BYTES				TIME	
		Data	Error Corr.	Format	Tot	Per Hc (msec)	Per A bus (456H Max)se
Acquisition/Shutdown	5.0	32	32	16	80	91.7	41.8
Normal Tracking	0.2	64	64	16	144	165	75.2
Emergency Shutdown	5.0	35	35	16	86	98.5	44.9
Calibration	---	12	12	16	40	45.8	---

TABLE II - TYPICAL COMMAND SEQUENCE

	Comm. Time (sec)	Frequency per day	% Comm Bus Use during Normal 8/hr. Operation Da
1. System Test	variable	1	*
2. Assign Master/Slave Modes	<.02	1	*
3. Send # of slaves per master	.06	1	*
4. Time Sync.	<.01	1	*
5. Initial Status Check	.2	1	*
6. Load ACQ & ESD Coefficients	86.7	1	*
7. Echo-back	86.7	1	*
8. Acquire Command(Auto Reference)	.1	1	<.01
9. Load Normal Tracking Coefficients	75.2	1	.26
10. Echo/back	75.2	1	.26
11. Power-on(Focus) Command	.06	1	<.01
12. Normal Operation including			
Time Sync	<.02	32	<.01
Status(All HCs)	.2	5760	4.00
Power Level Control	.06	32	.01
Interrogate individual	.05	100	.02
Calibrate	.48	480	.80
Failure reporting	.05	infrequent	0
Offset pointing	.1	"	0
Re-initialize	.75HC	"	0
Emergency shutdown	<.02	"	
13. Normal Power off	.1	1	<.01
14. Load Shutdown Coefficients	41.8	1	.15
15. Echo back	41.8	1	.15
16. Normal Shutdown Command	.1	1	<.01
17. Stow Command	.1	1	<.01
TOTAL			5.7%

* Prior to field operation

2.1.4.3 Heliostat Controller

2.1.4.3.1 Hardware

Figure 2-12 shows the detailed block diagram of the HC. This subsystem contains a single chip microprocessor which has internal program memory (ROM) and random access memory (RAM).

A single voltage DC power supply is used to power the entire board. It is protected from transients by the transient suppressor and fuse.

The microprocessor uses a crystal to establish a stable time base. The selected crystal is the same used in television sets and is low in cost. Due to our unique tracking algorithm, only short term (10 hrs.) stability is required, and accuracy is not critical since the microprocessor compensates for errors by comparison to the time base standard in the HAC.

Outputs to the motor controller are buffered as are inputs from the motor shaft encoders, benchmarks, and direction encoders. The motor shaft encoder produces a pulse each revolution, which the microprocessor accumulates to determine relative positions from the benchmark which is an accurate reference position sensor.

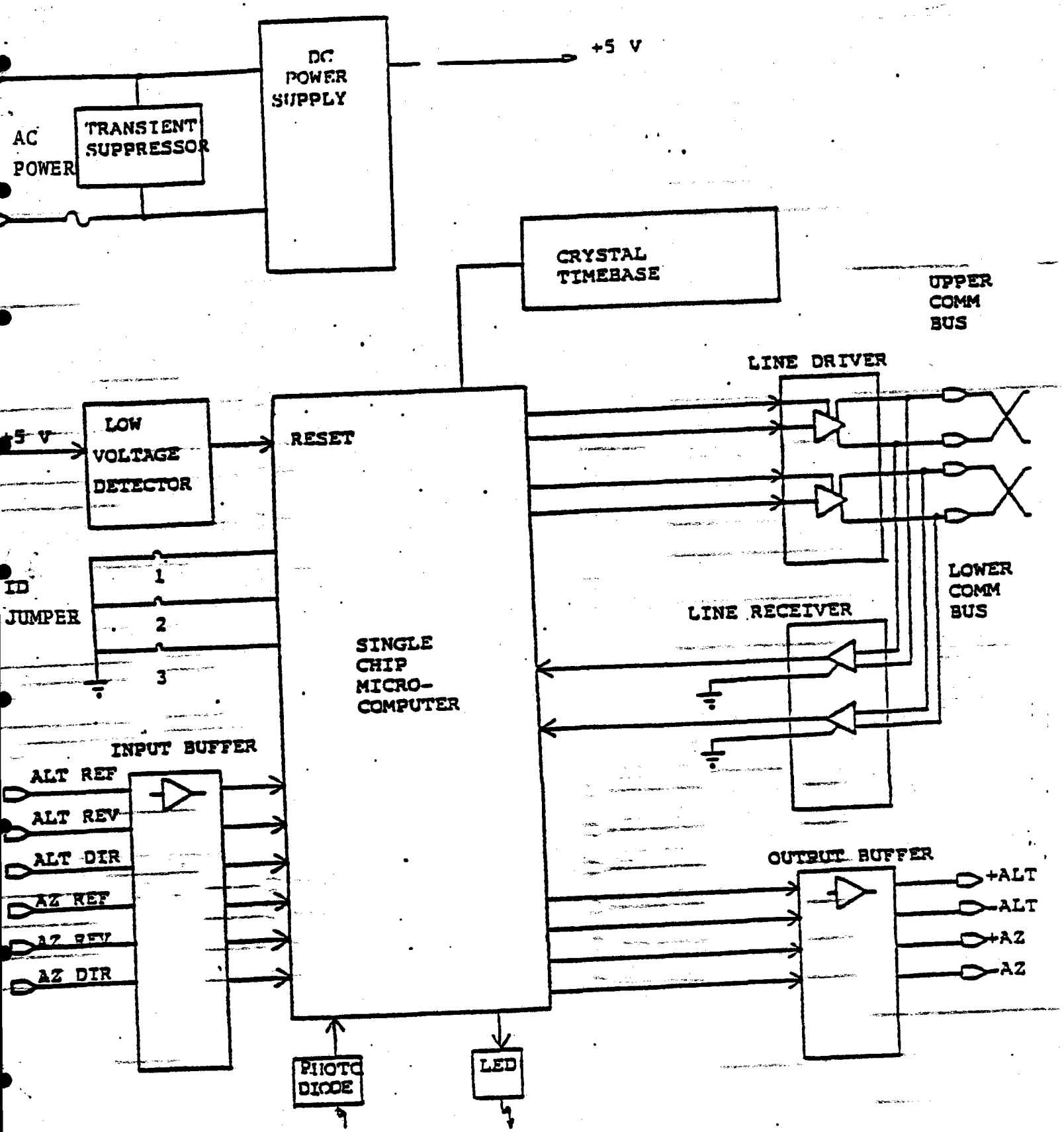

FIGURE 2 - 12 DETAILED BLOCK DIAGRAM - HELIOSTAT CONTROLLER

2.1.4.3.1 Hardware(cont'd)

Differential line drivers & receivers are used for the two communication bus lines.

A low voltage detector senses when the voltage drops below a level which could cause loss of data in the RAM. The power supply is designed to permit at least a 40 msec. AC dropout before tripping the low voltage detector. When power returns (or is initially turned on), a reset pulse is generated and the microprocessor requests new data from the HAC.

Local control is accomplished through an optical communication link. The light emitting diode (LED) is used to transmit data, and the photo diode receives commands and data from the external control unit. A small window with a diffusing lens provides an environmentally sealed path from HC to the external controller.

Three (3) Identification jumpers are used to code each board for one of eight (8) ID numbers.

2.1.4.3.2 HC Functions

2.1.4.3.2.1 Communications

The HC monitors both communication bus lines for messages. The upper level bus is treated as a control bus for commands and data.

2.1.4.3.2.1 Communications(cont'd)

The lower level bus is controlled by the HC.

Data messages are sent and received serially at 9600 baud with error detection and correction formats.

2.1.4.3.2.2 Drive System Interface

The HC monitors heliostat position and controls the movement of the heliostat as a function of time according to the tracking equations. Motor control commands are sequenced as a function of ID coding to prevent loading of the AC power line. That is, each time a motor is initially turned on, the current surge is high. If all motor controls were asynchronous, the probability of all motors starting at the same instant is finite and the AC power requirement is high and therefore expensive. By sequencing the motors, the maximum number of motors operating at starting current is reduced by the number of sequences (in this case eight(8)) and the cost of the AC power system is substantially reduced. Sequencing reduces the peak power demand also which is an economical operating benefit.

2.1.4.3.2.3 Normal Tracking

The control system uses a unique tracking algorithm which divides tracking responsibilities between the

2.1.4.3.2.3 Normal Tracking(cont'd)
HAC and HCs so as to reduce the cost of the HC with only minor impact on the HAC.

The first step in the tracking algorithm takes place during non-operating hours when the HAC would otherwise be idle. During the "pre-acquisition" time the HAC calculates the tracking positions for each HC at fixed intervals for the following day's operation. A solar ephemeris program (including atmospheric refraction) adapted from the Almanac for Computers is used. These tracking positions are then converted into a short polynomial expression using a least-squares curve fitting technique. This conversion results in the n^{th} order polynomial function of time which is accurate to better than 0.2 milliradians.

The algorithm converts "tilted" altitude directly into two polynomials, typically 3rd & 7th order. Optimization studies have shown that the use of two polynomials of lesser order is more efficient than a single high order polynomial.

In the case of "tilted" azimuth, an indirect method has proven to be more efficient than direct curve fitting. This method computes tilted azimuth from the intersection of the (already known) "tilted" altitude and a dummy variable. The dummy variable is then defined by two

2.1.4.3.2.3 Normal Tracking(cont'd) parameters(X&Y) in the same manner as altitude. In order to distinguish the operational coordinate system of the tilted axis mirror from the normal altitude-azimuth coordinate system, the tilted altitude will be called "tiltitude" and the tilted azimuth will be called "tizimuth". This will clarify the difference between normal coordinate system reference and tilted axis coordinate references.

Figures 2-13a,2-13b,&2-13c show 3 cases of tizimuth and corresponding X,Y,& tiltitude vectors. The drawings represent a three dimensional sherical system. Note that the X&Y origins have been chosen such that the intersection with the tiltitude is always at lease a 45^{o} angle and usually closer to 90 . This angular restriction guarantees that small errors in altitude produce equivalent or smaller errors in tizimuth. The choice of X&Y origins has also been optimized to simplify the mathematics involved in calculating the tizimuth.

Figure 2-13d shows the regions in which the X&Y variables are used. This decision is made by the microprocessor based on the tizimuth. The X&Y parameters are typically represented as 5th order polynomials(each).

The total data for normal tracking transmitted from the HAC to each HC is typically 64 bytes(1byte - 8 bits). A study of the HAC computation time reveals that all data for the entire field can be calculated in less than 24 minutes. The data is normally stored on disk for retrieval just before field start up.

X,Y CURVE FIGURE 2-13A

TILTITUDE = 90° - Z

X ARC = ▭▭▭▭▭

Y ARC = ● ● ● ● ●

Z ARC = ——·——·——

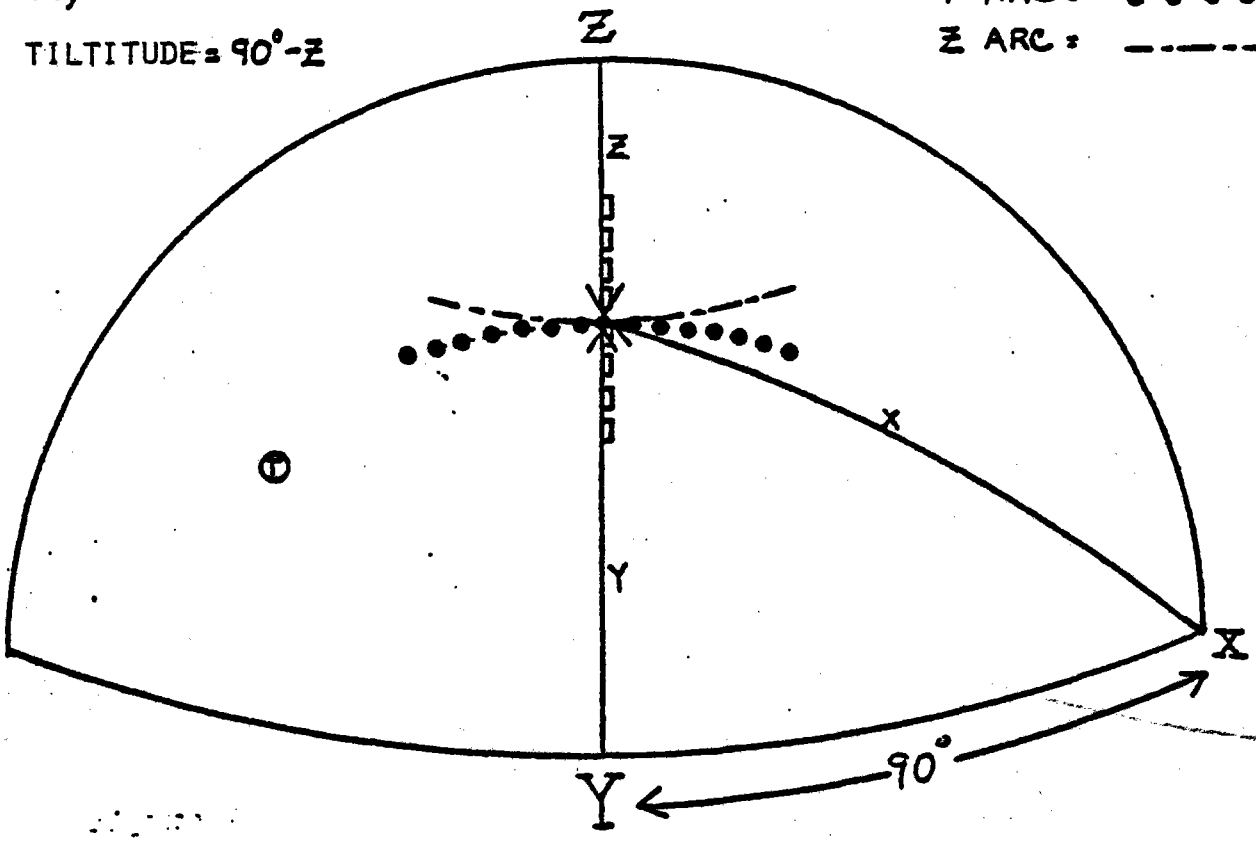

FIGURE 2-13B

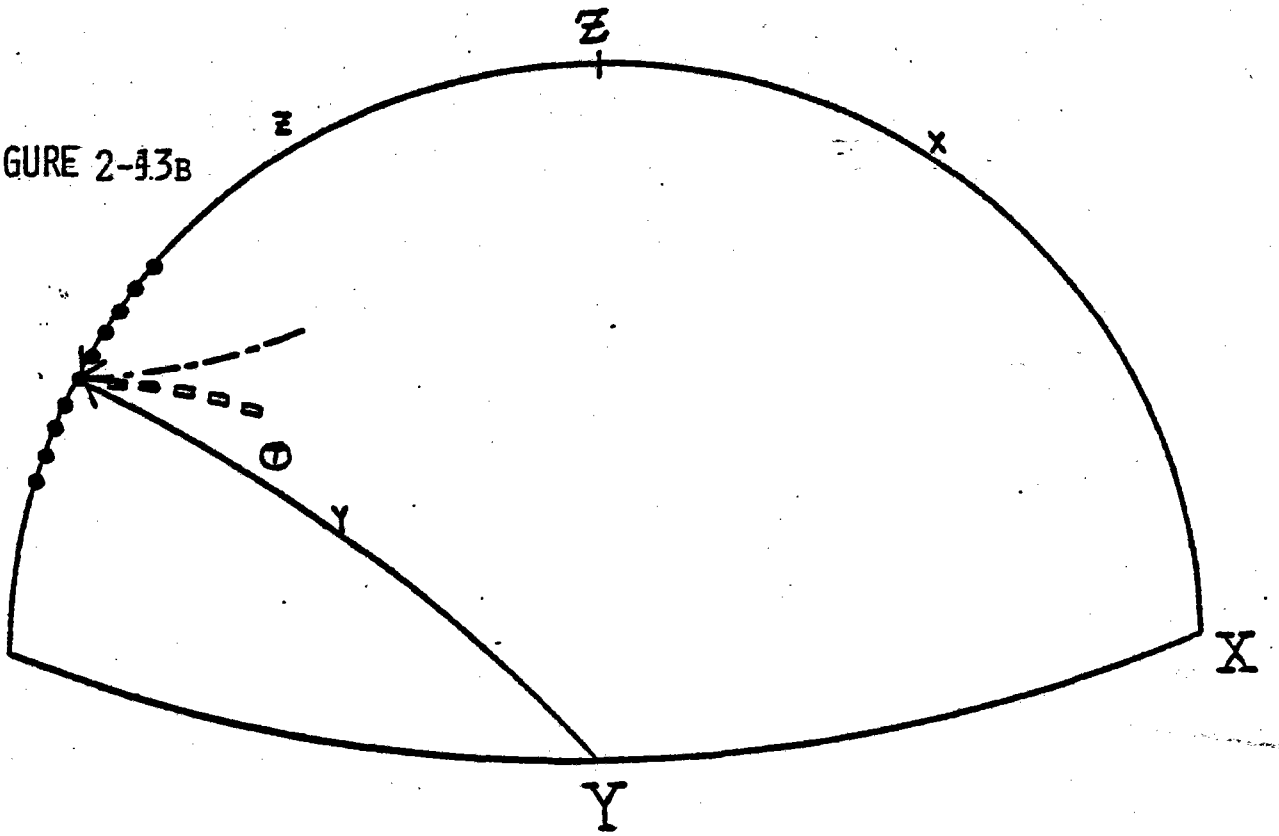

FIGURE 2-13c

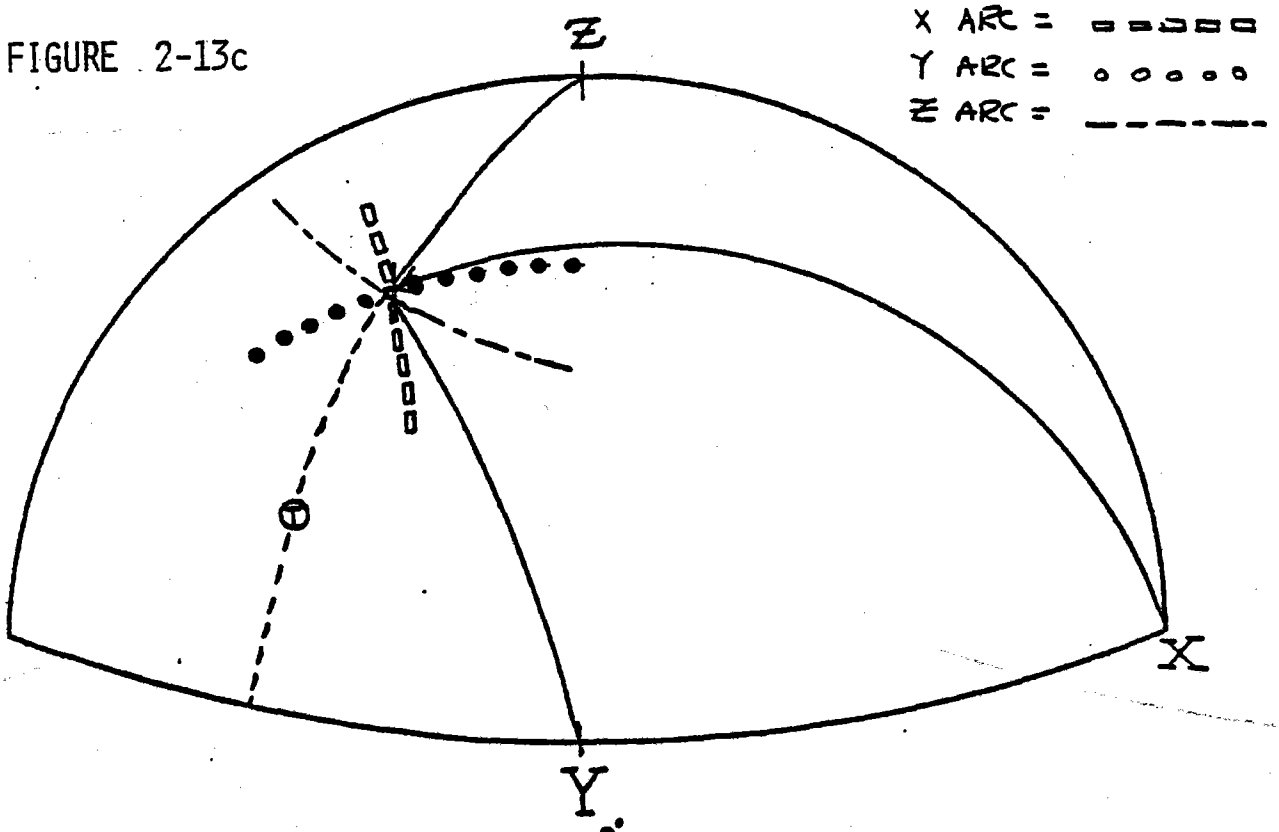

FIGURE 2-13D

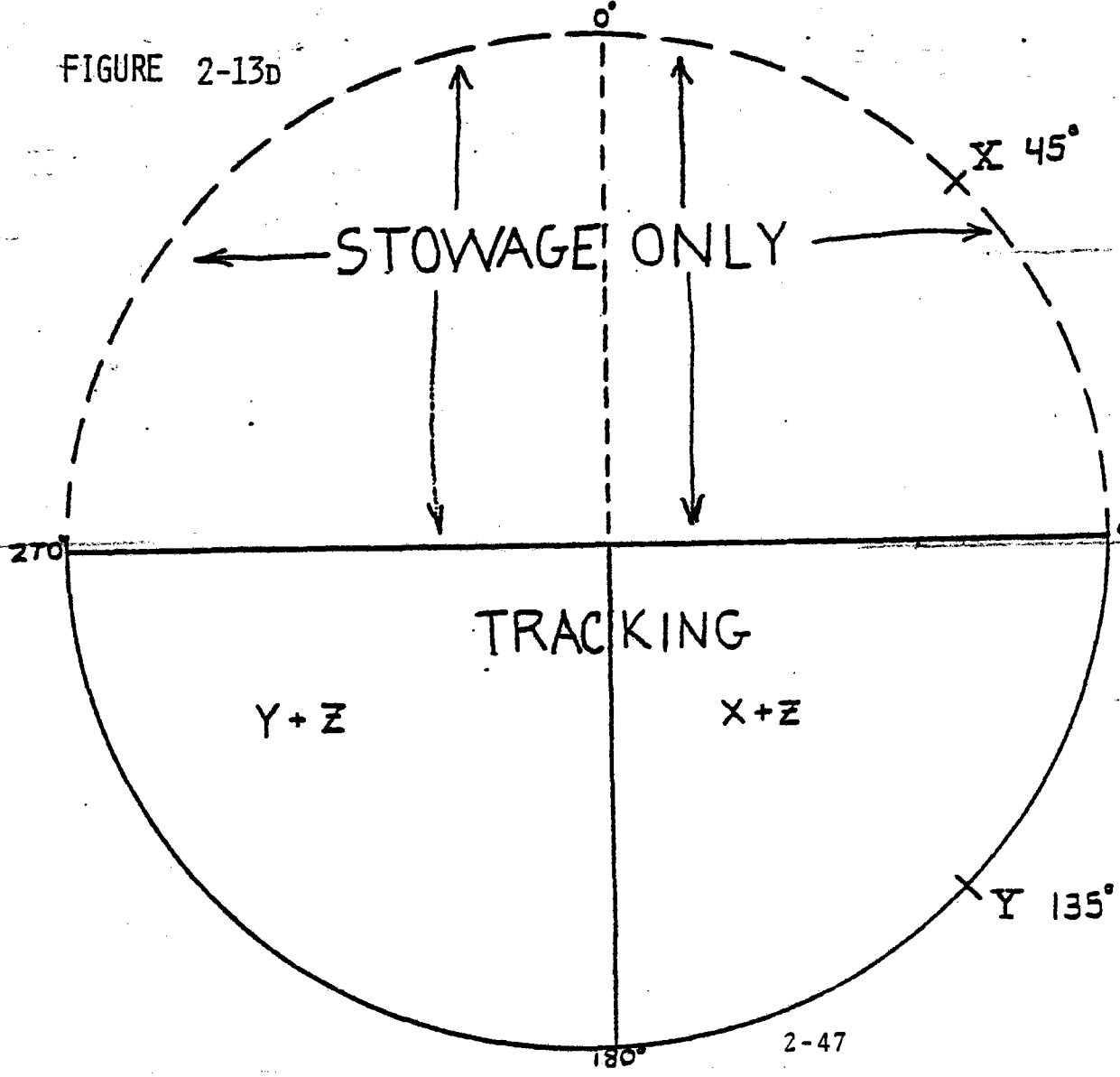

2.1.4.3.2.3 Normal Tracking(cont'd)

The second step in the tracking algorithm requires the transmission of tracking coefficients to all HCs. At a data rate of 9600 baud, the total time for transmission is less than 60 seconds. Data are transmitted serially using error correction codes. Echo-back is also used to verify both data link integrity and HC storage & operation.

The third step in the algorithm is the storage and use of the tracking coefficients by each HC. Tracking coefficients require 64 bytes & other data about 35 bytes of storage in each microprocessor. Currently available single-chip microprocessors have 128 bytes of RAM. The actual tracking equations are given below:

$$\text{Altitude} = \sum K_n \quad t^n$$

Where n is the polynomial order

K_n is the $_n$th coefficient

and t is time

$$\text{X and Y} = \sum c_n \quad t^n$$

Where n is the polynomial order

C_n is the $_n$th coefficient

and t is time

$$\text{Azimuth} = \cos^{-1} \left\{ \frac{\cos (\text{X or Y})}{\cos (\text{ ALT })} \right\}$$

2.1.4.3.2.3 Normal Tracking (cont'd)

Calculation time in the microprocessor is estimated at less than .1 sec.

Thus, the tracking algorithm permits the use of low cost, off-the-shelf microcomputer chips and other components. Testing is also simplified since all HCs are identical (except for ID jumper).

Furthermore, compensation for non-linear drives, offsets & misalignments, and mechanically restricted zones can be handled by the HAC by adjustment of tracking coefficients. This aspect represents a substantial decrease in the burden of the microprocessor.

The algorithm is also used during acquisition, shut-down & emergency defocus by simply substituting new coefficients.

An important feature of the tracking algorithm is its versatility. This benefit has already resulted in a cost saving which resulted when the tilted axis concept was shown to be the optimum solution to the mechanical drive requirement. The impact of changing to a tilted coordinate system had no effect on the design and studies concerning control. A versatile control system is also important in the area of beam safety where many requirements are initially heuristic and might

2.1.4.3.2.3 Normal Tracking (cont'd)

change significantly once the field is in operation. Changes in these areas would have minimal cost since only the HAC software requires modification as compared with other approaches which might require changing up to 1000 intermediate level multi-heliostat controllers.

Control over the field after a power failure can be reestablished rapidly. The "reload" time is the time required to transmit tracking coefficients last position and current time to each heliostat. Since the HAC has core memory and battery back-up for the timebase, no essential information is lost and the HAC can quickly calculate the position of every heliostat when the power was lost. The "reload" time is on the order of 120 seconds for the entire field.

2.1.4.3.2.4 Acquisition/Stowage

The acquisition/stowage method that offers the maximum in beam safety is the moving target method. In principal, an imaginary target slides up or down a "wire" from a point on the ground to the "prefocus" position for that group. During acquisition the heliostats in a given group track the target as it moves up the wire to the prefocus point. After reaching the prefocus point, the heliostats

2.1.4.3.2.4 Acquisition/Stowage(cont'd)

acquire the receiver.

This approach offers several distinct advantages:

1) Since the beams in the group focus on the moving point & diverge beyond it, the point of maximum flux is contained within the field's airspace.

2) The volume of airspace where high flux concentrations can occur during acquisition or stowage is further restricted since the maximum altitude of each beam is restricted by the path of the moving target.

3) The maximum number of beams potentially focusing in the distant airspace is no greater than the number of groups. For safety, the definition of the ground anchor point is critical.

Personal exclusion areas in the field can be defined for different heliostat group anchor points. Fixing the ground anchor at a distance from the group results in beams being parallel near the group. Before they become convergent the beams will be blocked by other heliostats between the group and its anchor point, thus reducing flux concentration hazards near the ground.

Before start-up of normal field operation, the HAC calculates Acquisition curves for each heliostat, which are converted to least-square polynomials. The least-squares co-

2.1.4.3.2.4 Acquisition/Stowage(cont'd)

efficients plus a starting acquisition time are loaded into each heliostat along with the "prefocus" tracking coefficients. Acquisition is automatic; each group starts at its predetermined acquisition start time. Normal shutdown is the same as normal acquisition, but in reverse.

The procedure for stowage or reacquisition at any other time is identical except that the HAC calculates acquisition/stowage coefficients in real time. This is possible because the acquisition/shutdown equations are greatly simplified versions of normal tracking equations.

In normal tracking, acquisition/shutdown, or emergency shutdown, the motion of the heliostat mirror normal in its coordinates (tiltitude-tizimuth) is a time dependent quantity.

To explicitly calculate the mirror normal position at any time requires:

1) Coordinates of beam aim point as seen by heliostat

2) Coordinates of Sun as seen by heliostat

For normal tracking only the latter is a function of time. For acquisition/shutdown both are functions of time.

2.1.4.3.2.4 Acquisition/Stowage(cont'd)

This means that the motion of the mirror normal is a complex function of a single variable, time. In the ECS algorithm we find a simple function of time that mimics the complex function to some desired accuracy.

This simple function is a least squares polynomial the order of which depends upon the form of the mirror position curve for each heliostat mirror normal (tiltitude & tizimuth of mirror normal versus time curves). This technique is illustrated by describing acquisition.

During acquisition beams are brought up by groups. The heliostats in each group move in a synchronized manner, keeping their beams aimed at a common point moving from a ground anchor point to the target.

Prior to the beginning of normal field operation the HAC determines how each heliostat in a group will move to maintain the group focus. For this the HAC uses the time at which the group will begin acquisition, an ephemeris for the sun for the duration of acquisition for the group, & the absolute position of the moving focus point in the field airspace as a function of time during acquisition. Thus, the motion of any heliostat during acquisition is solely a function of time.

2.1.4.3.2.4 Acquisition/Stowage(cont'd)

These quantities must be individualized for each heliostat. The solar ephemeris is transformed into each heliostat coordinate system. The moving focus point is a time dependent quantity since a fixed path (in the field air space) is defined for it, & moves along its "wire" to the focus at a predetermined speed. Its field position is transformed into each heliostat's coordinate system as each heliostat sees the same point in the field at different tiltitude & tizimuth.

The mirror normal position is calculated from these as a function of time subsequent to the start acquisition time. Its path is fit by least squares polynomials according to the algorithm. This is repeated for each heliostat in the group.

Normal shutdown occurs in a similar manner.

The result is, the heliostat beams follow the moving point focus as it slides up the wire, beginning at the start acquisition time for the group.

The heliostats move in a synchronized manner. All the beams step along the "wire" at the same time intervals subsequent to the starting time. Each HC has an internal time

2.1.4.3.2.4 Acquisition/Stowage (cont'd)

clock which is synchronized to the HAC at approximately 15 minute intervals. Accuracy of the HC time base is better than ± 0.05%, thus the HCs synchronism is always accurate to better than ± 0.5 seconds. This prevents heliostats spreading along the wire. All heliostats in each group are loaded with acquisition curve coefficients, emergency shutdown coefficients and a start acquisition time prior to beginning normal field operation. Different start times are assigned to each group. The heliostats need only time to calculate the mirror normal position during acquisition to the specified accuracy.

At the acquisition time for a group, its heliostats move from their ground anchor point along the wire to emergency shutdown position. Upon arrival at the ESD, the HAC loads the heliostats with normal tracking coefficients and the heliostats move their beams immediately onto the target, when commanded.

Flux loading on the target is controlled by having the heliostats wait at the ESD position after they receive their normal tracking coefficients. The HAC can bring them on target at a later time in whatever order desired.

The limiting factor in the time requirement for acquisition is not the

2.1.4.3.2.4 Acquisition/Stowage(cont'd)

loading time for coefficients, but the permitted slew rates.

The time required to load Acquisition and Emergency Shutdown coefficients into any heliostat is 0.2 seconds (with echo) or 86 seconds for the entire field. During acquisition the HAC will only be communicating with heliostats as they arrive at prefocus. Since their arrival times will be spaced, loading normal tracking coefficients have almost no effect on the time required for the entire procedure.

The entire acquisition procedure will be spread over 15-20 minutes.

The tilted heliostat avoids high tizimuth slew rates by moving the singularity outside the family of normal tracking curves for a heliostat.

The highest tizimuth rates occur when the mirror normal is near its maximum tiltitude. This tizimuth rate is about 2^{o}/minute corresponding to a maximum attainable tiltitude of 87^{o} (worst case). This is well within the available tizimuth slew rate of 22.3^{o}/min.

2.1.4.4 Emergency Shutdown

The purpose of the Emergency Shutdown (ESD) command is to decrease the insolation on the target to 3% of its initial value as fast as possible but in a controlled manner. This is accomplished

2.1.4.4 Emergency Shutdown (cont'd)

by giving each heliostat a set of ESD tracking coefficients in addition to the normal tracking coefficients. These ESD coefficients are determined by the HAC in a manner similar to the normal tracking coefficients except that the altitude and azimuth of the tower (as seen by the heliostat) are different from the real values. This substitution causes a heliostat beam to track a point in space off the target. Upon receiving an ESD command the heliostat substitutes the ESD coefficients for normal tracking coefficients, and moves to the ESD point.

The direction the beam moves depends upon the location of the ESD point with respect to the target. A horizontal displacement of the ESD from target center produces the best results in avoiding flux buildups during an ESD.

First, the target dimension is smallest horizontally; beams can move off target quicker. Second, the target is curved in this dimension resulting in a spreading of insolation as beams slew away from target center.

The place on the target where a "hot spot" is most likely to occur is on the target centerline as seen by the heliostats on a particular radius vector. Those heliostats are the primary cause of that flux buildup as dis-

2.1.4.4 Emergency Shutdown(cont'd)

tant heliostat beams catch up with beams from nearer heliostats. A constant "linear speed" algorithm minimizes the problem by maintaining the spatial relationships among beams as they slew off target. The constant linear speed at the target (in meters/sec) is produced by making the angular speeds of heliostats a function of distance.

The distribution of flux in the ESD mode is illustrated in Figure 2-14. Only groups of heliostats along a radius vector would focus at the same ESD point. The beams diverge beyond this point. Thus maximum fluxes are restricted to the inner airspace of the field.

Calibration - The calibration array is a square consisting of four (4) linear array segments (Fig 2-15) located below the target. During calibration, a heliostat nods its beam down across an array segment to a turnaround point, then sweeps up across the array back to the target (Fig. 2-15 b)

The calibration array is controlled by a microprocessor based Sensor Array Controller (SAC). The SAC frees the HAC from direct involvement in the calibration procedure during normal field operation. Prior to start-up of normal operation the HAC decides

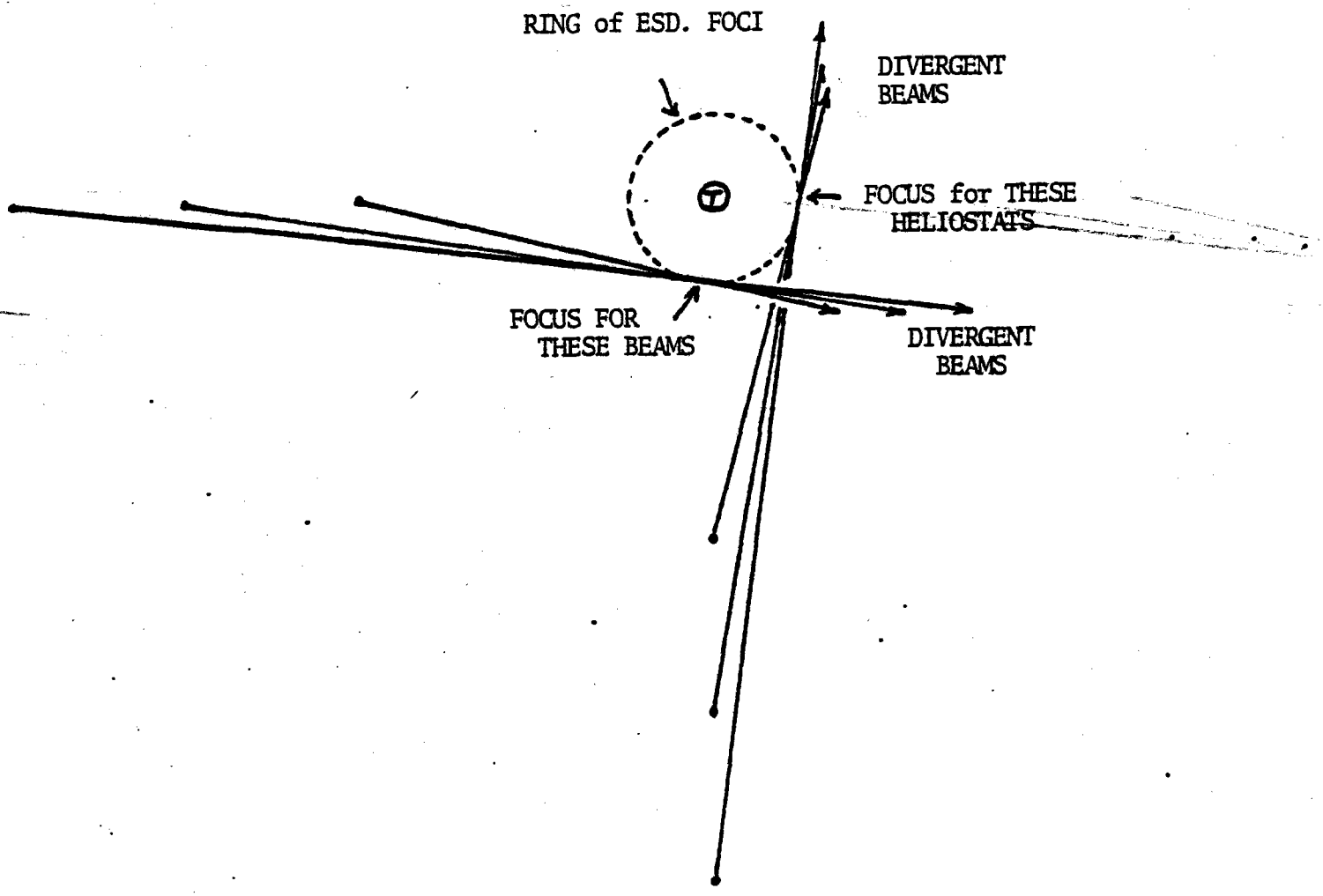

Schematic Emergency Shutdown Flux Distribution

FIGURE 2-14

Calibration (cont'd)

which heliostats are to be calibrated and calculates information the SAC needs for coordination of calibration data to be loaded into each heliostat which defines how the heliostats move during calibration.

During calibration the SAC monitors the array and saves sensor data for later analysis by the HAC. The analysis of multiple calibrations defines heliostat misalignments, pole leans, and coordinate rotations. Long term analysis determines these quantities with increased accuracy and also reveals trends in alignments.

The analysis is used to correct constants required to calculate the tracking coefficients for each heliostat, and consequently adjust tracking to compensate for these errors. When a heliostat is first brought on line, it is calibrated frequently. This break-in period is analyzed to check original alignments. After such a break-in period only periodic calibration is required.

The segments of the calibration array are independent allowing four(4) heliostats to be calibrated simultaneously. Each heliostat is calibrated once every seven (7) days. The structure of a typical array segment is shown in Figure 2-15c. The design re-

CALIBRATION ARRAY SCHEMATIC

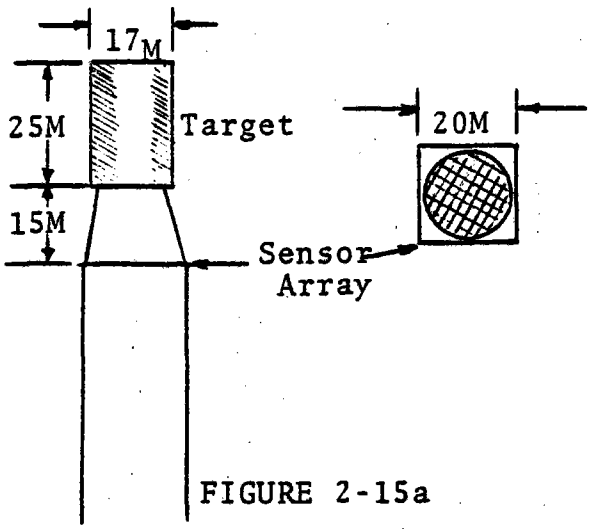

FIGURE 2-15a

CALIBRATION BEAM PATH

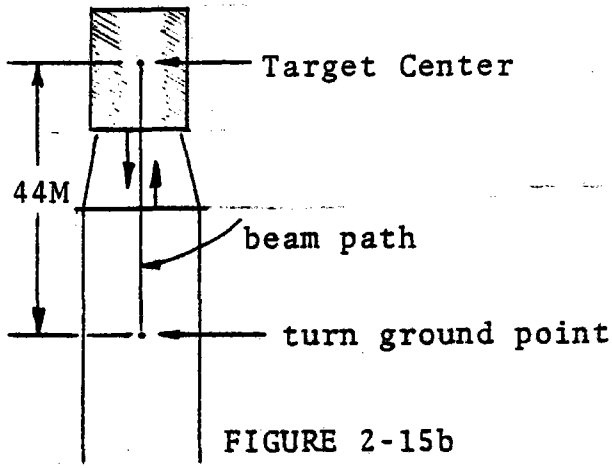

FIGURE 2-15b

SENSOR ARRAY STRUCTURE

Top View Ψ' = unrestricted field of view ≃ 80'

Side View
ϕ = Angle between horizontal and sensor centerline ≃30
Ψ = restricted field of view ≃70°

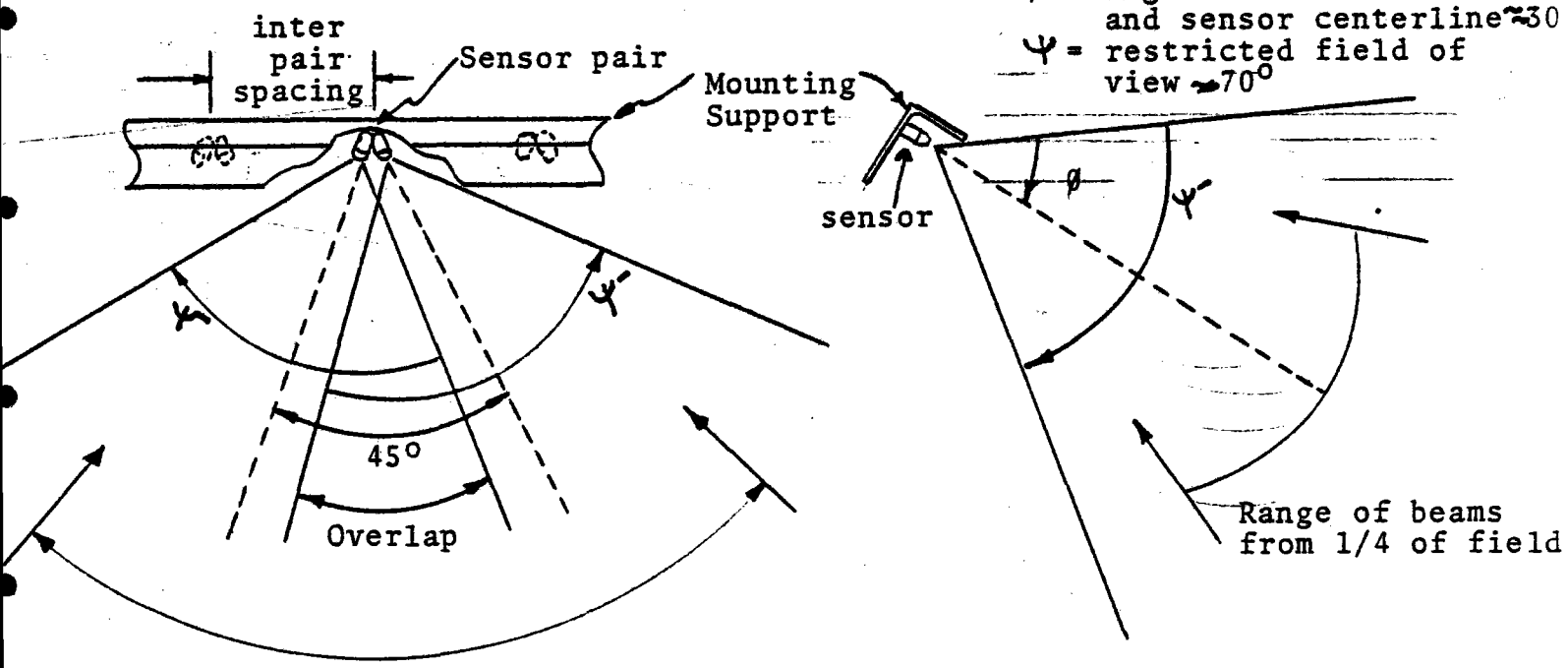

Solaramics, Inc.

FIGURE 2-15c

Calibration (cont'd)

requires sensor pairs to obtain full coverage of the part of the field assigned to each array segment.

2.1.4.6 Offset Pointing

Offsets are incorporated into normal tracking by changing the height of the target point on the receiver in calculating HC tracking coefficients.

For three (3) aimpoints on the receiver, heliostats are assigned to an aimpoint as a function of distance from the tower. This keeps the maximum flux on the target and minimizes insolation lost through tracking errors. Table Y shows these effects. The data is presented for worst case vertical beam pattern on the target (Column 2). Column 3 relates motion of a beam from target centerline before insolation is lost above or below the target, and reflects sensitivity to tracking errors.

The most distant heliostats are the most sensitive to tracking errors & are assigned to the middle focus. Thus if insolation is lost off the target from these heliostats it will be above the receiver rather than on the tower. The nearest heliostats are assigned to the lowest focus. They are the least sensitive to tracking errors, and the safest for that focus.

2.1.4.7 Local Control

Local control of any HC is accomplished by optically coupling a remote controller to the HC. Local control has first priority, and once the local mode begins all other commands from the communication bus are ignored. This feature is required for safety. The optical communication link is two-way, and enables testing of the HC, motor controls, motors, and all other functions.

The local mode is normally used for maintenance and checkout. It can also be used for emergency control.

TABLE Y

Heliostat Distance (meters)	Beam size (meters)	mr/meter	Allowed mr motion
210	14.5	2.0	10.3
310	12.8	2.0	11.9
410	12.5	1.8	11.9
510	12.8	1.6	9.8
610	13.2	1.4	8.2
710	13.9	1.2	7.0
810	14.6	1.1	6.0
910	15.3	1.0	5.0
1010	16.0	0.93	4.2
1110	16.8	0.86	3.5
1210	17.6	0.79	2.9

2.0 PRELIMINARY DESIGN

2.2 Performance

2.2.1 Beam Quality

The beam quality has been evaluated for the target specified in Para. 3.2.2.1 of Specification 001. It consists of a vertical cylinder 17 m diameter by 25m high, the center of which is elevated 250m above ground level. Field positions evaluated are those described in Para. 3.2.3.1 of the above specifications.

FIELD POSITIONS

Position	North of Tower,m	East of Tower,M
A	1200	430
B	800	860
C	-400	430

The sun was assumed to be a uniformly illuminated disc with a half angle of 4.63mr. This sun model was selected to obtain a clearer evaluation of the effects of heliostat performance variation due to structural deflections and tracking error. The performance reported would be expected to decrease with more realistic sun models considering limb darkening and atmospheric attenuation.

The target was constrained to receive energy only within 60^{o} angle of incidence from the surface normal.

The analysis was performed with the

2.2.1 Beam Quality (cont'd)

Helios computer program developed at Sandia Labs (Sand 76-0346). The heliostat parameters utilized for the evaluation were as follows:

- Each 4' X 10' facet focused to a point at the center of the target
- Pointing error of 1 mr RMS at all heliostat positions
- .5mr RMS manufacturing and construction uncertainty

DEFLECTIONS

	Heliostat Elevation 10^{o}	Heliostat Elevation 80^{o}
Gravity on panels & Structure	Elevation 2.4mr	1.2mr
	Azimuth .3 mr. max	.3mr. max
Wind (@ 12m/s)	Elevation -2.7--0.6 mr.	-0.7--1.6mr.
	Azimuth -3.1--2.0	1.3--1.7

The static and dynamic wind deflection were added to the deflections due to gravity and these were then converted to a function expressed as a constant on a sinusoid with time. The wind velocity distribution provided in Specification 001 has been simulated by a Gaussian Distribution in which the peak amplitude of the time varying function represents the wind deflection of the panel. The pointing errors & manufacturing errors were introduced by increasing the Sun Disc by the Rms. value.

2.2.1 Beam Quality(cont'd)

The Gaussian distribution dispersion of the accumulative time dependent errors was convoluted with the sun distribution to produce a broader distribution which includes both the sun and heliostat wind deflections.

The error function which was calculated from the mean squares of the above deflections and the time dependent wind deflections is expressed as:

ERROR = 1.13 + 2.10 Sin wt(milliradians)

The constant 1.13 is treated as a pointing error and the time dependent function is incorporated into the helios program as a sigma error in the Gaussian distribution.

The results of the Helios program output are presented in Fig. 2-16. Since the Helios program integrates intensity of energy received by a point grid representing the target, a range of uncertainty exists in the integration. The range of uncertainty for positions A and B is approximately ± .5% and for position C is typically ± 2%.

2.2.1.1 The Net Reflected Power

The net reflected power has been computed from the following parameters:

	SPRING	SUMMER	FALL	WINTER
Position A	8 hrs X 98.5%	12 hrs X 98.3%	8 hrs X 98.5%	6 hrs X 98.5%
Position B	8 hrs X 99.3%	12 hrs X 99.5%	8 hrs X 99.3%	6 hrs X 99.3%
Position C	8 hrs X 98.7%	12 hrs X 98.4%	8 hrs X 98.7%	6 hrs X 98.8%

Ave % Reflected Energy Rec'd
X the number of hrs. is 8.397 hrs.

2.2.1.1 The Net Reflected Power(cont'd)

1) The life cycle Reflective efficiency has been estimated to be 0.90%, with an initial as installed efficiency of 0.95.

$$\eta = .90$$

2) Insolation I_o 41. = 950 w/m^2

3) Heliostat Area A_H = 39 M^2

4) Motor Energy Reqmt. E_m = 389 Kw_T hrs/yr

NRP = 365 X (1) X (2) X (3) X (4) - (5)

NRP = 101,857 Kw_T hrs./year

2.2.2. Structure

2.2.2.1 Foundation Analysis

The pedestal is designed to be installed in a bored hole and stabilized with a dense urethane foam called "pole set". For the purpose of this analysis, the soil properties shown in Table 5-1 have been assumed as typical for site locations. The foundation design must be re-examined for specific site characteristics.

FIG.2-16 BEAM QUALITY ANALYSIS

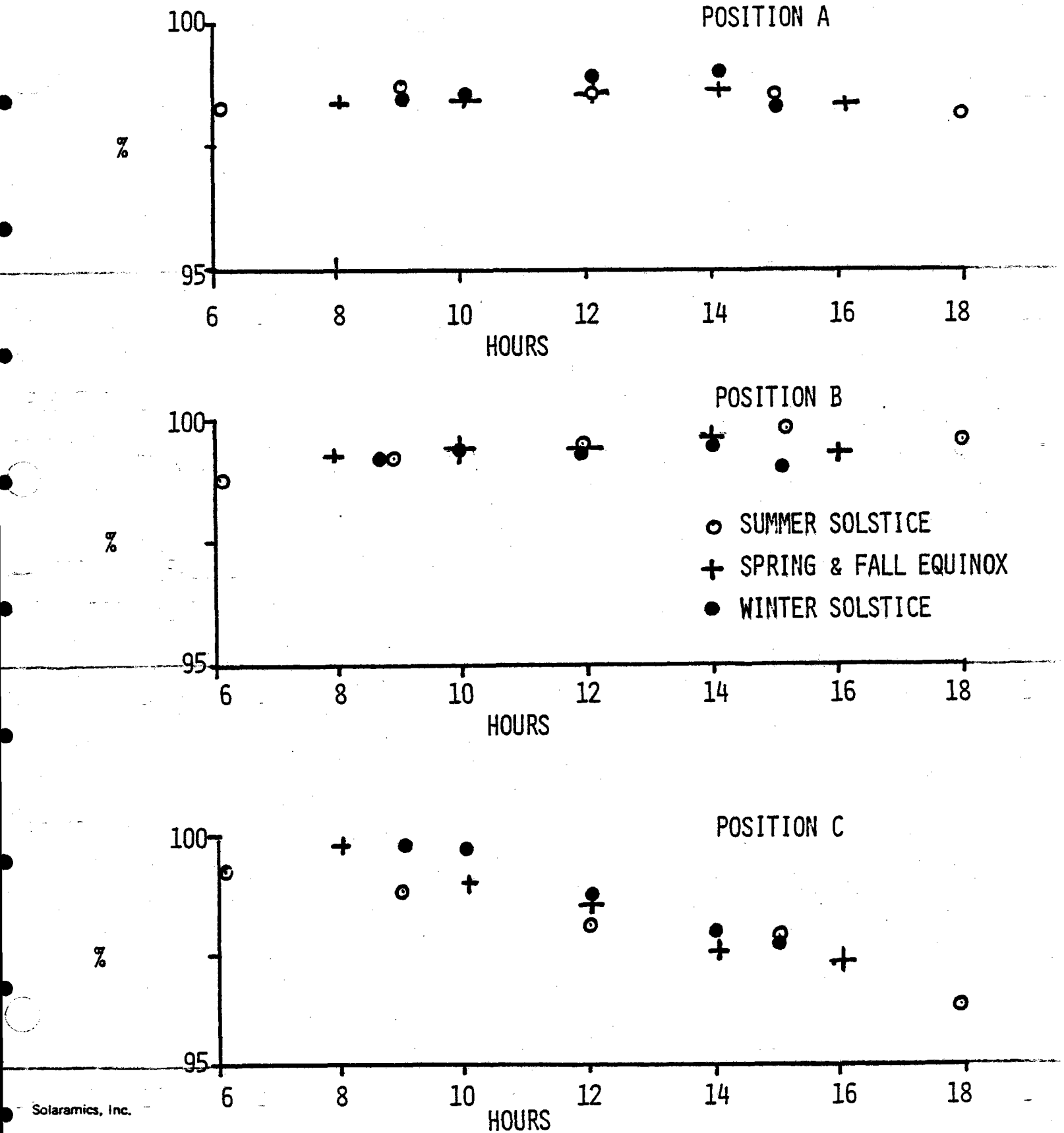

TABLE 5.1: SOIL PROPERTIES (ASSUMED)

The surface deposits of silty sand, which extend to depths of from 0.3 m to 1.5 m (1 ft to 5 ft), are only moderately firm. The sand below a depth of about 1.5 m (5 ft) is firm but contains thin layers of relatively soft silt. In general, the sand is firmer below 3 m (10ft) and layers of soft silt are not encountered.

G, Shear Modulus, and E, Secant Modulus

$$\text{Shear Modulus} = G\,\frac{B\,(h+z)}{2(1+u)} = \frac{By}{2.6}$$

$$\text{Secant Modulus} = E^* = B(h+z) = By$$

Where B = function of soil depth (see chart)
h = depth of burden
z = depth from burden
u = constant = 0.3
y = depth from surface

Soil Depth(y)		Density		B	
(m)	(ft)	(kg/m^3)	(Lb/ft^3)	(MPa/m)	(psi/ft)
0-1.5	(0.5)	1600	(100)	1.7	(75)
1.5-3.0	(5-10)	1840	(115)	2.5	(110)
3.0	10ft below	1920	(120)	3.4	(150)

At depth of 1.5 m (5ft) G = 10 MPa, (1500psi)
*E = 28 MPa (4000psi)

At depth of 3.0 m(10ft) G = 32 MPa, (4600psi)
*E = 83 MPa (12,000psi)

2.2.2.1 Foundation Analysis(cont'd)

The analysis has been performed with the aid of a computer program (COM 622) developed by Lymon C. Reese at the University of Colorado, Boulder. The program provides a solution to the differential equation for a laterally loaded pile considering the pile as a linear elastic beam and the soil reaction as a line load.

$$EI \cdot \frac{d^4y}{dX4} + P \times \frac{d^2y}{dX2} - p=0$$

where y = lateral deflection of the pile at X
x = length along the pile
EI = stiffness of the pile
P = axial load
p = soil reaction per unit length=f(x)

The loading conditions imposed on the Pedestal at the ground line are as follows:

LOAD CONDITION	BENDING MOMENT	VERTICAL FORCE	HORIZONTAL FORCE
Survival 22 m/sec	38,333 ft lbs	4400 lb	3200 lb
Operation 14 m/sec	11,500 ft lbs	4400 lb	952 lb

FIGURE 2-17 FOUNDATION ANALYSIS

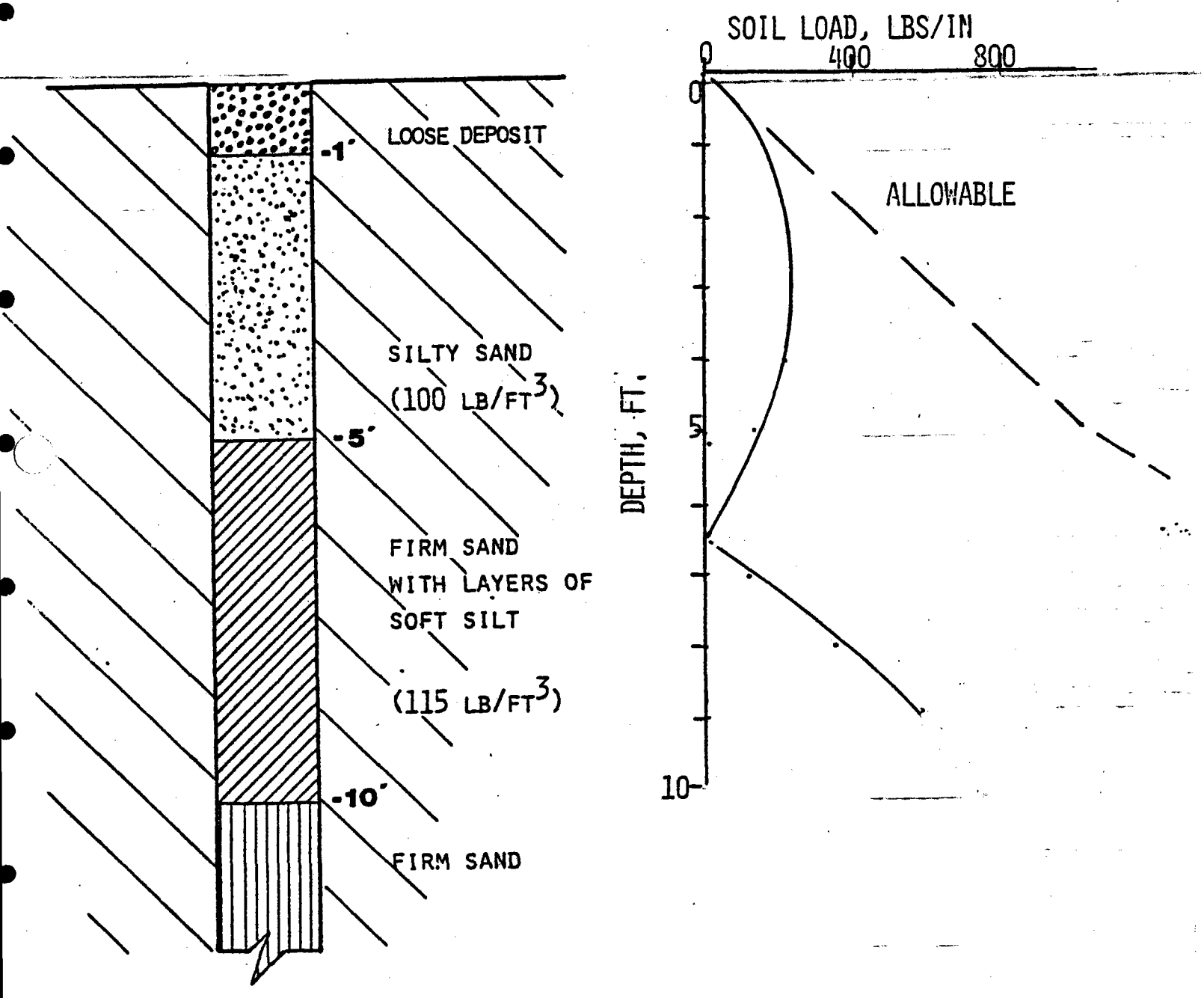

2.2.2.1 Foundation Analysis(cont'd)

The Foundation was analyzed at three (3) installation depths -9, 10, and 15 feet. The deflection and rotation at ground level determined were as follows:

INSTALLATION DEPTH	LOAD CONDITION	DEFLECTION(in)	ROTATION(mr)
9	22 m/s survival	.186	2.58
10	"	.152	2.03
15	"	.109	1.14
9	14 m/s operation	.055	.76
10	"	.049	.68
15	"	.033	.33

The soil allowable and the calculated soil pressures are shown in Fig. 2-17. Since high margins exist for all conditions, the design depth is determined by the cost effectiveness/stiffness function.

2.2.2.2 STRUCTURAL AND DYNAMIC RESPONSE

To insure the operability of the heliostat design, calculations were performed with the EASE 2 structural dynamics code to determine the panel deflections from gravitional and wind loading. To insure the survivability of the heliostat over the design-basis life, calculations were performed to determine stresses in the structural components under conditions of high winds, tornadoes, earthquakes & ice or snow loading. An analysis of the potential for structural fatigue due to prevailing wind loads was also made, considering a 30 yr. system life.

Two orientations of the heliostat panels were considered in each analysis: the near-horizontal orientation with the panels tilted 10^{o} from the horizontal plane, and the near-vertical orientation with the panels tilted 80^{o} from the horizontal plane(see Figures 2-18a & 2-18b). The near-horizontal orientation was modeled two (2) ways, with the elevation linkage tilted down to represent an operating condition and with the linkage tilted up to represent a stowed condition, as applicable to operability and survivability analyses respectively.

Finite Element Model

The EASE2 model used for the final structural analyses included 124 lumped mass nodes connected by beam and shell elements. Both the elevation and azimuthal linkages were modeled in detail. The dynamic response of the structure was determined by the superposition of the lowest ten eigenmodes.

THIS FRAME DISPLAYS BEAM AND SHELL ELEMENTS
HELIOSTAT
ORIENTATION AT 80 DECREES FROM HORIZONTAL
(FRAME NUMBER 1 VIEW NUMBER 1
RUN DATE 04/28/78
EHC/CSI/EASE2/E2PLOT
UNDEFORMED GEOMETRY

FIGURE 2-18a

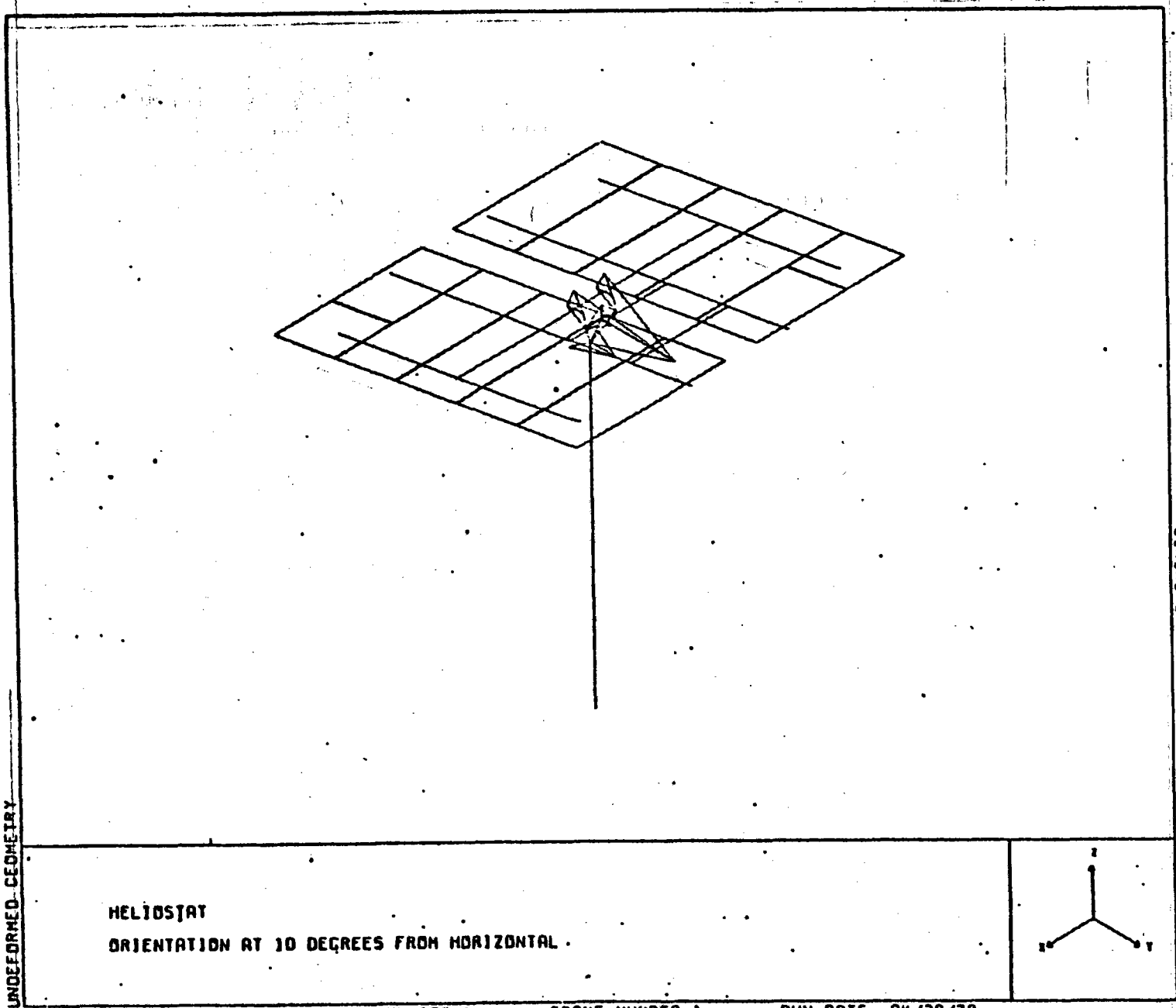
UNDEFORMED GEOMETRY
HELIOSTAT
ORIENTATION AT 10 DEGREES FROM HORIZONTAL.
Z
X
Y
EAC/CSI/EASE2/E2PLOT
VIEW NUMBER 1
FRAME NUMBER 1
RUN DATE 04/28/78
THIS FRAME DISPLAYS BEAM AND SHELL ELEMENTS

FIGURE 2-18b

Gravitational Deflection

Calculations were run with EASE2 to determine the static structural deflections of the panels due to gravitational loading. For the near-horizontal orientation, the outer edges of the panels deflect about 2 milliradians, with a mean panel deflection of about 1.2 milliradians. For the near-vertical orientation the panel configuration tilts about 1 milliradian due to gravity.

Wind-Deflections-Vortex Shedding

Vortex shedding is considered the most likely source of excessive oscillation under wind conditions. At a critical angle of attack with respect to the wind flow separation will occur, creating alternating vortices on the low pressure leeward, surface of the heliostat panel array. The vortex shedding condition needs further investigation, with wind tunnel model testing, to establish the critical separation angles. Typically, the critical angle of attack for flat plates is reported to vary between 30^{o} and 40^{o}. Variation of the critical angle is expected to be significantly affected by the presence of the support frame, especially when on the leeward side, hence the need for wind tunnel testing.

Vortex shedding is not predicted to occur in the stowed position, and the survival calculations in stowage have not included this condition.

The Vortex Shedding Frequency is estimated by the formula:

$$f = \frac{St.\ V}{L \sin \alpha}$$

Wind-Deflections-Vortex Shedding (cont'd)

WHERE St = Strouhal Number - .15 for flat plates
V = Wind Velocity
L = Length in the windward direction
α = Angle of attack

An angle of attack of 10^{o} was assumed. For wind deflection analysis to determine the panel deflections for use in the beam quality analysis, the analysis was performed for the near horizontal position and the near vertical position. The panel loading criteria is shown in Fig. 2-19 and the deflection modes are illustrated graphically in Figures 2-20a -- 2-20b (the deflections are exagerated in the plot for clarity).

Maximum Panel Deflections from the Panel Array Due to Wind Loads (X-Axis Parallel to Cross-bar, Y-Axis Parallel to Panel Supports)

Near-Horizontal Orientation		Near-Vertical Orientation	
Deflection about X-Axis (mrad)	Deflection about X-Axis (mrad)	Deflection about X-Axis (mrad)	Deflection about X-Axis (mrad)
1.7 to 4.0	1.6 to 2.0	-1.5 to 1.8	-3.4 to 1.7

Survival Conditions

Two conditions were considered for structural survivability based on the RFP specifications; in any orientation the structure must withstand a 22 m/sec wind prior to stowage, including an oscillating wind load due to vortex shedding; in the horizontal orientation, representing a stowed condition, the structure must withstand the static load from a 40 m/sec wind. Maximum stresses calculated for the fluctuating load on the near-vertical

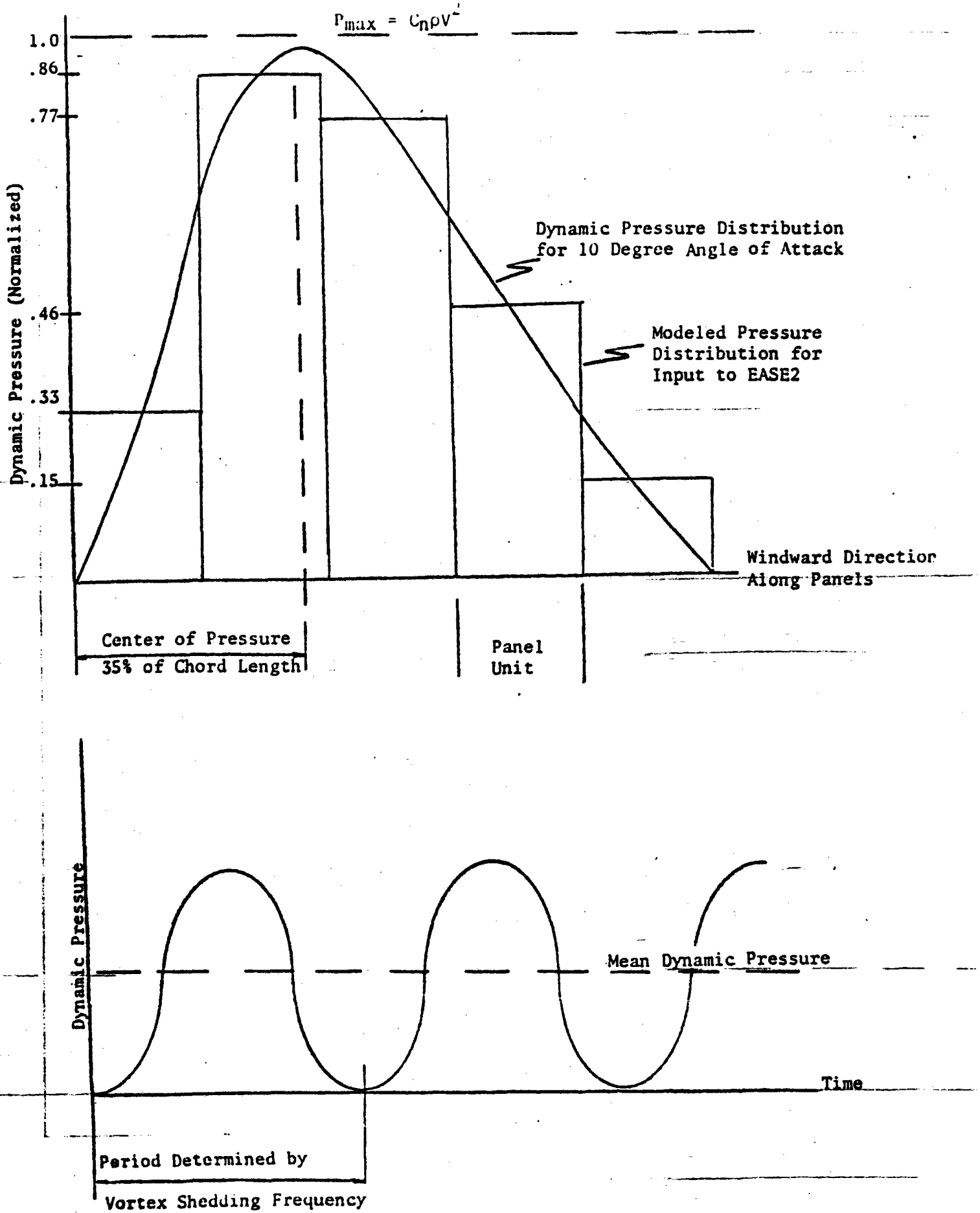

FIGURE 2-19 WIND LOADING MODEL FOR DYNAMIC DEFLECTIONS FROM VORTEX SHEDDIN

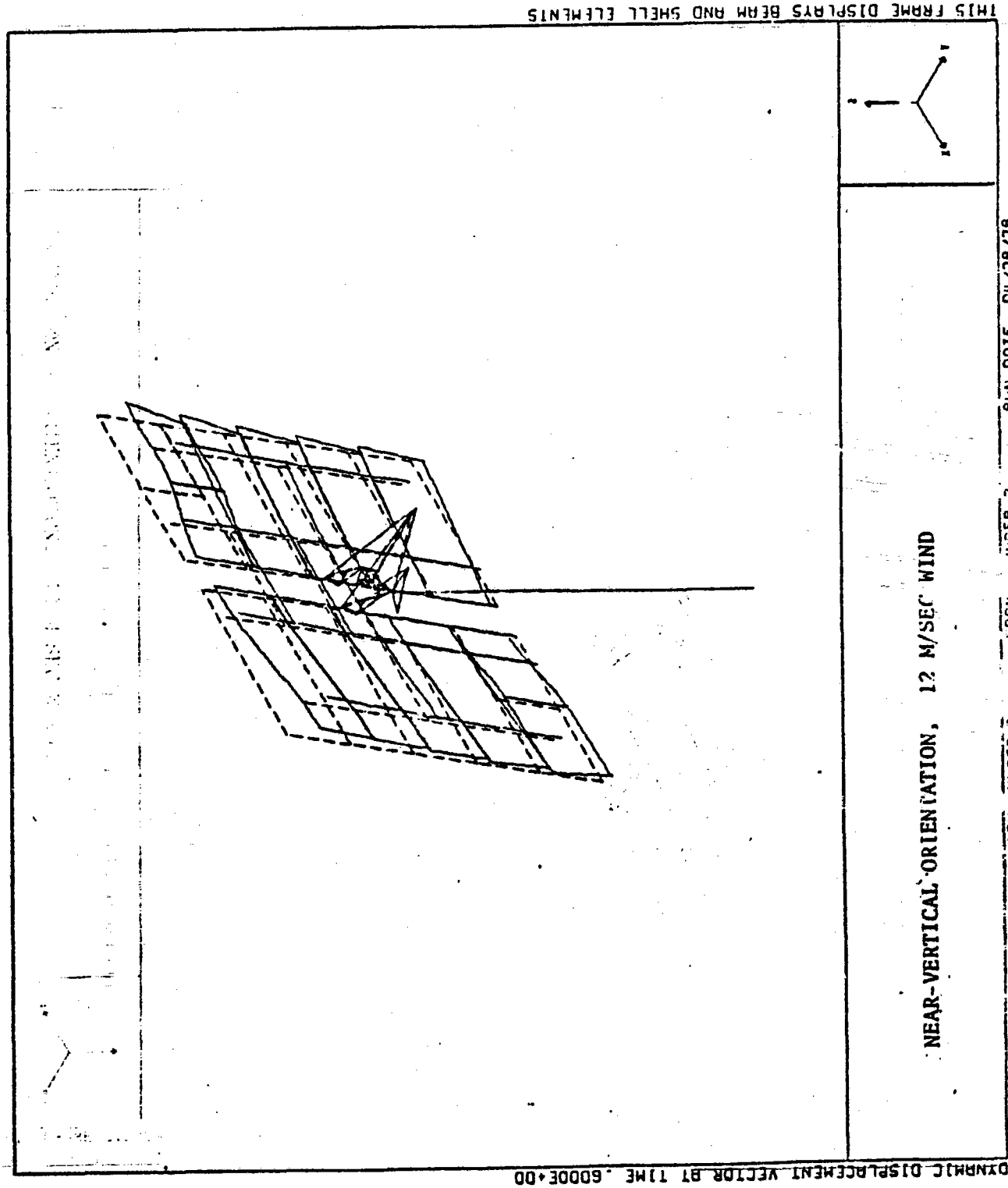

FIG. 2-20a

DYNAMIC DEFLECTION OF HELIOSTAT MODEL

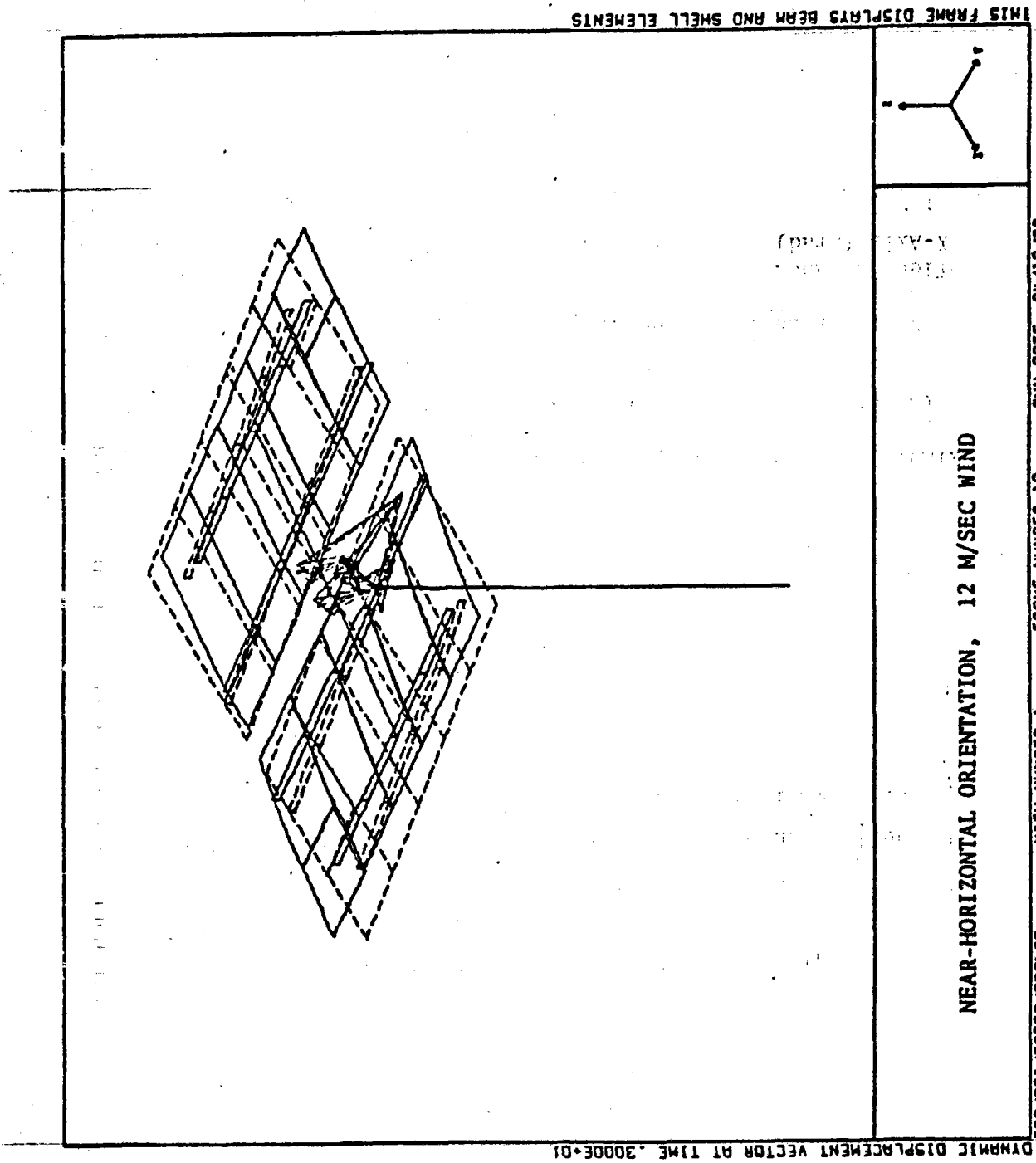

FIGURE 2-20b

DYNAMIC DEFLECTION OF HELIOSTAT MODEL

Survival Conditions(cont'd)

orientation in a 22 m/sec wind were 2,400 psi tension in the pedestal, 13,000 psi compression in the azimuthal linkage threaded thrust bar, and 30 psi compression in the foam glass panels. All stresses are below the yield point of the particular material. Maximum stresses calculated for the stowed condition in a 40 m/sec wind were 120 psi shear in the pedestal, 10,000 psi compression in the elevation thrust bar, 8,300 psi tension in the inner panel supports and 20 psi tension in the foam glass panels. All stresses are well below the yield point of the particular material.

Dust Devils

The heliostat was found to be capable of survival in the dust devil environment. The condition considered critical is represented by a rotational wind of 18 m/s, located with its centroid at the pedestal centerline, the array positioned in a vertical orientation. The wind profile was conservatively considered uniform, reversing at the core. The rotating moment of 142,000 in lbs. was calculated for a C_D of 1.2. This produces a load of 20,000 lbs. in the azimuth actuator which is within its capability.

Ice and Snow

The critical loading condition is generated by an ice pack 2 inches thick on the horizontal position. This generates a loading of ten(10) lbs./ft^2 on the panel which when coupled with the panel weight of 4#/ft^2, produces a maximum bending stress of 50 psi in the panel, which is 20% of the ultimate strength of the panel.

2.2.3 Control Mechanism

An analysis of control and tracking vector motions required for the specific field geometry and latitude range discloses that 180° of azimuth drive is more than adequate to provide all tracking functions if the azimuth axis is inclined 20° from normal. The inclination is specifically advantageous in the south field and for the inner circle of heliostats at the tower base. Inclination is not required in the north field; however, it is provided to achieve interchangeability objectives and does not introduce any undesirable performance. It is significant to note that with the inclined axis system, no control singularities occur! An additional 3° of axis inclination is provided for installation tolerance reduction of azimuth slew rate, and potential site grade.

A number of locations exhibiting singularity have been examined and are presented in figures 2.4 through 2.8. The tracking motions required for the normal azimuth-elevation drive are shown on the left, and the tracking motions for the proposed modified system on the right which is identified as tizimuth & tiltitude for clarity. The field has also been adequately examined for the modified system to assure performance and to verify that the singularity was not merely shifted to another location. The tilted heliostat avoids high tizimuth slew rates by moving the singularity

2.2.3 Control Mechanism (cont'd)

outside the family of normal tracking curves for a heliostat.

The highest rates occur when the mirror normal is near its maximum tiltitude. This tizimuth rate is about 2^{o}/minute corresponding to a maximum attainable tiltitude of 87^{o} (worst case). This is well within the available tizimuth slew rate of 22.3^{o}/minute. A typical case is illustrated in Figure 2-21.

FIGURE 2-21 "WORST CASE" TRACKING ANALYSIS

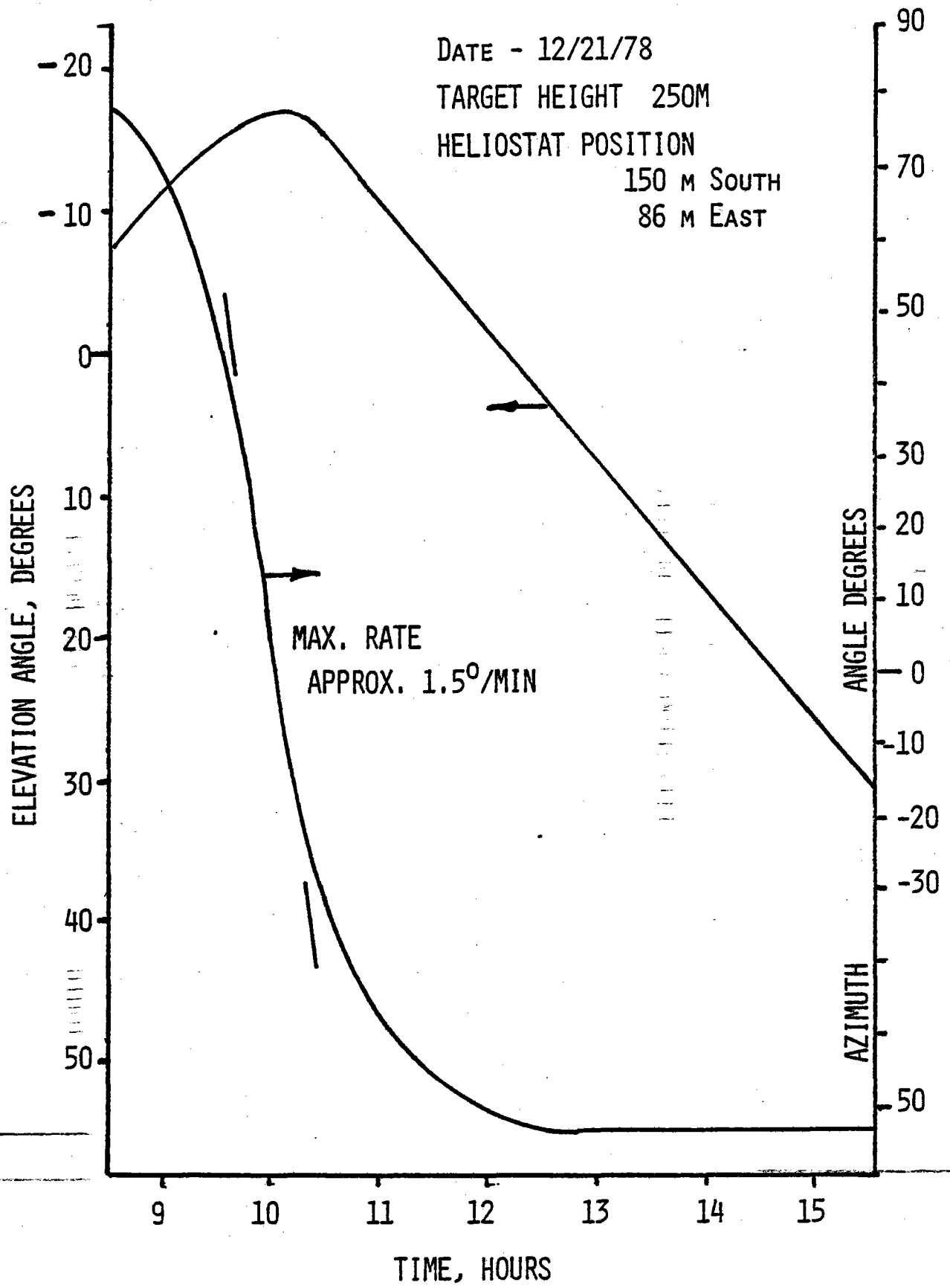

3.0 PRODUCTION PROCESSES

The manufacturing plan described herein represents the concept for high production and is based upon utilization of mass production techniques. Concentration of much of the effort is planned for production facilities at centralized locations. Maximum use of automated equipment and of special handling devices is planned to minimize labor costs.

Manufacturing operations will be considered at three (3) levels:

1) component and/or detail parts fabrication such as mirror module substrate or actuator link fittings or steel support structure.

2) subassembly and assembly such as mirror module assembly, and bonding or welding and painting of steel support structure, and fitting and checkout of linkage & drive mechanisms.

3) on-site final assembly of those structures too large or delicate for cost effective transport except as details or subassemblies.

The logistics or material flow with adequate reserves to accommodate emergencies such as natural disasters and strikes or transport problems are recognized as complex problems. They have not been addressed at this point. However, the criticality of storage and staging of inflowing materials is recognized as an essential ingredient to successful quantity production and to cost control.

The manufacturing concept is presented here but no attempt has been made to formalize the selection of material sources and make or buy potentials. Commercially available items such as actuators and motors will in all probability be purchased. Because of the impact on potential vendors or

the quantities involved in producing 25,000 or more heliostats annually, multiple sources are indicated and recommended.

In most cases major components will require development of facilities dedicated to satisfying SOLARAMICS requirements.

The facility and rate requirement, described herein are for a baseline quantity production of 25,000 heliostats per year. Higher production rates can be attained by expanding facilities accordingly and will not affect cost effectiveness.

3.1.1 Microglass Mirror Manufacturing Process (Fig. 3-1)

The concept advanced for the production of microglass (.010 in. thick) embodies a continuous down draw of molten glass from a thermally controlled bushing in the fore hearth of a glass furnace. The glass would be further conditioned as it is drawn over a temperature controlled platinum surface. The technique provides flow control and thermal conditioning. CO_2 Laser trimming of the edge beads will occur shortly thereafter at a temperature at which the edge is fused without reformation of an edge bead. The glass is then passed through a stannous chloride surface to achieve an electrically conductive surface. The glass ribbon will then be slowly cooled to avoid thermal stresses. At the end of this process the glass ribbon (24 in. width) would be stored as a large Roll to maximize the advantages of continuous processing.

CONTINUOUS MICROGLASS REFLECTOR PROCESS

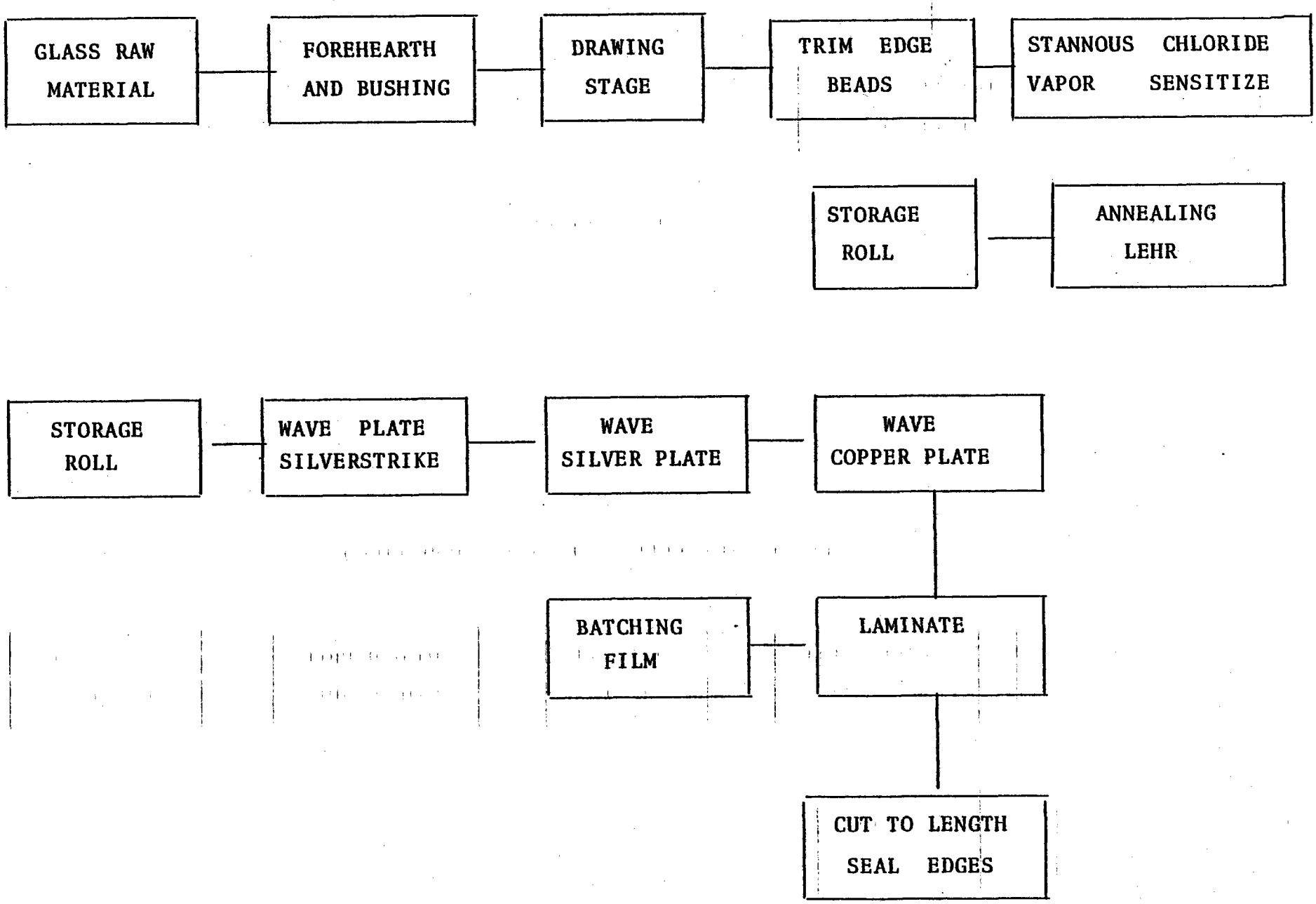

FIGURE 3-1

The glass ribbon would then be fed back off the roll through a series of wave plating stations which would deposit a silver strike, a silver deposit, and a copper deposit.

The silvered microglass will then be bonded to a thin carrier material to improve handling and impact resistance characteristic of the very thin glass sheet. The carrier materials currently considered include mylar films, urea impregnated paper laminates, and steel foil. The lamination temperature can be controlled to assure compressive stresses in the glass layer of the laminate.

The advantages to be accrued from this process include Cost Reduction by virtue of the continuous nature of the process and very high reflectivity achievable with very thin glass.

3.1.2 Glass Foam Manufacturing Process (Fig. 3-2 & 3-3)

The primary support base for the microglass mirror is a "foamed" glass panel, 2" X 4' X 10', weighing 170 lbs. Initially, waste scrapped glass is processed in a crushing mill at a rate exceeding 80 tons daily. The coarse crushed glass is then washed and passed through a pulverizer and air classifier to provide the desired mesh size and uniformity. It is then stored in tanks sized to insure a continuously available supply. The proprietary foaming agent is pulverized and classified in a similar manner. The glass and foaming agent are then precisely measured and blended into a homogenous mix-

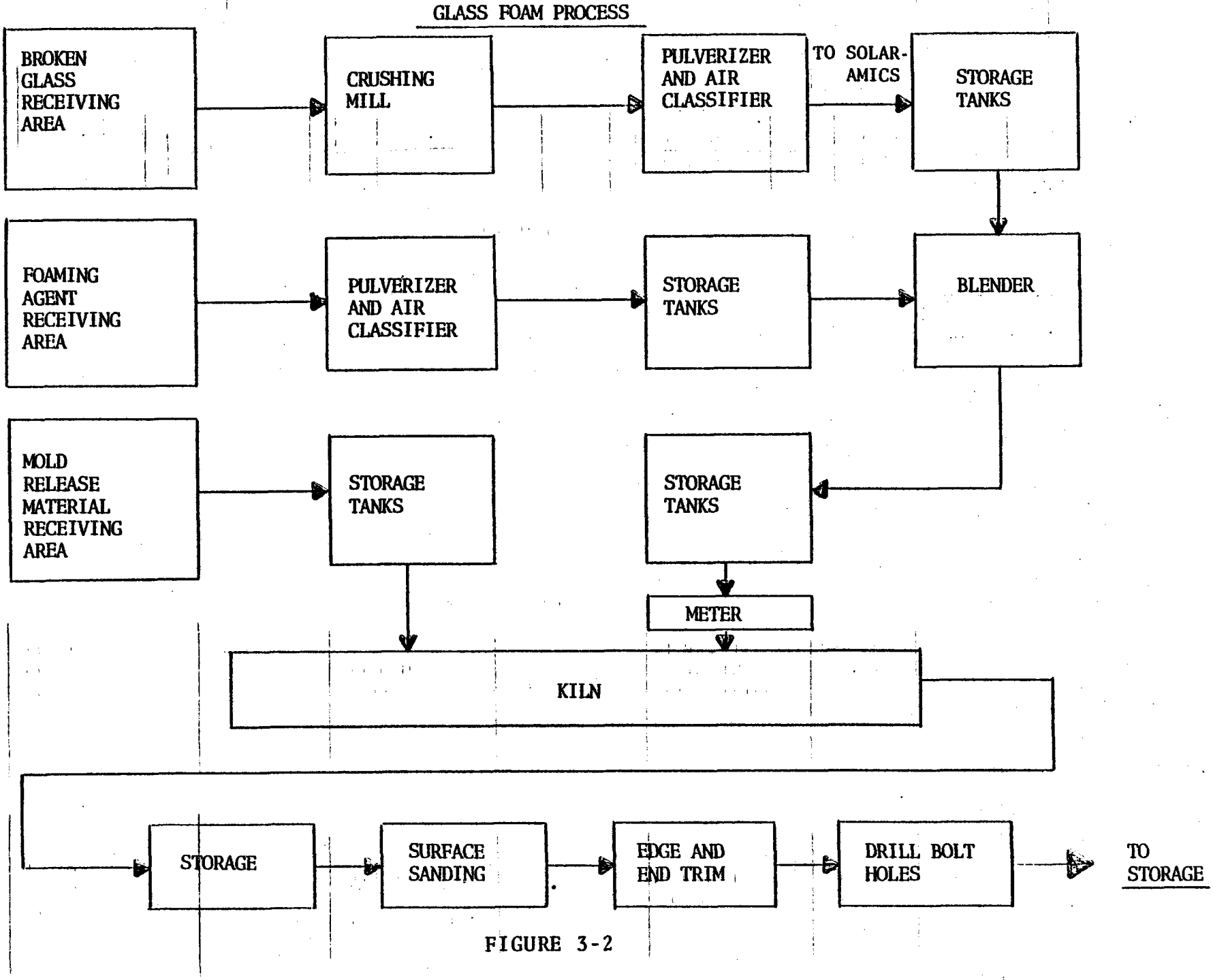
GLASS FOAM PROCESS
BROKEN GLASS RECEIVING AREA
CRUSHING MILL
PULVERIZER AND AIR CLASSIFIER
TO SOLAR-AMICS
STORAGE TANKS
FOAMING AGENT RECEIVING AREA
PULVERIZER AND AIR CLASSIFIER
STORAGE TANKS
BLENDER
MOLD RELEASE MATERIAL RECEIVING AREA
STORAGE TANKS
STORAGE TANKS
METER
KILN
STORAGE
SURFACE SANDING
EDGE AND END TRIM
DRILL BOLT HOLES
TO STORAGE

FIGURE 3-2

GLASS FOAM PROCESS

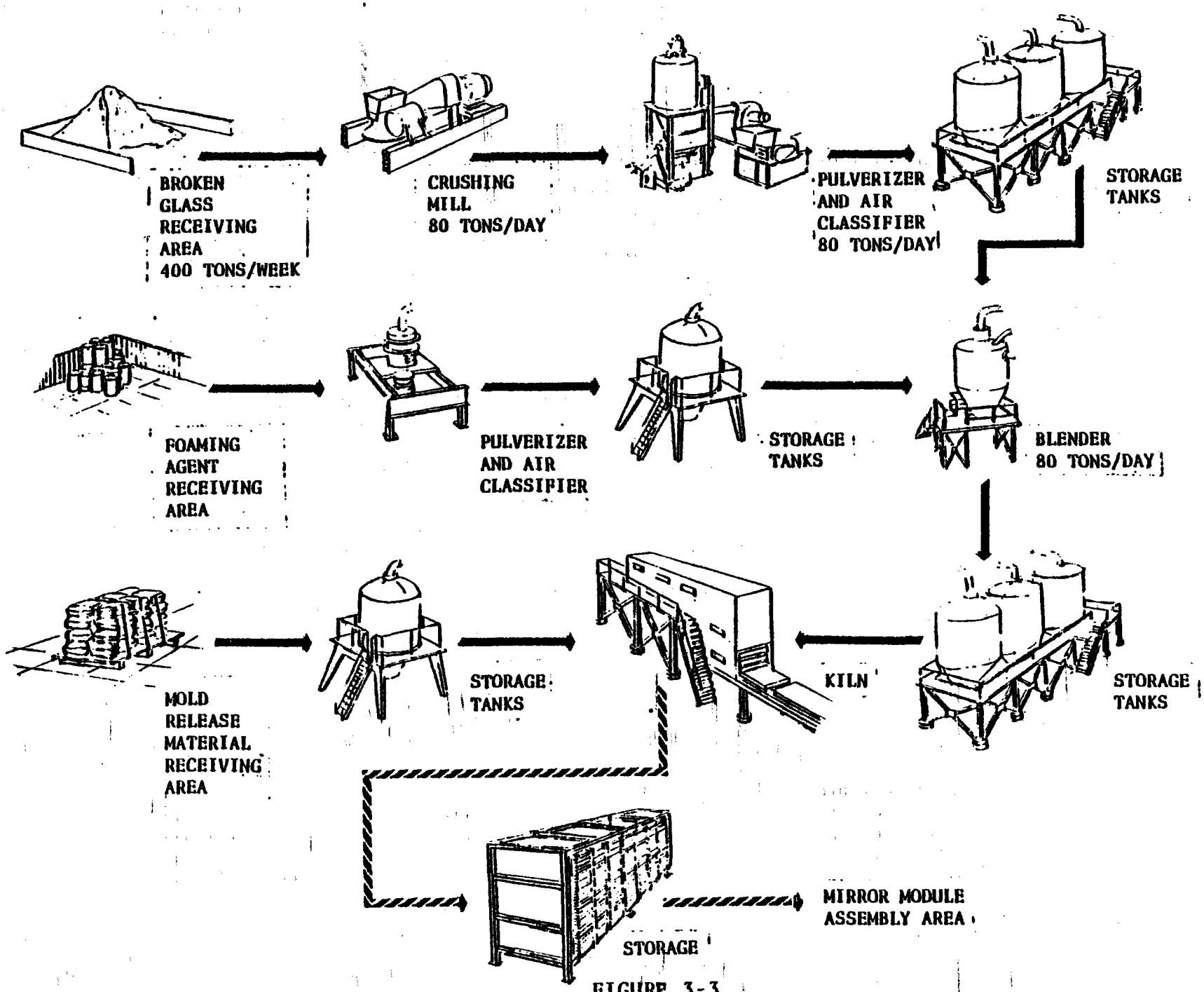

FIGURE 3-3

ture and again stored. Stringent quality measures are a prime requisite at all stages of the process. The foaming time process that provides the necessary rate of 765 panels daily to support a 25,000 heliostat annual production. The rough panels are then stored and transferred as required to the sanding & finishing line to be trimmed and drilled to their finished configuration. They are then palletized for shipment to the mirror module assembly area.

3.1.3 Mirror Module Assembly(Figs. 3-4, 3-5)

The mirror module assembly will consist of a series of work stations at which assembly and bonding will take place. These stations will be flat platens on which two(2) 24" X 10' long strips of microglass mirror will be vacuum chucked face down. Specially designed automatic spray equipment will be utilized to apply an adhesive coating to the back of the mirrors. The required production rate is 60 modules per hour during two(2) shifts five(5) days a week. The predrilled and trimmed foam glass panels will be transferred by conveyor from the storage area to the assembly area. En route, semi-automatic stations will be established for the insertion and potting of the elevator bolts used to attach the mirror module mounting brackets. Adhesive will be applied between the bracket and foam glass panel to guarantee proper load distribution. Urethane compounds will be used for all bonding and adhesive applications to insure chemical compatability. The attach brackets will be fabricated using conventional high production techniques. The tooling concept includes the use of pre-slit coil stock fed through straightening rolls into a

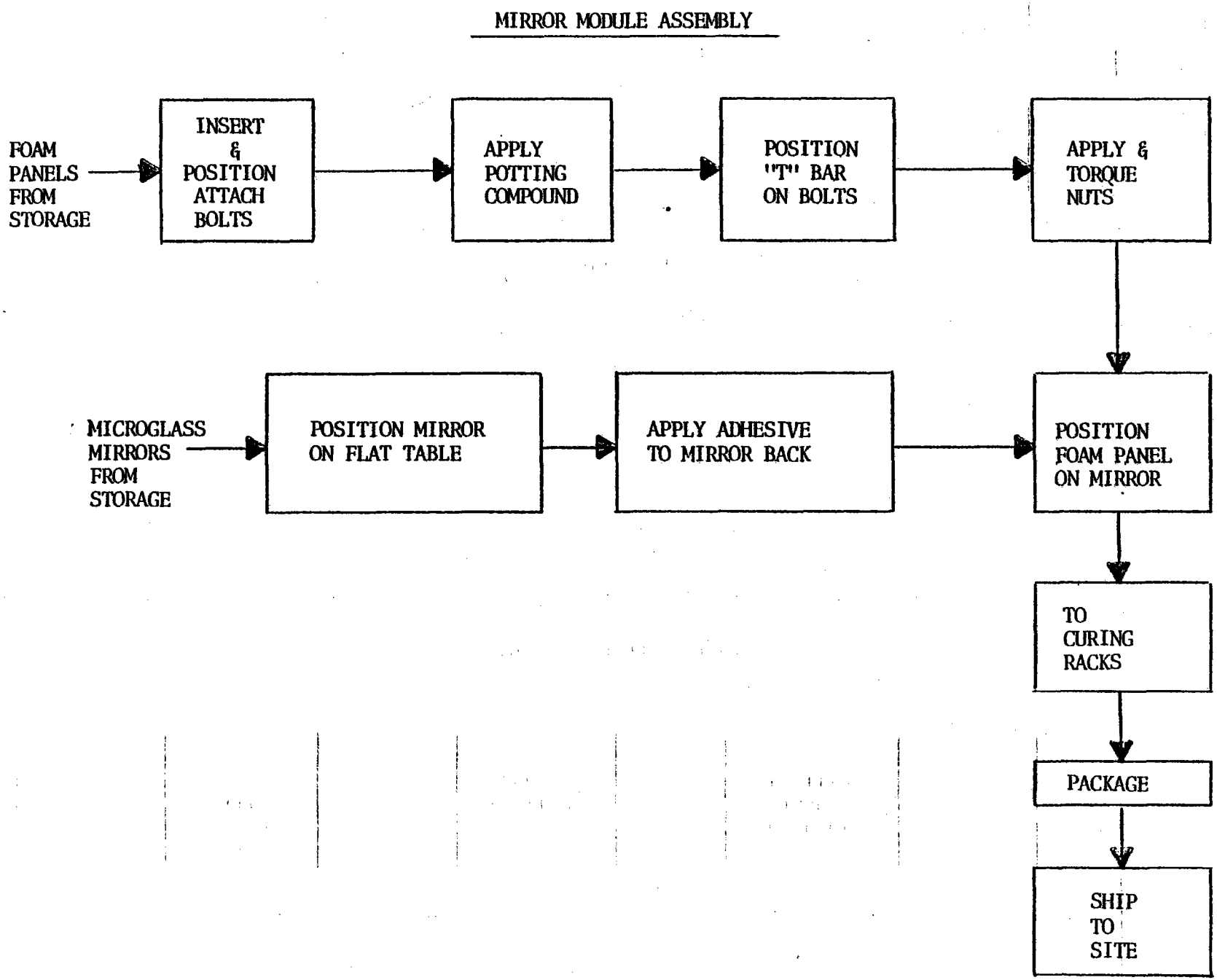
MIRROR MODULE ASSEMBLY
FOAM PANELS FROM STORAGE
INSERT & POSITION ATTACH BOLTS
APPLY POTTING COMPOUND
POSITION "T" BAR ON BOLTS
APPLY & TORQUE NUTS
MICROGLASS MIRRORS FROM STORAGE
POSITION MIRROR ON FLAT TABLE
APPLY ADHESIVE TO MIRROR BACK
POSITION FOAM PANEL ON MIRROR
TO CURING RACKS
PACKAGE
SHIP TO SITE

FIGURE 3-4

MIRROR MODULE ASSEMBLY

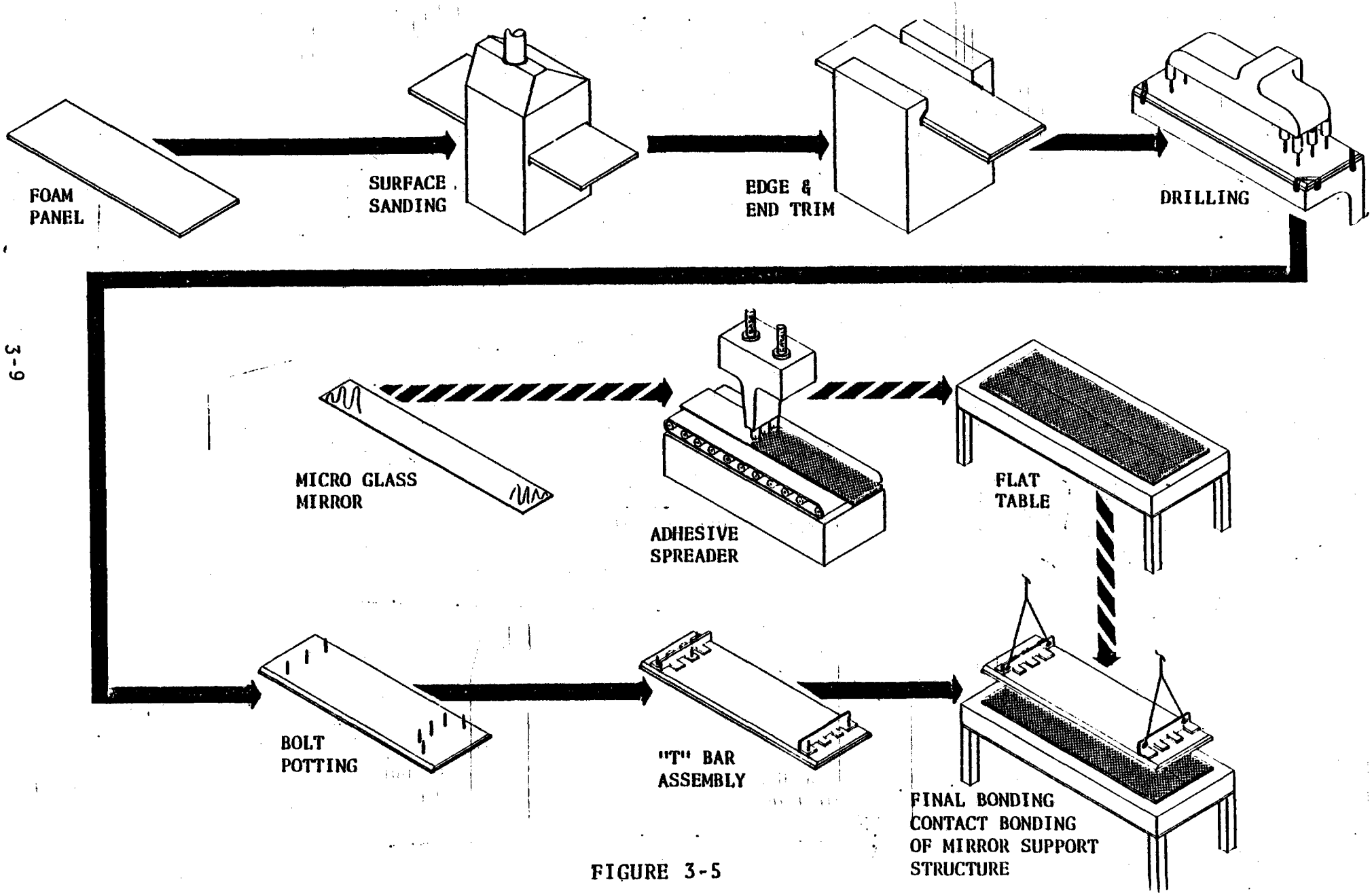

FIGURE 3-5

progressive die in a high speed automatic press, in order to meet the production rate of 2,000 units per day needed for modules. The formed brackets will be cleaned and phosphate coated on an automatic line prior to electrostatic painting in a continuous process through the drying oven.

After the brackets are bolted to the foam glass panels an air balance lift will be used to position the foam assembly onto the microglass mirror already positioned in the bonding fixture and coated with a quick curing adhesive. As a final operation, the edges of the facet assembly will be coated with sealant to seal the edges of the assembly.

After cure, the assembled mirror module will be prepared for shipment to the on-site assembly plant as described in the transportation plan.

3.2 Heliostat Support Structure Fabrication & Assembly

3.2.1 Pedestal Manufacturing Process(Fig. 3-6)

The pedestal on which the heliostat is mounted will be a 21' long ceramic pole manufactured utilizing a batch firing process and de-airing pug mill. The basic material was developed by the SOLARAMICS' parent organization (ECP, INC.), for use as a power pole for the public utilities. Its primary advantages are extremely long life with zero maintenance at a very low cost. The basic raw materials are waste glass and fly ash from coal burned by the

PEDESTAL FABRICATION
(Ceramic Material)

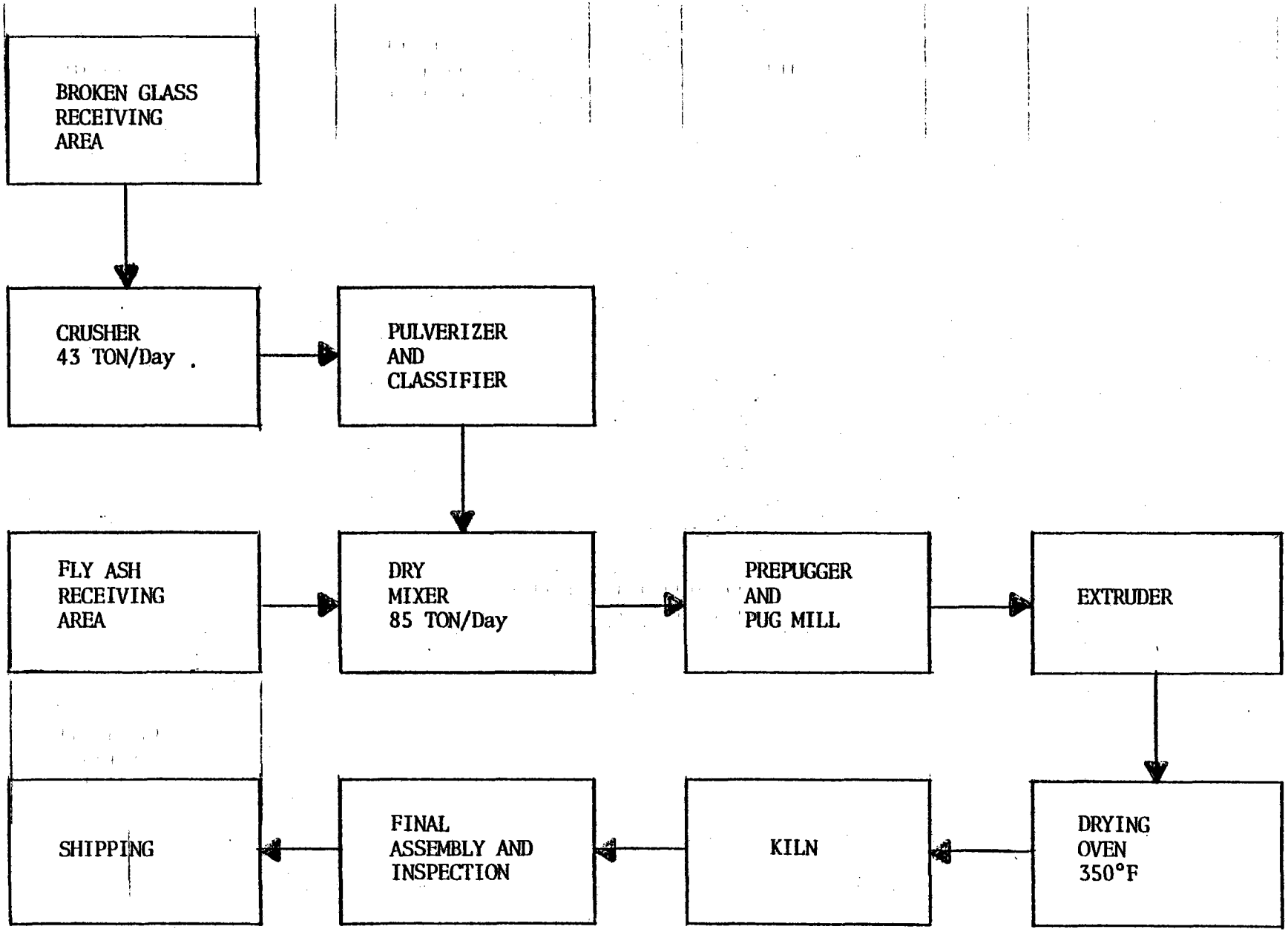

FIGURE 3-6

utilities. The glass will be crushed, pulverized and dry mixed with the fly ash at a rate exceeding 85 tons daily. The mixture then will be processed through a pre-pugger and pug mill and extruded into the desired size and shape and trimmed to length while still in the uncured stage. The 'green' pole is baked in a 350° drying oven and then fired at elevated temperatures into a true ceramic with good strength and stiffness.

The final operations are assembly, locating, and potting of the slant base for the trunnion mount. The 21' long, 2,500 lb. pedestal will then be shipped to the heliostat site as described in the transportation plan.

3.2.2 King Pin and Base Plate Fabrication & Assembly Process

The King Pin assembly will consist of a torch cut base plate welded to a precut bar and then machined on a numerical controlled lathe. (Required rate is 6 per hr during (2) two shifts, (5) five days). This rugged design will permit ultra high speed machining using ceramic cutters to reduce costs. The bolt circle will be drilled with a multiple spindle drill using carbide tipped drills guided by a drill jig. The base mount for the King Pin will be made from 5 sections of 1/2" steel plate plasma torch cut to shape and metallic inert gas welded. The six studs which provide the attachment and adjustment for the King Pin will be inertia welded onto the slant face in bolt circle that matches the King Pin base.

Corrosion protection will be provided by the same phosphate coating and electrostatic spray described in 3.1. The slant base will be bonded to the pedestal at the manufacturing site.

3.2.3 Trunnion Fabrication and Assembly

The modular iron castings required will be machined on an automatic transfer line designed specifically for this operation, at a rate exceeding 100 per day for this 150 lb. unit. Machining will be limited to boring out the bearing races for the king pin and milling and drilling the attach points for the azimuth control & mirror module support frame and facing the target bosses for precision alignment of the heliostats. Bearings will be installed at the factory after masking and electrostatic painting of the machined trunnion. The king pin and trunnion will be assembled at the main plant in order to protect the bearings and seals and shipped as a unit to the on-site assembly area.

3.2.4 Frame Fabrication and Assembly

Each half of the frame will be manufactured using conventional "Steel Fabrication" techniques.

39' X 120" sheets of 10 gauge hot rolled and pickled steel will be sheared into a pair of 19-1/2 X 9" X 120" tapered blanks. These blanks will be transferred to a large punch press in which the developed detail for mating to the torque tube and all of the necessary notches and

holes will be blanked. Forming of the left and right sections will be done in four strokes each of a conventional press brake. This cost effective design precludes any requirement for special equipment for this operation. The torque tube, manufactured from standard schedule 5 pipe will be in two sections approximately 9' ft. long. The hinge brackets will be plasma arc cut from plate steel using a multiple pantagraph method. The components of each frame half will be assembled in a fixture & welded with wire fed metallic inert gas guns for maximum strength at minimum cost.

After welding, the frames will be primed & painted for maximum corrosion resistance. The in board ends will be masked and protected for field site welding. The welded and primed frame assemblies will be trucked to the field site factory by special transport as described in the transportation plan.

3.3 Heliostat Drive System Fabrication & Assembly

3.3.1 Actuators

The actuators will be purchased items modified to accept the SOLARAMICS motor mounting & attach fitting requirements.

3.3.2 Actuator Links

The links for the elevation & azimuth drive systems will be fabricated by welding end fittings to heavy wall mechanical tubing. Multiple usage of component parts will reduce costs. The end fittings will be machined from closed die steel forgings whenever it is the most economical method.

Automatic methods will be used to weld the end fittings to the tubes. Low friction bearings will be installed in the rotating linkage joints. The completed link assemblies will be shipped to the site, in kits, for installation.

3.3.3 Motors and Encoders

The motor assemblies will be purchased complete. They are planned as "off the shelf" gear reduction drive units selected for dependability and low cost. The encoders will be purchased to meet the design parameters described in Section 2.2.5--Assembly and checkout will be performed at the intermediate site and both the encoder and motors will be kitted and shipped for on-site assembly.

3.3.4 Mfg. Process/Heliostat Control Board(Fig. 3-7)

The simplicity of the microprocessor-based heliostat control board eases the manufacturing & testing processes.

The specification of components is a key item for this application since reliability has been shown to be of paramount importance. Specification of each component shall be required on the basis of cost effectiveness, plus negotiated phases with component manufacturers.

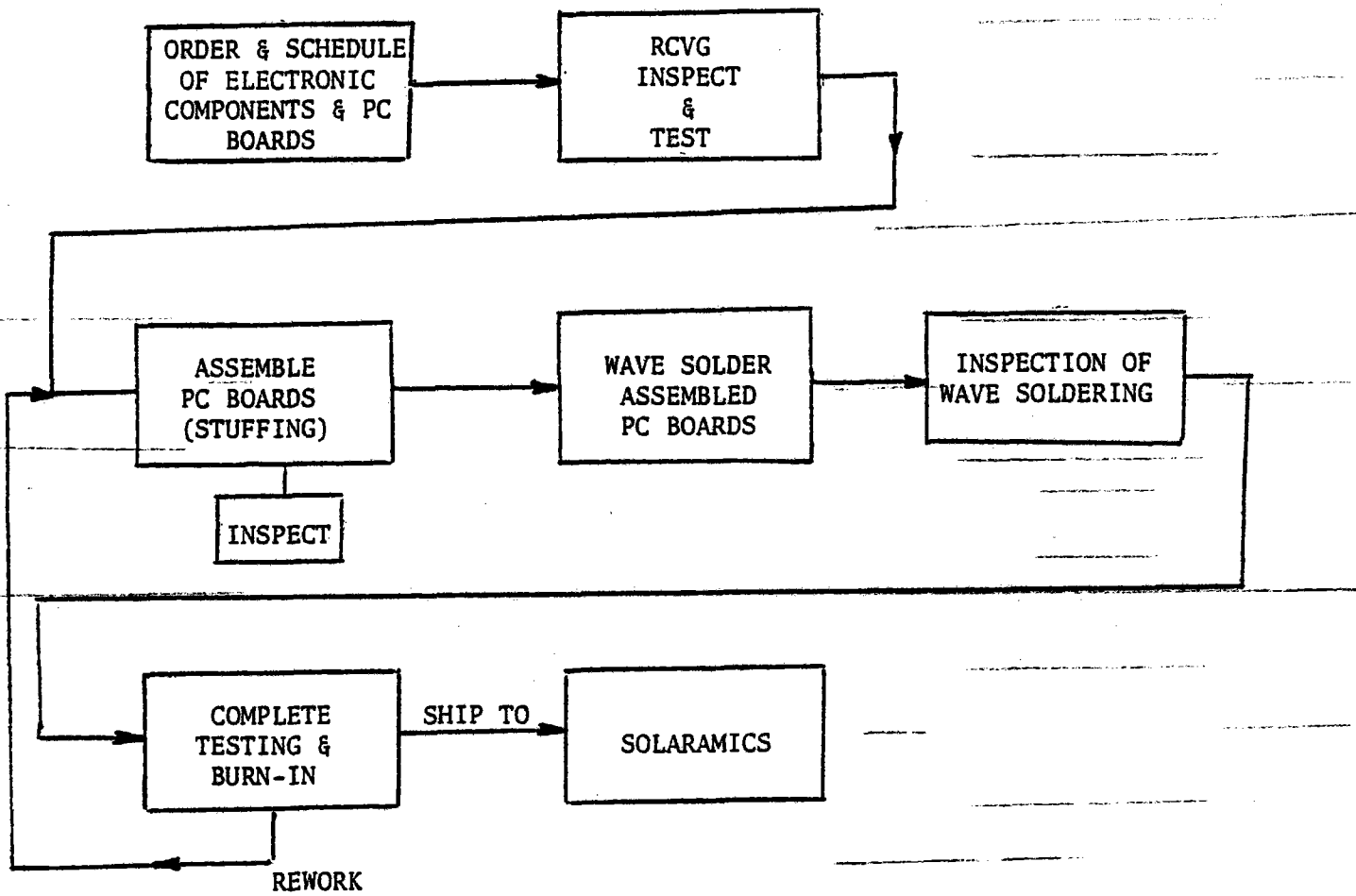

MANUFACTURING PROCESS - MICROPROCESSOR

FIGURE 3-7

Incoming inspection shall functionally test all components to the degree that the cost reliability studies indicate. A high level Quality Control system shall exist at this phase and in lessening degrees as the product nears final assembly.

Circuit board assembly shall be 100% automatic, including component lead forming and insertion. Clean room procedure will be utilized and QC inspection shall be applied to fully populated boards prior to soldering.

Soldering shall be accomplished by automatic wave soldering followed by a QC inspection of each board. Sampled boards shall receive complete analysis with substantial attention to incompatibilities between component leads, circuit board foil, solder (and flux) and precleaning agents, which is a leading contributor to lowered reliability. Conformal coating is applied as the last manufacturing process.

Final burn-in and testing shall include power shock, vibration, and thermal shock to detect potential solder joint failures and mechanical problems.

Accepted units will be packaged for shipment to the site, and all documentation filed for QC analysis if required.

3.5 Transportation Plan

Heliostat physical characteristics have determined the nature and amount of packaging and

transportation required to deploy one solar farm or 25,000 heliostats. The overall transportation philosophy takes into account the designed weatherability of the components while at the same time recognizing the characteristics of the mirror modules.

3.5.1 Incoming Materials

3.5.1.1 Bulk Materials

The quantity of bulk materials, crushed glass, fly ash, foaming agents and mold release agents required to produce 25,000 heliostats annually indicates the desirability of using rail transport and a factory siding. Trade-off studies will be made between rail and truck transport at each of the factory locations.

3.5.1.2 Sheet & Coil Steel

The coil stock used and the sheet sizes required are all commonly used. Transportation is similar to that currently being used by many steel warehousing & fabricating companies.

3.5.1.3 Forgings, Castings & Bar

The larger castings will be received palletized. The plan envisages four (4) trunnion castings on reuseable pallets designed to accommodate the entire manufacturing flow. The same analysis will be used where applicable to all components.

3.5.1.4 Finished Components

Purchased items such as motors, actuators and etc., will be transported by common carrier using the manufacturers' standard methods.

3.5.2 Out-going Parts & Assemblies

3.5.2.1 Mirror Modules

Shipping the mirror modules will be on standard trailer trucks with special racking. It is planned to stack and bundle one(1) heliostat's requirements of modules with suitable edge and face protection. Eight(8) of the bundles will make one 40 ft. trailer load. To minimize handling costs the trailers will be left loaded at the site while the tractors either dead head back or return empties. A precise turn around schedule will be developed for each site and factory location.

3.5.2.2 Pedestals

Sixteen(16) poles, each 21 ft. long & weighing 2,500 lbs., each, can be loaded on a standard flatbed trailer. For a 25,000 heliostat solar site over 1,560 loads will be required.

3.5.2.3 King Pin and Trunnion Assembly

The king pin and trunnion assembly will be palletized in sets of four(4) using the trunnion pallets. Approximately 100 assemblies can be shipped on a 20 ft. trailer.

3.5.2.4 Frame Assemblies

The frame halves will be stacked vertically on low bed trailers to stay within the height limits required of highway travel without special permits. Further consideration of site plant welding vs transportation costs will be made.

3.5.2.5 Heliostat Drive System Components

The actuator assemblies, link assemblies and encoder assemblies & related hardware will be factory checked and kitted for trans-shipment to the site. No special requirements are entailed in shipping or handling.

3.6 Heliostat Assembly & Checkout

3.6.1 Site Preparation(Fig. 3 - 8)

On-site activities are initiated by the set up of a portable, modular, field operations office. The office will be located strategically along the main roadway so that it can serve as both an operations base for the site activities and, as a construction office for the final assembly building. Erection of the final assembly building, will be accomplished in parallel with site preparation. Equipment will be moved on site to commence site preparation. The

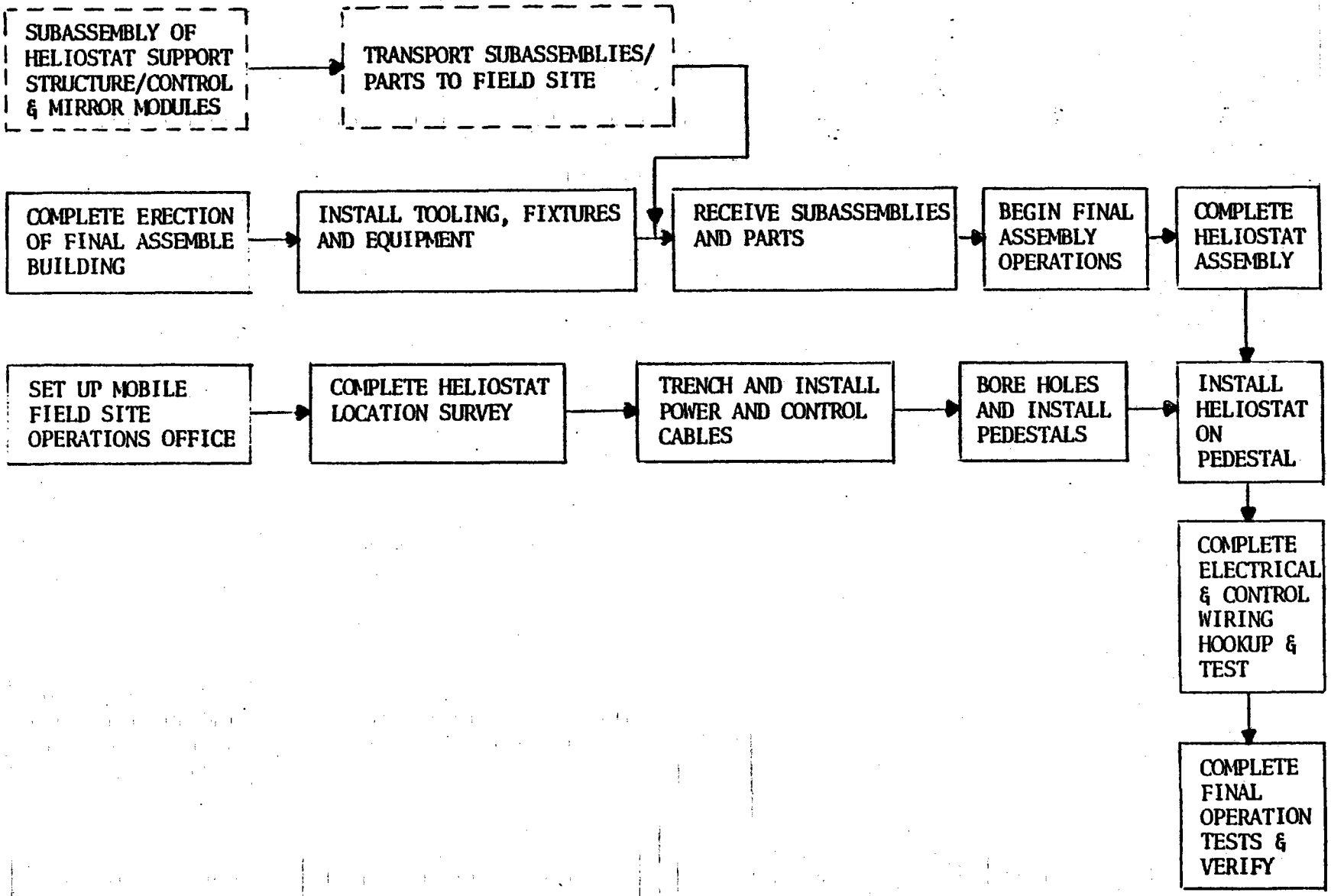

HELIOSTAT FINAL ASSEMBLY AND INSTALLATION SEQUENCE

FIGURE 3-8

logistics support for this phase of construction such as fuel, water & supplies, will be provided by portable, vehicle mounted containers typical to the types used by remote construction work camps.

It is presumed that the site selected is relatively level and without excessive growth of trees or other vegetation, large rocks or obstructions which would require other than minimal grading and hauling to prepare the site for installation. Heliostat location surveys will be accomplished by use of electronic Distance Measuring Equipment (EEM) and a theodolite. Other methods of surveying are to be reviewed to determine if state-of-the-art improvements are available to improve the cost effectiveness of the field survey.

Electric power and control cables have been selected for direct burial and the most economical distribution has been established by computer mapping. Trenching will be accomplished by use of a crawler type trenching machine. The layout for control cable distribution is divided into(8) eight segments of the circular field. A typical segment will have a main distribution trench from the heliostat central control to the outer radius of the field.

All cable will share the common trench and will be branched to each of (8) eight sectors. Each sector will contain eight(8) groups of fifty-seven(57) heliostats. See Figure 3-9. A cable of #22 gauge twisted pair shielded wire in a protective jacket will be used.

The power distribution network provides 240V, 1Ø, 60 Hz power to the heliostat 1/3 h.p. drive motors. Each motor draws approximately 1.0 amps under slewing conditions. This sizes the distribution network to efficiently distribute this power to the 25,000 heliostats on site. Twenty-five(25) primary feeders will emanate from the central power plant and to fifty (50) secondary groups. Each secondary group of 20 heliostats will be reduced in voltage through a transformer to the operating voltage of 240V. By splitting the 3Ø distribution into single phase distribution at the secondary group point, further cost reduction is achieved. Two (3) three conductor, 5000V rated jacketed cables will be used for primary feeders, one cable being used for ground return.

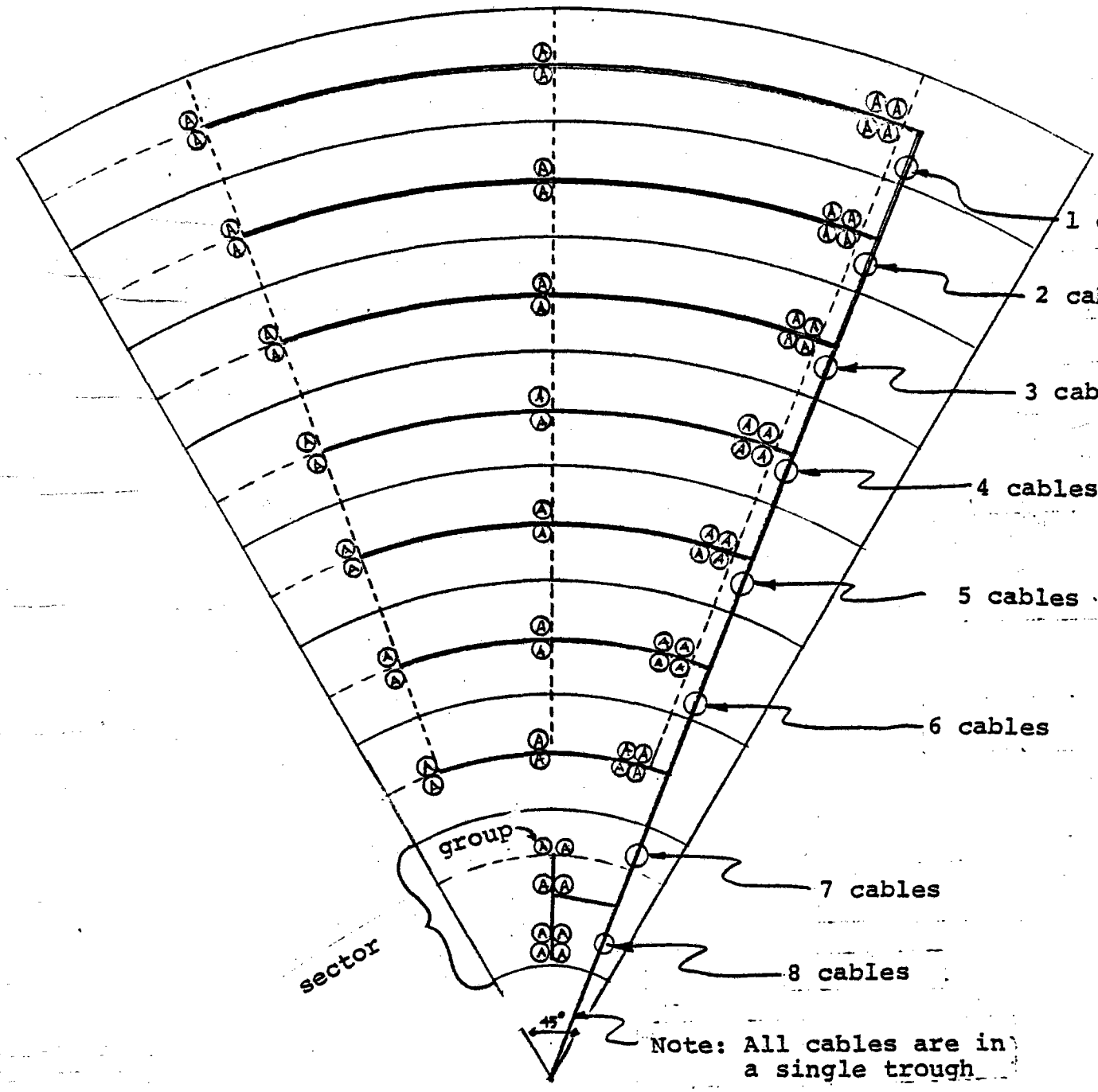

Typical of 1/8 of total field
Ⓐ= Bus for group of 57 heliostats

CONTROL CABLE LAYOUT

FIGURE 3-9

Two conductor 5000V rated jacketed cables will be used for the secondary distribution to the transformers. 600V rated, two conductor cable will be used to each heliostat from the transformers. Distribution circuit protection will be provided in each distribution junction box.

3.6.2 Heliostat Final Assembly

3.6.2.1 Assembly Building

The final assembly building will be erected along the main roadway at the outer boundary of the site to reduce the time required to transport the pedestals, heliostats & controls to the installation site. The location will also enhance the suitability of the building for use as a maintenance & storage facility following installation and test. The building will be an all steel, prefabricated structure erected on a concrete slab and will contain approximately 20,000 ft^2 of assembly space. The building will house all final assembly operations and provide storage for certain components & subassemblies which will not be suited to outside storage. A covered 30 ft. wide loading dock

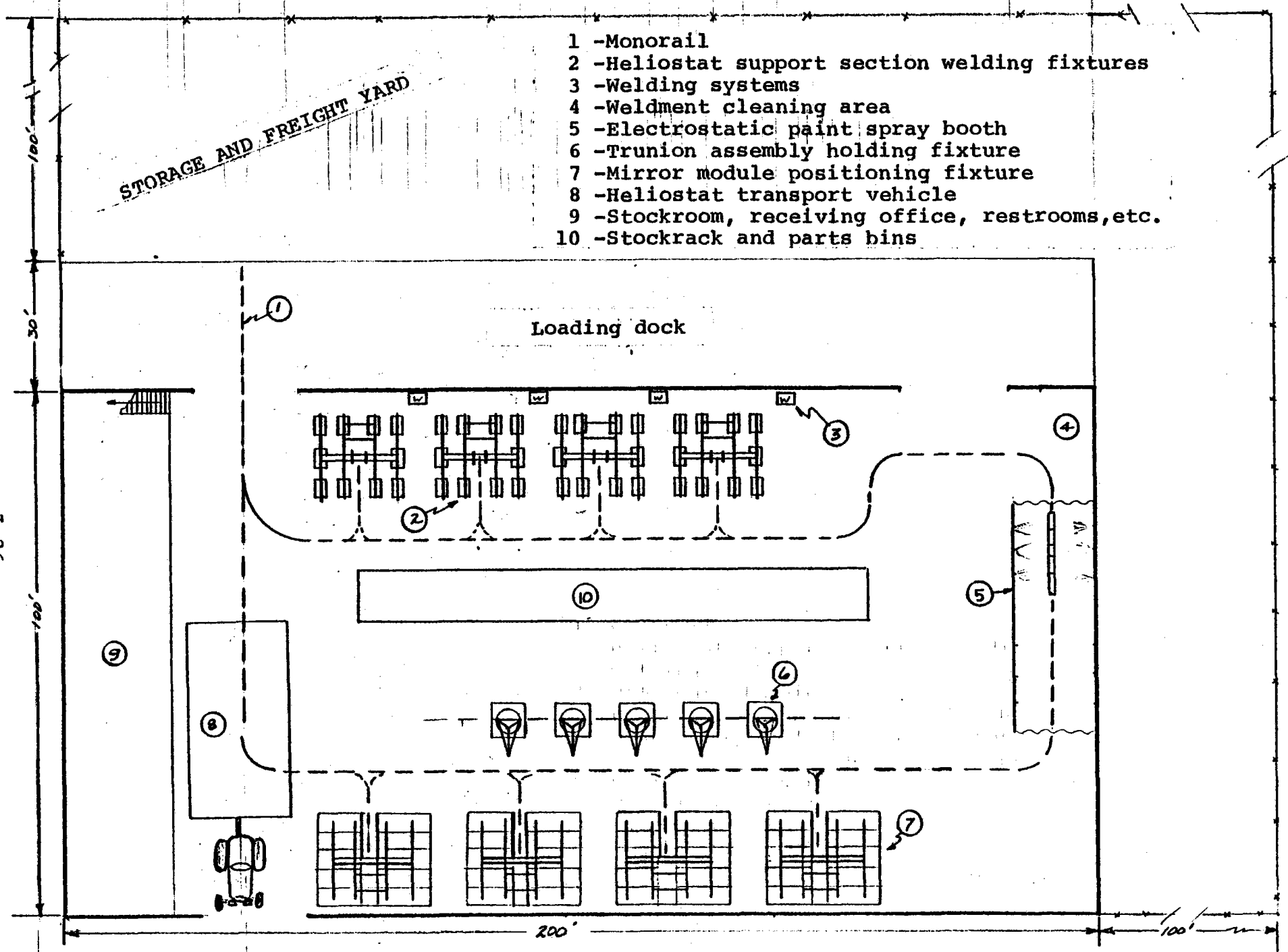

FINAL ASSEMBLY BUILDING
FIGURE 3-10

will run the length of the building (200 lin. ft.) and be truckbed high (52") for efficient unloading. A paved, fenced area shall be provided for outside storage of large components, equipment & shipping containers. This building is also intended as a maintenance/ storage building for the utility user when the site is put in operation.

3.6.2.2 Supply

The following components and subassemblies will arrive at the site via truck from the manufacturing plant(s). (Described for one unit):

Pedestal w/King Pin Mounting Plate Installed
Heliostat Support Structure (2 sections)
Center Mirror Inter Costal (2)
Trunnion w/King Pin Assembly
Drive Mechanism w/Actuators & Motors
Drag Links & acuator (1 set)
Controller w/Wiring Harness
Mirror Modules (11)
Misc. Parts and Hardware

3.6.2.3 Final Assembly Operation(Fig. 3-11)

The two support structure half sections are clamped in a welding fixture which precisely aligns the torque and mirror support structure. The tube is welded by an automatic, programmed pipe welding system with mofified welding head. Following the tube welding operation the two small mirror support intercostals are positioned and welded in place.

The structure is removed from the welding fixture and moved by monorail

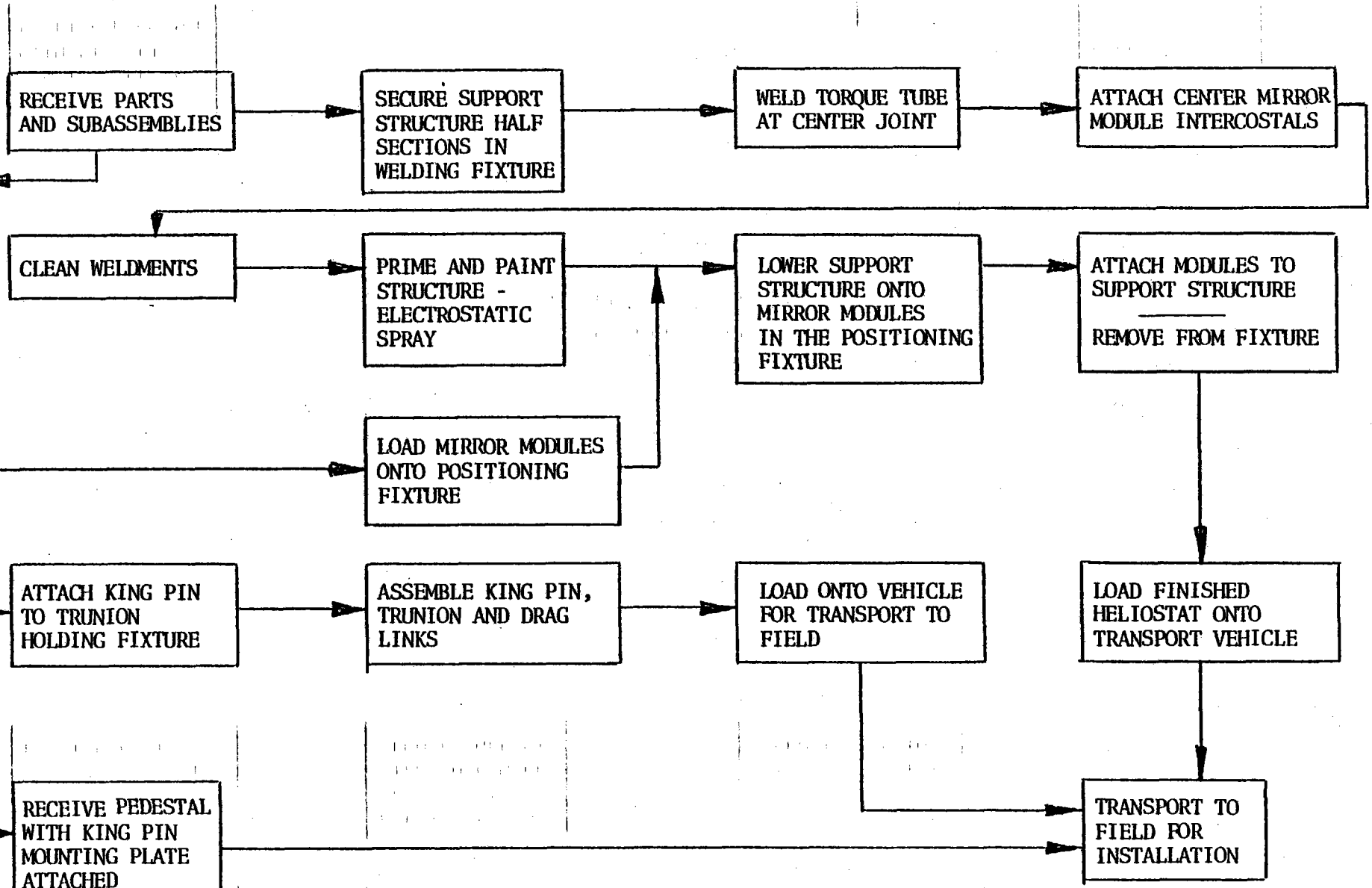

ON-SITE FINAL ASSEMBLY SEQUENCE
FIGURE 3-11

through the paint booth. The structure is primed and painted electrostatically by an automatically controlled paint spray system.

The mirror modules are positioned, mirror down, on a positioning fixture in the exact positions to mate to the support structure mounting holes. The support structure, moves from the paint booth to the mirror positioning fixture via monorail and is attached to a special handling fixture which is used to rotate the structure to a horizontal position and lower it onto the mirror modules. The bolt holes are aligned & bolts, nuts, and lock washers are installed & torqued.

The completed heliostat frame assembly is moved by monorail to a loading position and placed on the heliostat transport vehicle(HTV). The HTV is designed to carry (8) eight heliostats to the installation site and provides a means of interim storage. It also affords maximum protection to the heliostats while stored or in transit. The vehicle is designed for towing by truck or tractor.

3.6.3 Pedestal Installation

The pedestal with king pin mounting plate attached, will be moved to the site on the same trailer which transported them from the factory. The economics of using the same trailer are primarily the elimination of labor in unnecessary handling and the need to move large quantities of pedestals to the site to meet the de-

mands of the high installation rate. The holes for the pedestal are bored in the earth by use of a rough terrain vehicle with a high torque hydraulic auger system capable of boring precise, vertical holes in the earth at a high rate of speed. The pedestal is picked up and set in place in the hole by rough terrain fork lift with a specially designed, rotating, hydraulic clamp. This forklift will have special features such as wide side shift, rotating head & tilt to allow placement and alignment of the pedestal.

With the pedestal in place, the hole will be backfilled with a dense polyurethane foam which expands to (15) fifteen times in volume and cures rapidly (reaches (60-80% of its strength in 8-10 minutes). Once cured, the foam has a compression strength of 100 psi. The foam is applied by use of a truck mounted, high production dispensing unit which meters the two foam components from two(2) eighty gallon steel tanks. As 35-CFM air compressor and controls provides pressure to force the material through two 50 ft. dispensing hoses and a mixing and control valve. This method of pole setting has been used successfully for several years by electric utility companies in setting power poles and street light bases.

3.6.4 Heliostat Installation & Checkout

3.6.4.1 Trunnion & King Pin Installation

The trunnion assembly, complete with king pin, drive mechanisms, actuator assembly and drag links, is positioned over the pedestal by use of rough terrain vehicle with telescopic boom and a special handling sling. Technicians standing on a mobile work platform guide the assembly onto the mounting bolts, the nuts are attached and torqued. The handling fixture is disengaged from the trunnion and final alignment adjustments and completed.

3.6.4.2 Heliostat Array Installation

The heliostats are transported from the final assembly building to the site by a special heliostat transport vehicle (HTV) designed to haul eight (8) completed heliostats at a time. This vehicle is also used to store heliostats as they are removed from the final assembly position and is configured to offer maximum protection during storage & transportation. The HTV is towed along the access roadways to a position adjacent to the installation site. The heliostat is picked up by a special handling fixture mated to

a rough terrain vehicle with telescopic boom and moved a short distance to the pedestal. The heliostat is then lifted above the trunnion and lowered into position while guided by the technicians. The two bell cranks on the heliostat torque tube are mated to the trunnion pivot and the two elevation drive drag links. Bolts and nuts are installed. The handling fixture is then disengaged and removed from the heliostat.

3.6.4.3 Controller Installation

The controller with wiring harness is attached to the pedestal at ground level and wired to the azimuth and elevation drive motors and to the power and control cables.

3.6.4.4 Check-out

After installation is completed verification and checkout tests are performed to assure the correct functioning of controllers and heliostats in the various operational modes.

3.7 Alignment Procedures and Checkout

The following alignment critical functions are identified:

1. pedestal installation, gross alignment
2. mirror module alignment upon assembly to structural support
3. precision king pin axis alignment
4. gimbal axis encoder bench mark

3.7.1 Pedestal Installation

The "pole set" techniques planned for the pedestal installation with its quick cure characteristis (15 mins.) allows the pedestal to be held in a close alignment position during installation with a minimum of special tooling. It is desirable to obtain a good alignment of the pedestal to minimize the range of adjustment which must be provided for in the design for subsequent precision alignments.

The pedestal positioning fixture establishes vertical and azimuth orientation with respect to the tower.

3.7.2 Mirror Module Alignment

The mirror module is assembled at a canted angle to achieve a "Focus" on the tower. The field is divided into five(5) radial zones, each having a nominal "Focal" length. The position of the modules are established by adjustment of the heliostat array assembly fixture. As the modules are attached to the support structure with lock fasteners, this focus becomes a permanent characteristic of the array.

3.7.3 King Pin Axis Alignment

As the King Pin Trunnion assembly is installed on the pedestal, a precision alignment fixture is attached to the trunnion. The alignment fixture shown in Fig. 3-12 provides precision indication of the azimuth axis orientation together

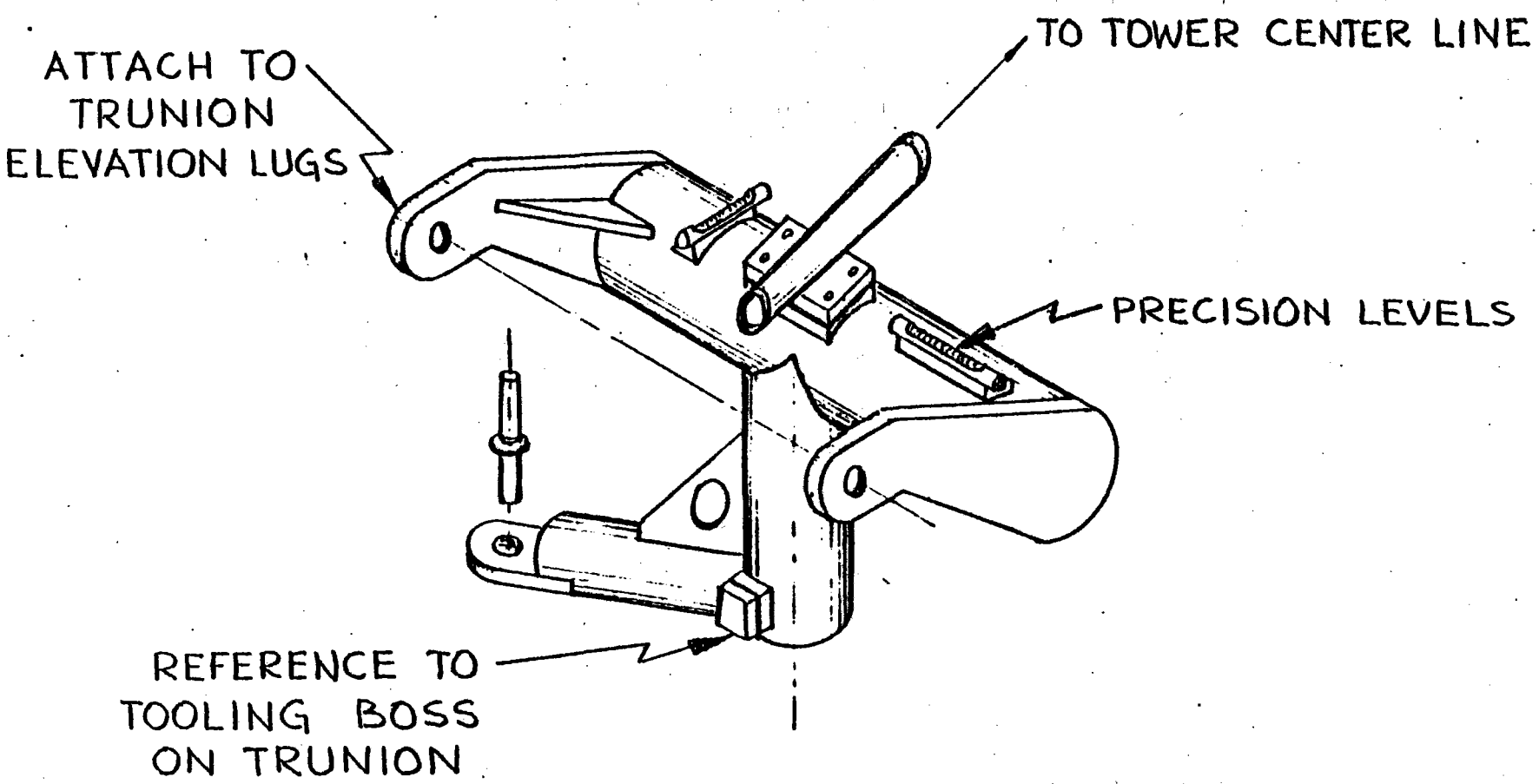

KING PIN/TRUNION ALIGNMENT FIXTURE

FIGURE 3-12

with the orientation of the fixed lug for the azimuth drive mechanism with respect to the tower centerline. Adjustment of the King Pin base plate is achieved by the double lock nut design. A rotating eccentric permits adjustment of the azimuth drive lug pivot point. Upon completion of the alignment the fixture is removed.

3.7.4 Gimbal Axis Encoder

After the heliostat array is installed, and all power connected, the gimbal axis encoder adjustment is accomplished with the aid of a manual controller. With the azimuth drive positioned at 90°, i.e.-vectored toward the tower, the elevation drive positions the mirror array in a vertical position, indicated by a precision level at the center mirror module. The elevation gimbal axis mirror is adjusted to obtain an indication from the elevation gimbal axis encoder.

The azimuth vector is established with a theodolite attached to the trunnion. The azimuth drive is manually oriented through the auxiliary motor drive to achieve alignment with the tower centerline.

The azimuth mirror is then adjusted to obtain an indication from the azimuth gimbal axis encoder.

3.7.5 Checkout

The heliostat control is accessed through the manual controller, and all functions and drives of the heliostat operation are checked out in accordance with a predetermined checklist. The heliostat is now ready to be turned over to the master control.

3.8 Maintenance Plan

Maintenance functions will be considered in(3) three categories:

1. Cleaning
2. Preventive
3. Corrective

Cleaning:

Cleaning techniques and dust/dirt accumulation are currently being investigated by several agencies, esp. Sandia Laboratories, Albuquerque and Battelle Pacific Northwest Laboratories. Cleaning high velocity water spray jets mounted on a special tank vehicle operating in evening hours is envisioned. The preferred cleaning solution additives are expected to vary with location depending upon the alkalinity of the deposit. A recent verbal communication with Mike Lind of Battelle indicated that the side exposed to tin in a float glass process was more readily cleaned than the opposite side by a factor of 2 to 1. If this effect is a result of ion exchange at the tin interface it suggests a possible advantage could be accrued through exposure of the glass surface to a stannous chloride vapor as it exits the hot end of the glass line.

The above technique is widely utilized in the glass container production to obtain a more scratch resistant surface by an ion exchange where tin replaces the majority of the sodium and calcium surface ions.

Preventive Maintenance:

The preventive maintenance functions primarily are concerned with the actuators & gear reducer elements of the drive mechanisms. Periodic checks and adjustment of the backlash unit together with inspection for lubrication leakage through shaft seals are planned. At the same time, inspection of the rubber bellows which protect the actuator drive shafts from contamination will be performed. These operations would also be performed in the evening hours.

Corrective Maintenance:

The considerations for modular replacement have been incorporated into the design. For example, the microprocessor is replaceable as a clip in circuit board module, as is the motor controller circuit.

A service vehicle will be provided with the necessary test equipment and spare components, which can be dispatched upon indication of a malfunctioning heliostat report from master control. The local control test box will access the microprocessor and by sequencing operational instructions the failure mode can readily be identified. The service vehicle will also contain an auxiliary DC motor for manual control to position the heliostat for ease of maintenance if required.

3.9 Tooling and Handling Plan

The tooling philosophy at SOLARAMICS is based on a full identification of the scope of the tasks required by the size, complexity and necessary production rates of heliostat manufacturing and installation. All tools, molds, processing facilities and special handling devices will be designed to produce the components for a minimum of 100 complete heliostats daily. The equipment will vary from (2) two 14 ft. eight gauge capacity squaring shears worked (8) eight hrs./day to a dozen or more 60 ft. conveyorized automatic kilns operating on a 24 hr. basis.

The tools and special equipment required are delineated in the following sections:

3.9.1 Foam Glass Fabrication

Skip Loaders-modified for loading kilns

Glass Crushers - initial glass processing

Pulverizers - final stage of glass crushing

Air Classifiers - to control the particle size of the crushed glass

Mixer/Blenders - for blending crushed glass and foaming agent

Special Kilns - to provide continuous process for foamed glass panels, this will be a SOLARAMICS development

Trim Saws - conventional type equipment specially mounted & controlled to automatically trim the panels

60" Belt Sander - to surface the glass panels- these are standard machines used in wood fabrication but with special abrasives developed for SOLARAMICS

Spec. Drilling Machines - air actuated automatic drill heads mounted on a bridge frame for drilling mounting holes

Conveyors - Primarily powered roller type with switch stations for transporting of foam glass panels throughout the facility

Dust Collectors - To meet OSHA requirements

3.9.2 Mirror Modules Assembly

Conveyors - for transporting components

Air Balance Lifters - for transporting components

Vacuum Head Lifters - for transporting components

Mirror Module Assembly Tables - 4 ft. X 10 ft. granite surface plates equipped with positioning devices & clamps. The surface plate is a standard measuring tool that will provide the necessary flatness & dimensional stability required to maintain satisfactory optical flatness during assembly.

Adhesive Dispensers - several types for spray or potting - all with automatic mixing heads for two-component adhesive systems. The mixing heads are current state-of-the-art & will require only mounting & control

Nut Runners - Torque set for bolting or mounting brackets.

3.9.3 Pedestal Manufacturing

Grinding & Screening Equipment

Batch Weighing & Mixing

Batch Wetting Systems

De-airing Pug mills

Drying Ovens

Extrusion Press

Kilns

Cranes

Transport Dollies

3.9.4 King Pin Fabrication

Plasma Torch - Pantograph mounted for cutting base plate

Plasma Arc Cut Off Saw - for cutting king pin bar to length

Inertia Welder - for welding base plate & bar

Turret Lathe - automatic with tracing attachment or numerical controlled

Spindle Drill - tooled for the bolt circle on the base plate

3.9.5 Trunnion Fabrication

Gantry Crane - from incoming pallet to machining center

Machining Center & Transfer Line - a dedicated machine tool to automatically finish machine the trunnion casting. This is conceived as a direct numerical control tool similar in size & facility to those used for automotive transmission housings

Freezers & Ovens - for bearing installation

Fork Lifts

3.9.6 Frame Fabrication

Bridge Crane - 40,000 lb. capacity for handling sheet & coil steel

De-coiler, Roller, Leveler & Cut-off Shear

Squaring Shear - 12 ft. 12 gauge, equipped with roller table & take off conveyor

300 Ton Mechanical or Hydraulic Press Brake for 2" frame bending

500 Ton Backgeared Press - straight side with roller feed for attach bracket fabrication

3.0 PRODUCTION PROCESSES (cont'd)

Frame Welding Jigs - precision tools equipped with automatic weld heads & wire feeds designed so that all welds are programmed and done simultaneously. Each weld head will be powered by an individual generator.

Metallic Inert Gas Welders - to power welding jig

Monorail Conveyor

Spray Cleaning Line - for paint preparation

Electro Static Paint System & Booth
FULLY automatic

Paint Drying Oven

Forklifts - equipped with "grabber" arms for manuevering and positioning frame assemblies.

4.0 BENCH TESTS

4.1 Glass Foam Characterization Tests

A series of tests were conducted to determine the strength and performance characteristics of selected densities of glass foam. This effort provided the preliminary design data required for the application of glass foam as a structural material in the heliostat design.

The following is a summary of the results of these investigations.

Flexural Strength and Young's Modulus (ASTM Method D 790 Four Point Loading)

Sixteen (16) specimens were tested, three (3) with a target density of .3 specific density, but actually measuring .241, .247 & .261; seven(7) specimens with a target density of .4 specific gravity, but actually measuring .339, .356, .359, .360, .364, .373 & .444; and five(5) specimens with a target density of .6 specific gravity, but actually measuring .517, .527, .538, & .542.

The specimens were positioned and the load applied as shown in Figure 4-1. The test results are shown in Figures 4-2 & 4-3.

Compressive Strength(ASTM Method C 165 Procedure A)

Four(4) specimens from each of sixteen panels were tested. The densities were as for the Flexural Strength Test. The specimens were positioned and the load applied as shown in Fig. 4-4. The test results are shown in Figure 4-5.

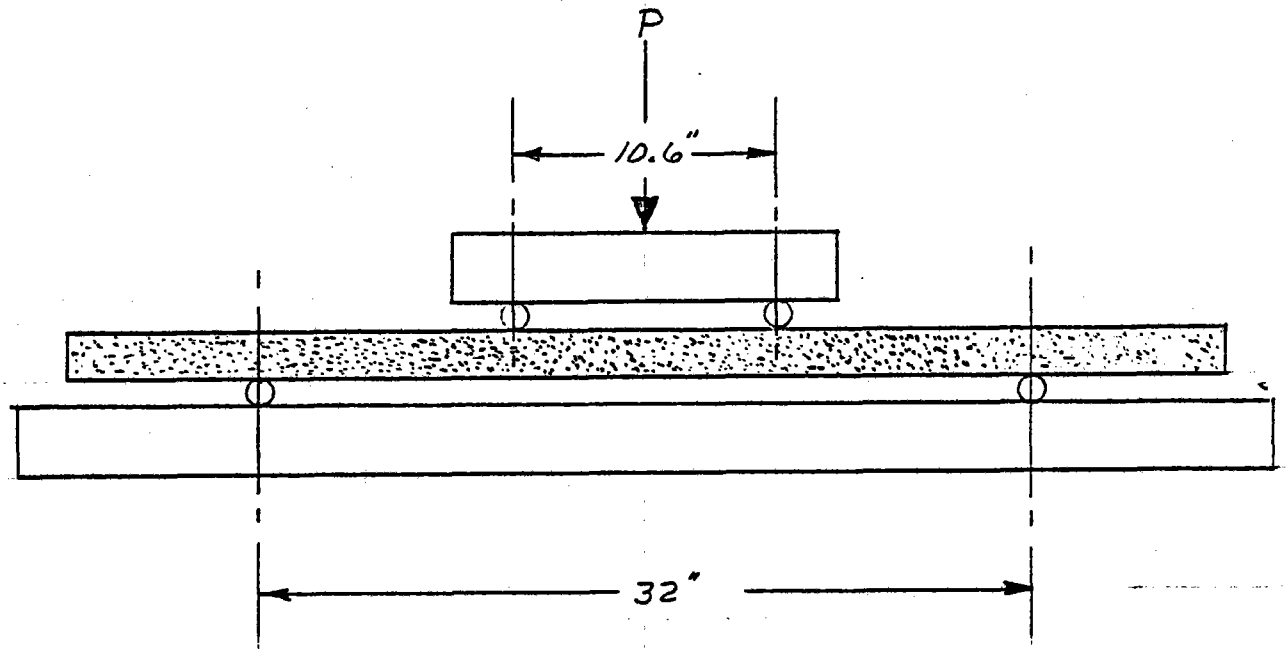

FIGURE 4-1 FLEXURAL STRENGTH - 4-POINT LOADING

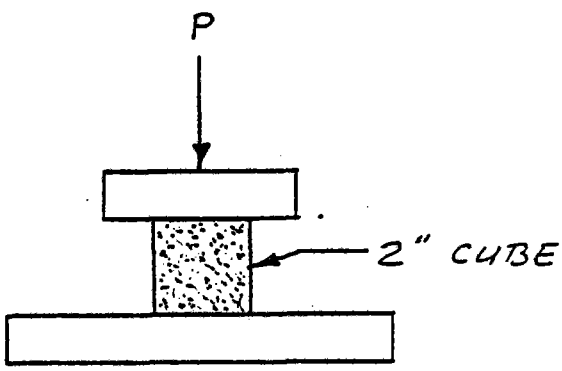

FIGURE 4-4 COMPRESSIVE STRENGTH

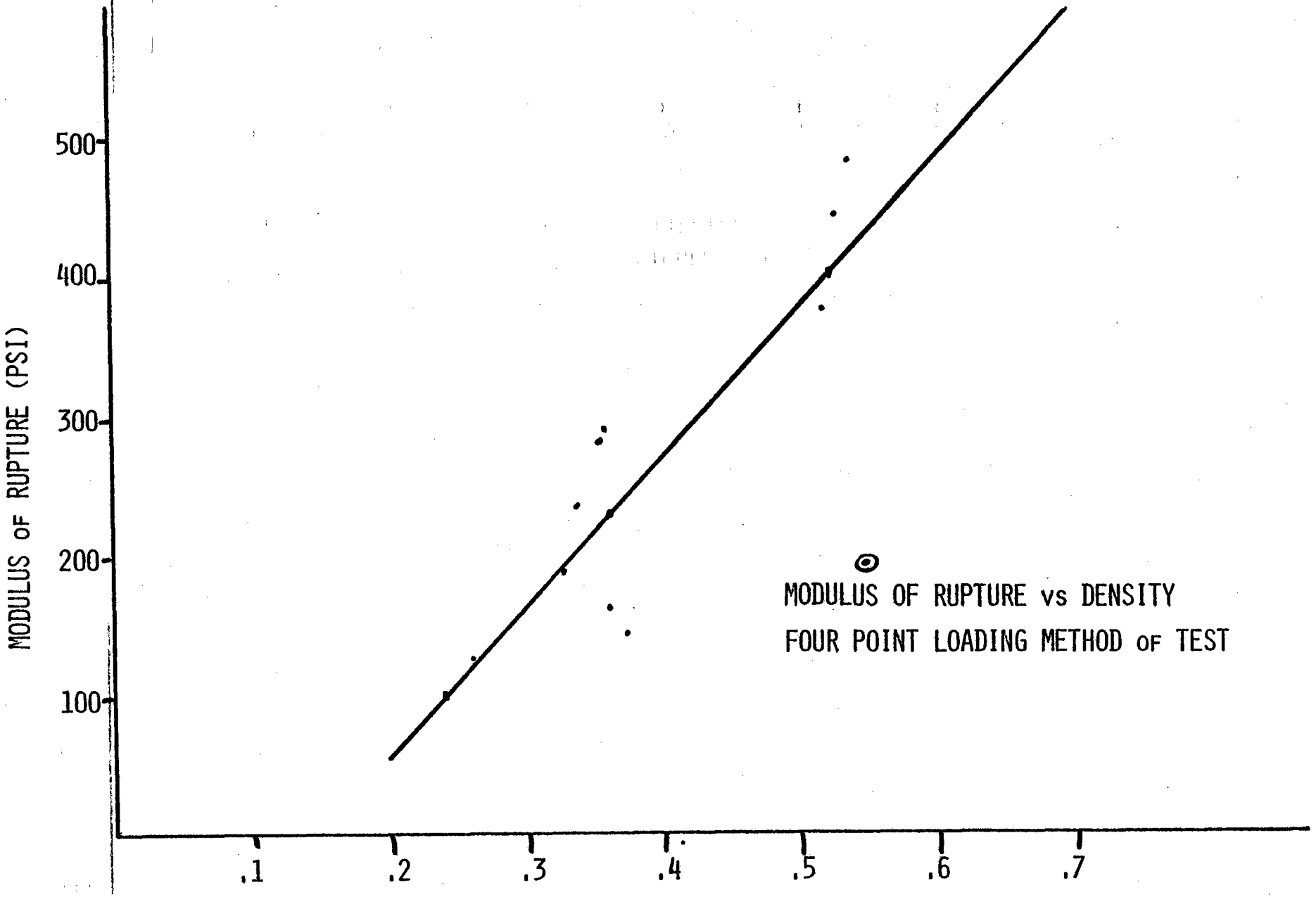

FIGURE: 4-2

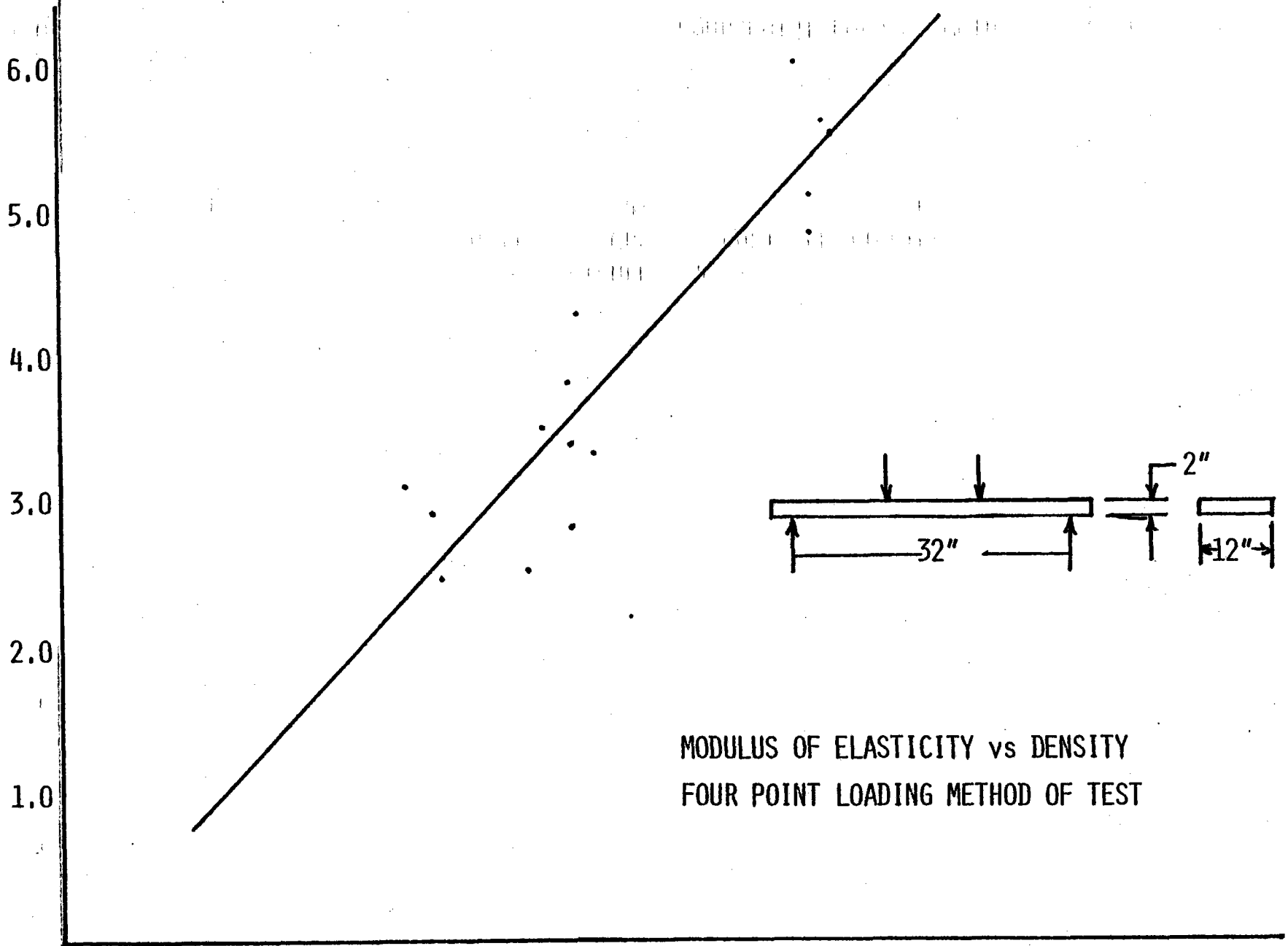

FIGURE: 4-3

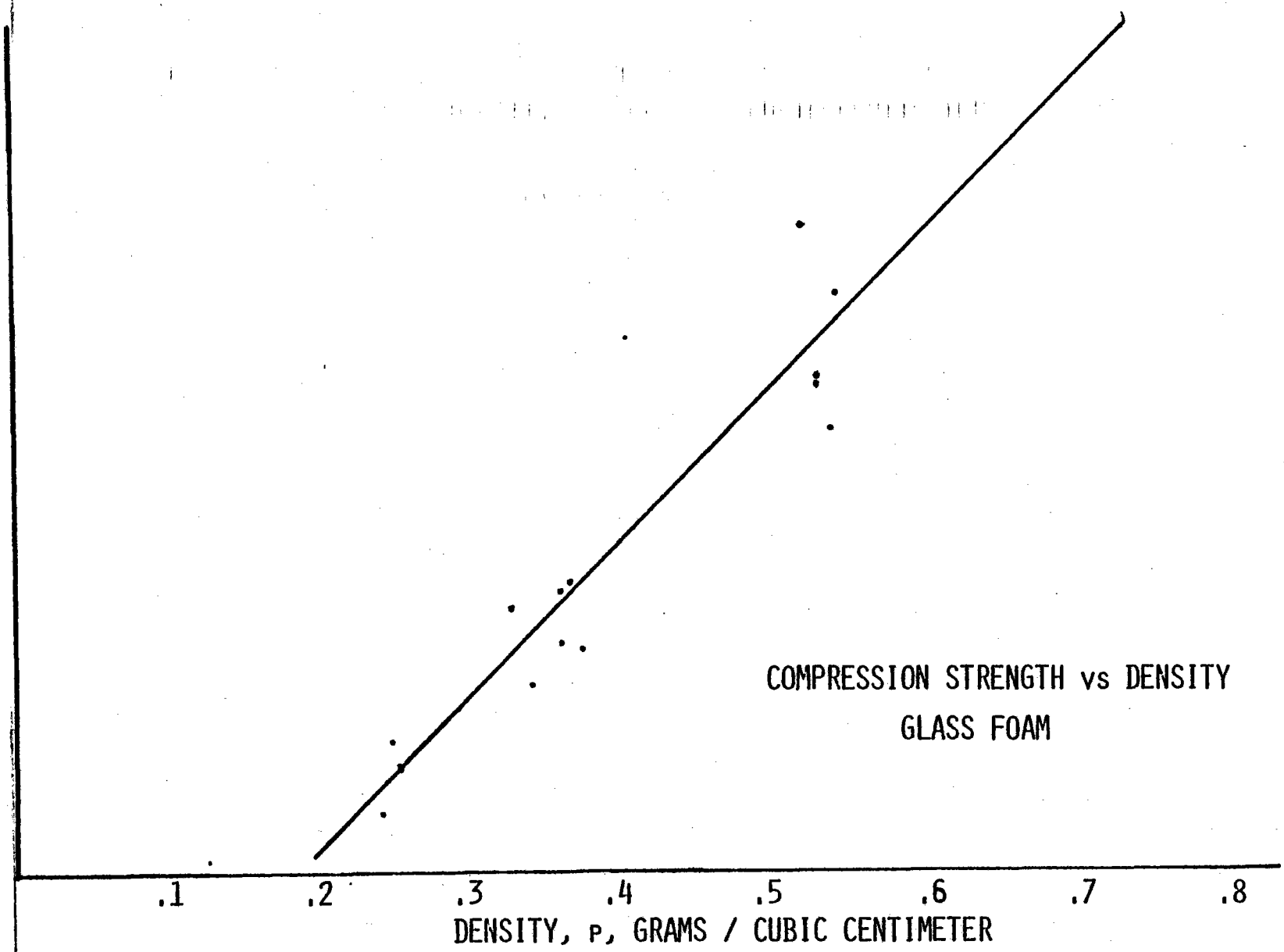

FIGURE: 4-5

4.0 BENCH TESTS

4.1 Glass Foam Characterization Tests(cont'd)

Thermal Expansion(ASTM Method C337)

Thermal Expansion of glass foam, .364 specific gravity, was determined to be:

α = 9.5 $\pm$ 0.5 ppm/^{o}C over the range 72^{o}F to 400^{o}F

The test was conducted by Analytical Research Laboratories, Inc., Los Angeles, California

Water Absorption(ASTM Method C240)

Water absorption for a 2"X12"X18" specimen, sanded on all faces & edges was determined to be 125% by weight. The results of this test indicate the need for a closed cell structure or a water-proof coating. Additional investigations are required to understand fully the nature of the cell structure.

Fastener Attachment Test

The loads required to dislodge a large heated bolt, small headed bolt and a threaded rod which have been potted in the foam with polyurethane adhesive are shown in Figure 4-6.

Freeze/Thaw Test

After 20 cycles of exposing water-soaked specimens to -20^{o}F temperatures in a freezer for eight(8) hours, one of four(4) specimens has failed.

Three specimens, with attachment brackets mounted with bolts & adhesive, have been cycled between the freezer set at -20^{o}F and room temperature air 20 times with no visual evidence of failure. These specimens have not been exposed to water except for ambient humidity conditions.

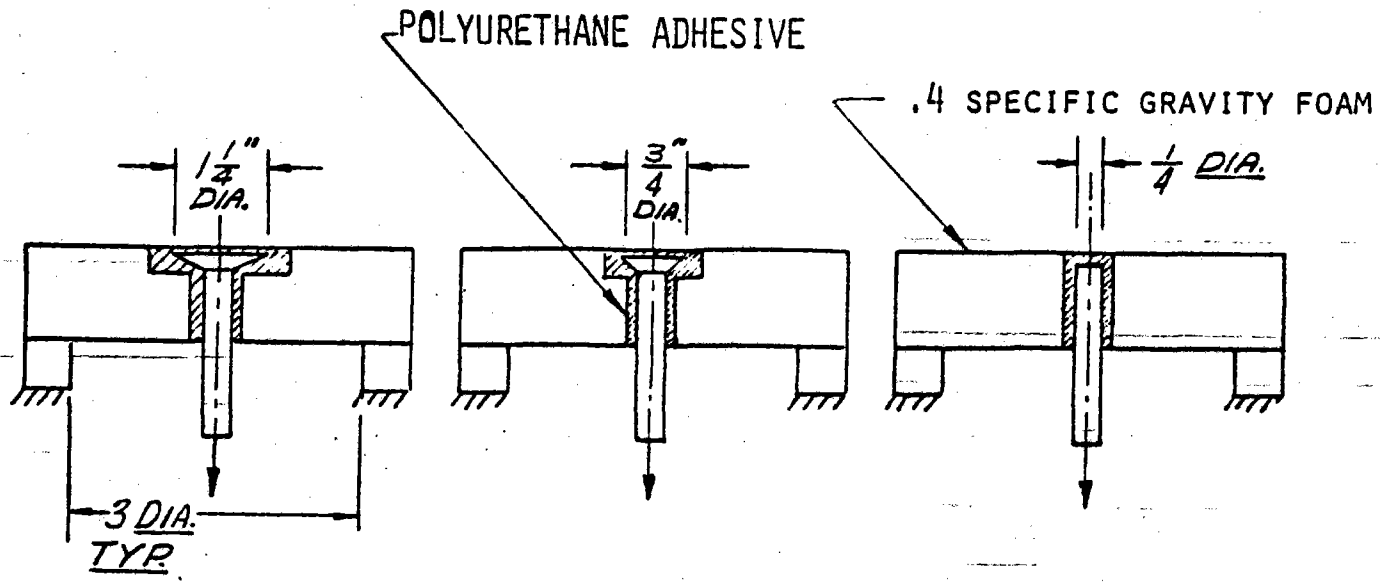

P = 930#
1260#
1490#
1285#

P = 900#
980#
1170#

P = 250#
670#

FIGURE 4-6

FASTENER TEST ARRANGEMENT

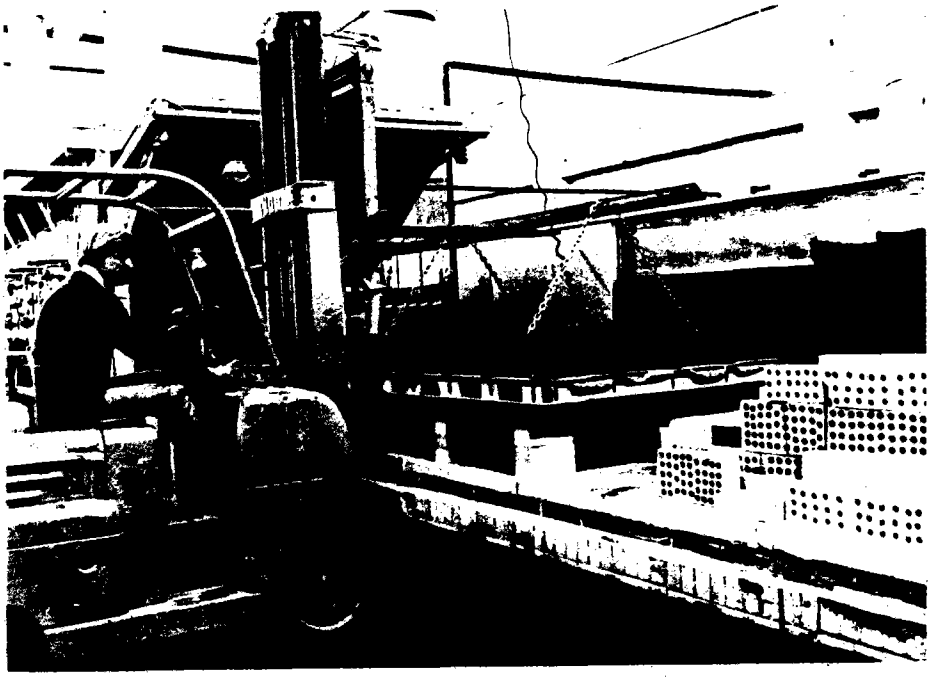

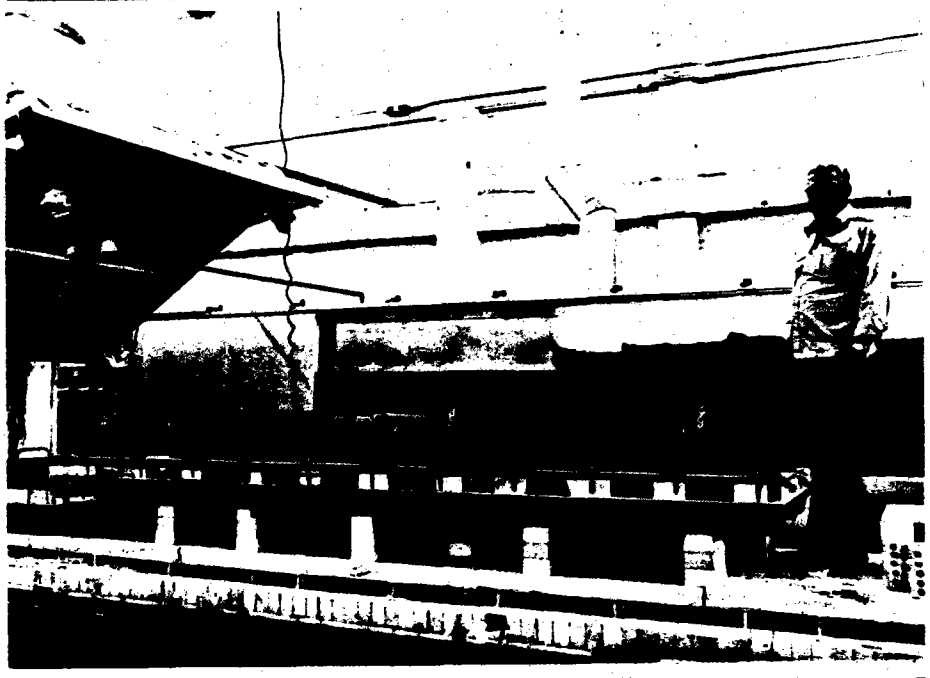

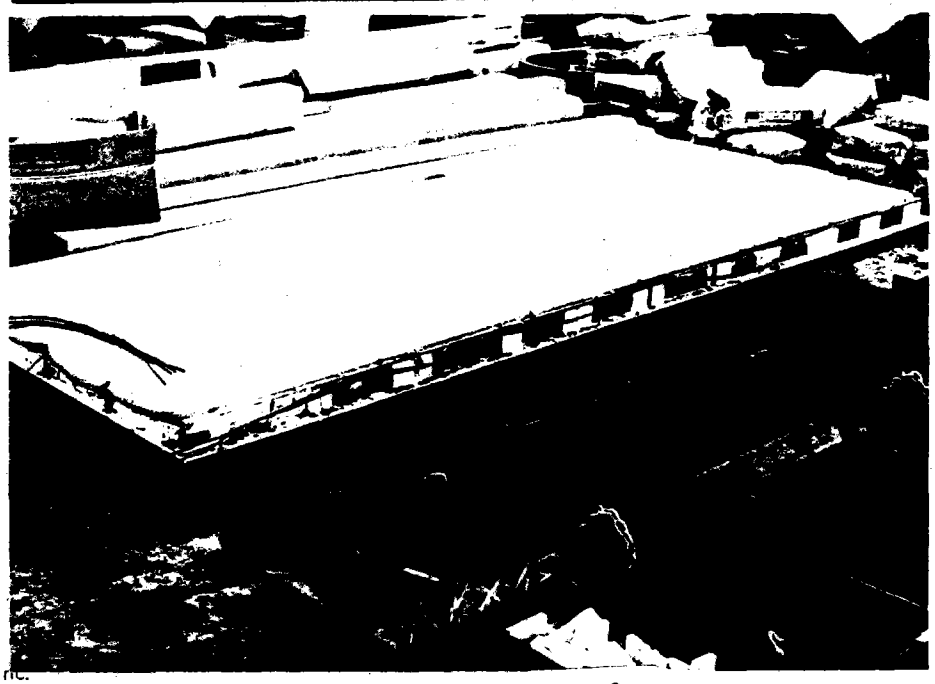

4' x 10'

CELLULAR GLASS PANEL

PERIODIC KILN PROCESS

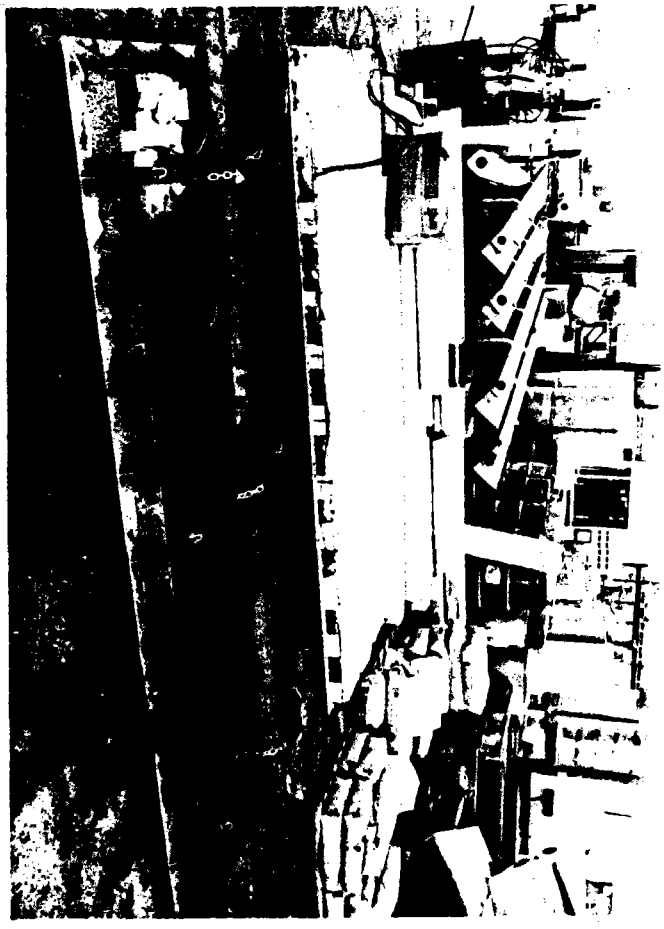

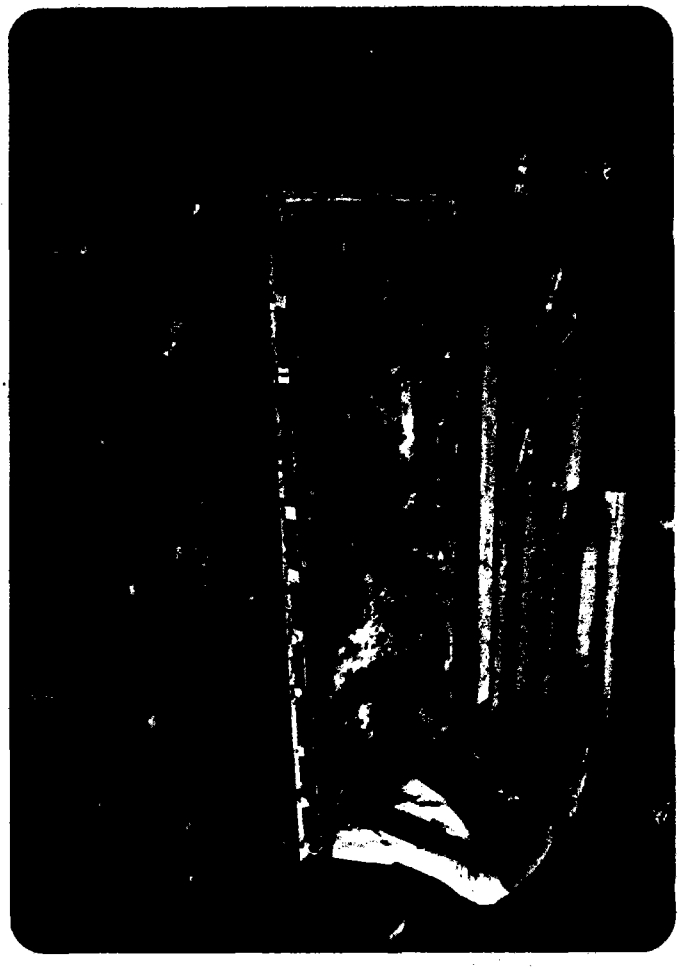

Solaramics, Inc.

4.0 BENCH TESTS

4.2 Drive Mechanism Stiffness Tests

Since the central tracking bench model mechanism had been fabricated full scale, the test plan was expanded to include stiffness measurements of the drive mechanisms. The bench model hardware was modified to achieve close simulation of the elevation mechanism preliminary design, while the azimuth mechanism contained several components, especially the torque arms, not representative of the preliminary design stiffness.

The stiffness measurements observed are presented in Fig. 4-7 to 4-17. The following observations and design recommendations resulted.

Elevation mechanism: Deflections of the elevation mechanism were observed to occur primarily in:

1) the entended actuator shaft
2) distortion of the trunnion between the actuator pivot & the cross tube pivots
3) bending of the Kingpin
4) diaphragm deflection of the large plate

Design Recommendations:

1) increase the diameter of the actuator drive,(from 1.1 sq in to 2.2 sq in root area)
2) increase bending rigidity of the cross tube support points of the trunnion, & increase the diameter of the center tubular support(see Fig. 2-1)
3) increase diameter of Kingpin & change to a ductile iron casting. The pin now becomes an integral part of the pedestal cap. (see Fig. 2-1)

4.2 Drive Mechanism Stiffness Tests(cont'd)

4) support Kingpin by integral truncated cone and thereby eliminate diaphragm plate

5) support trunnion on preloaded tapered roller bearings to reduce tolerance fits and ease assembly.

Azimuth Mechanism: Deflections were observed to occur principally in the two torque arms. A poor tolerance fit of the actuator pivot bearing contributed significantly to the backlash observed.

Design Recommendations:

1) implement the design modifications shown in Figure 2-1,of the torque arms, together with the increased torsional stiffness of the trunnion.

2) utilize the specially designed actuator with 2" diameter drive shaft(2.2 sq in root area)

3) examine potential application of fibre filled teflon bearing with split collar at the actuator pivot on the Kingpin.

It should be noted also that azimuth stiffness is primarily of interest in the range from -55^{o} to $+55^{o}$. Review of tracking motions indicates that the higher azimuth positions are only employed with elevation positions near horizontal, with low azimuthal moments.

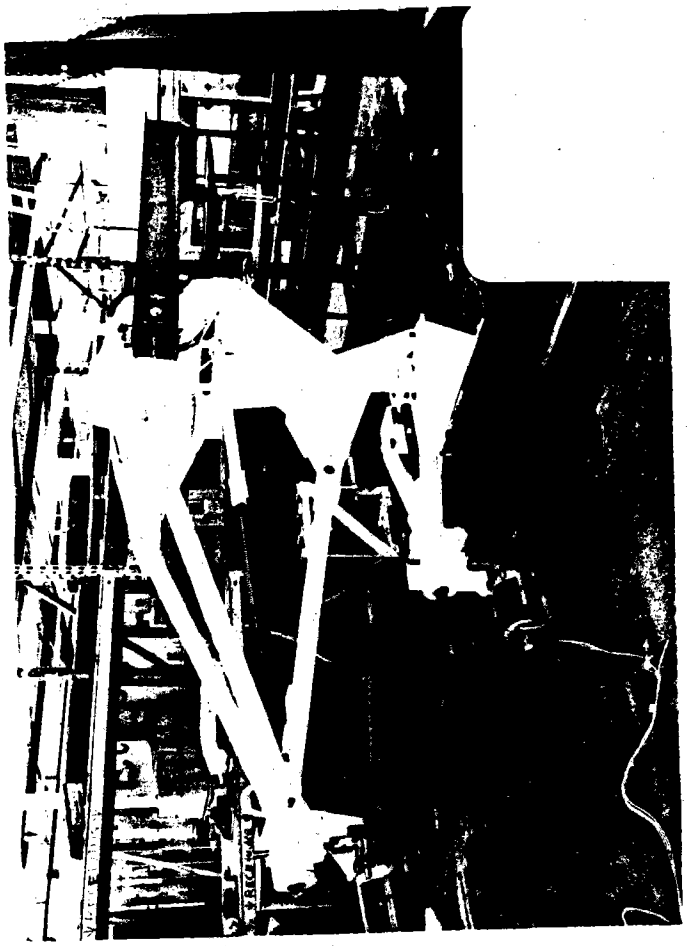

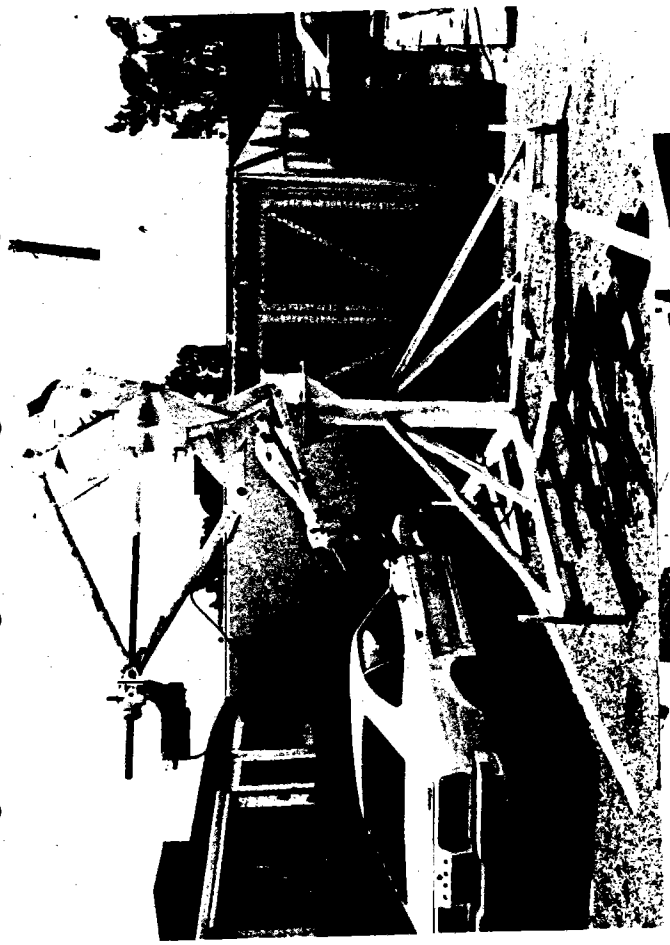

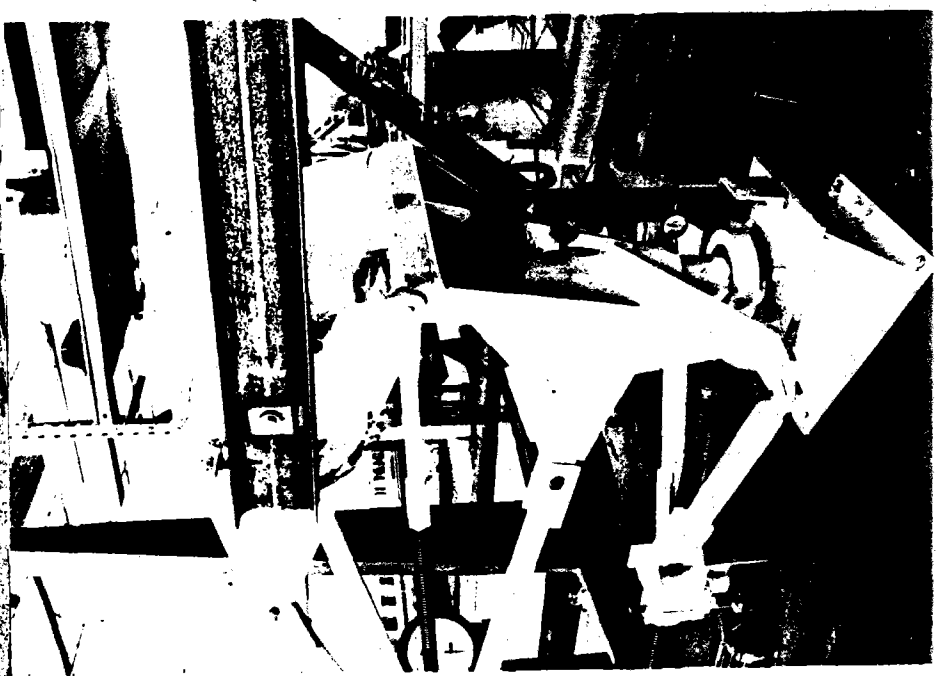

Solaramics, Inc.

FIGURE: 4.7 ELEVATION MECHANISM
-23° POSITION

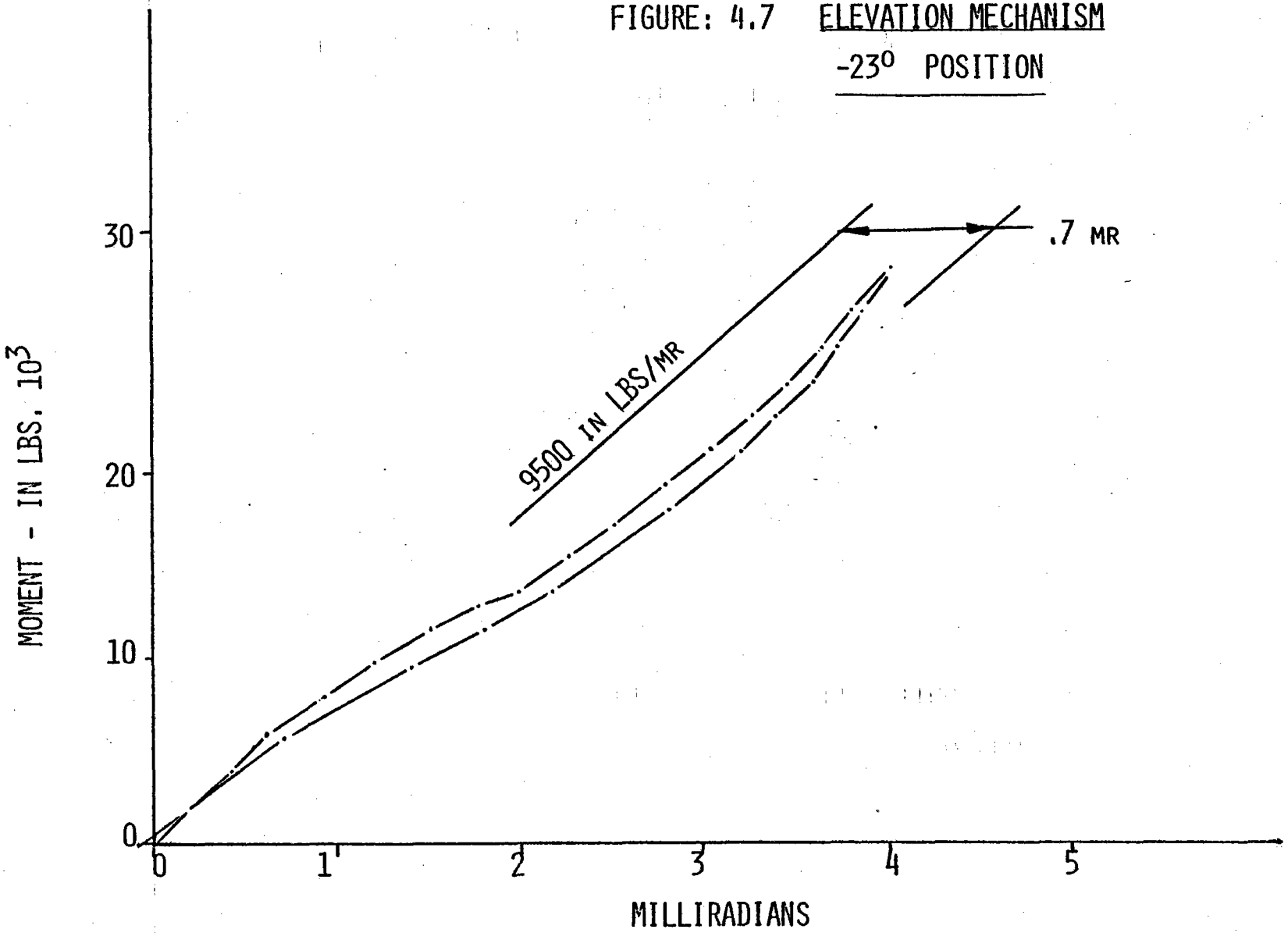

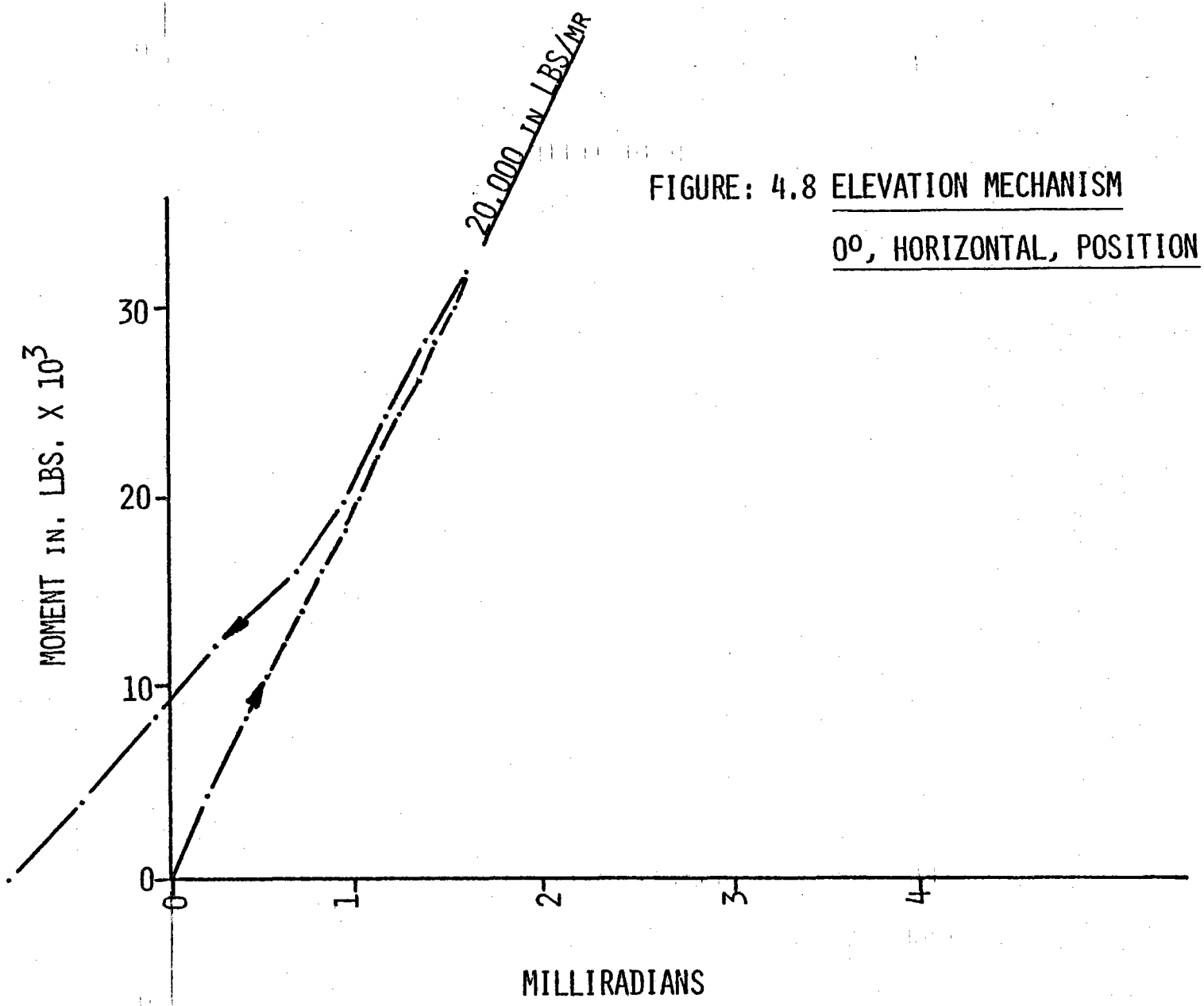

FIGURE: 4.8 ELEVATION MECHANISM

0°, HORIZONTAL, POSITION

FIGURE: 4.9 ELEVATION MECHANISM
45° POSITION

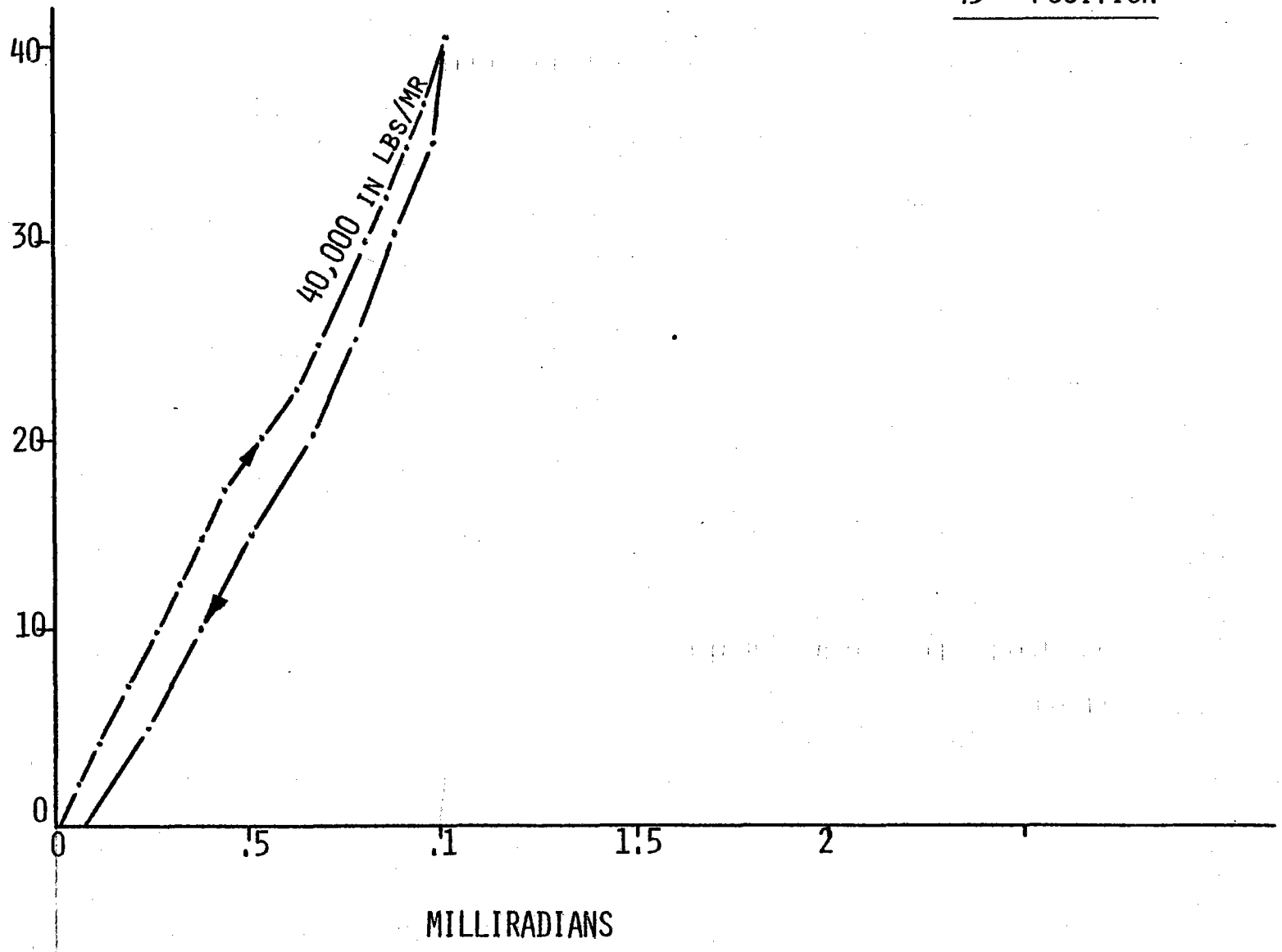

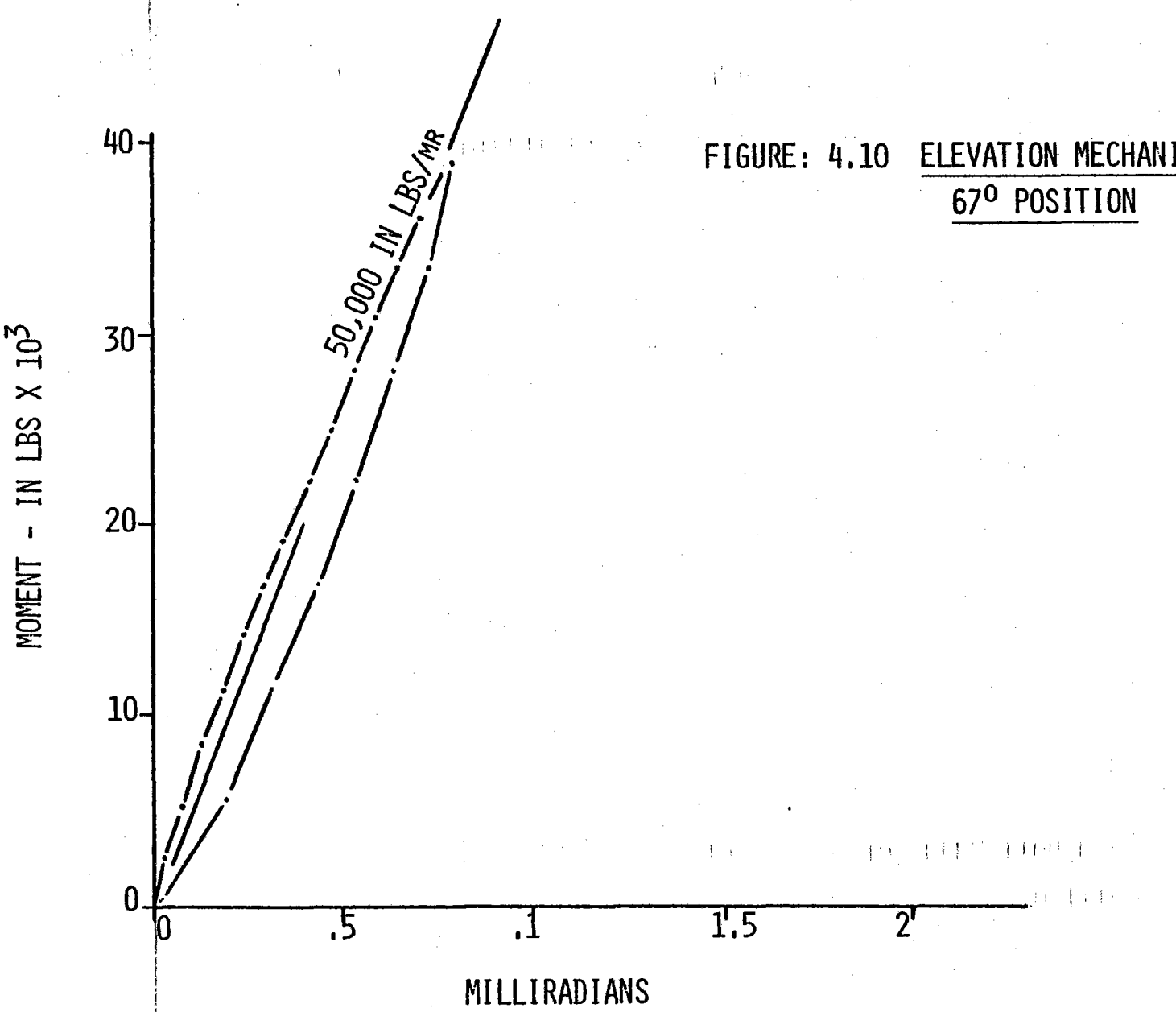

FIGURE: 4.10 ELEVATION MECHANISM
67° POSITION

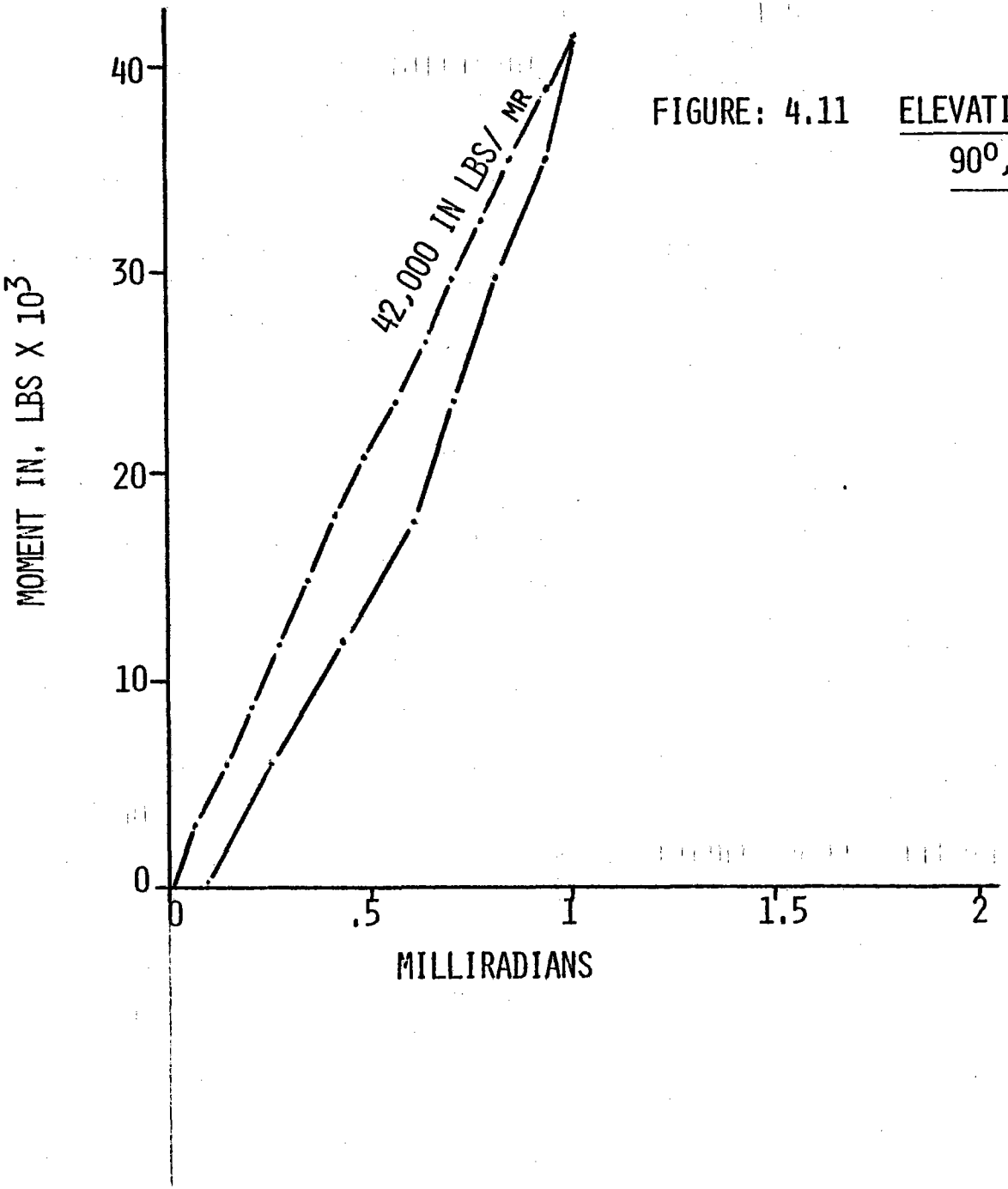

FIGURE: 4.11 ELEVATION MECHANISM
90°, VERTICAL POSITION

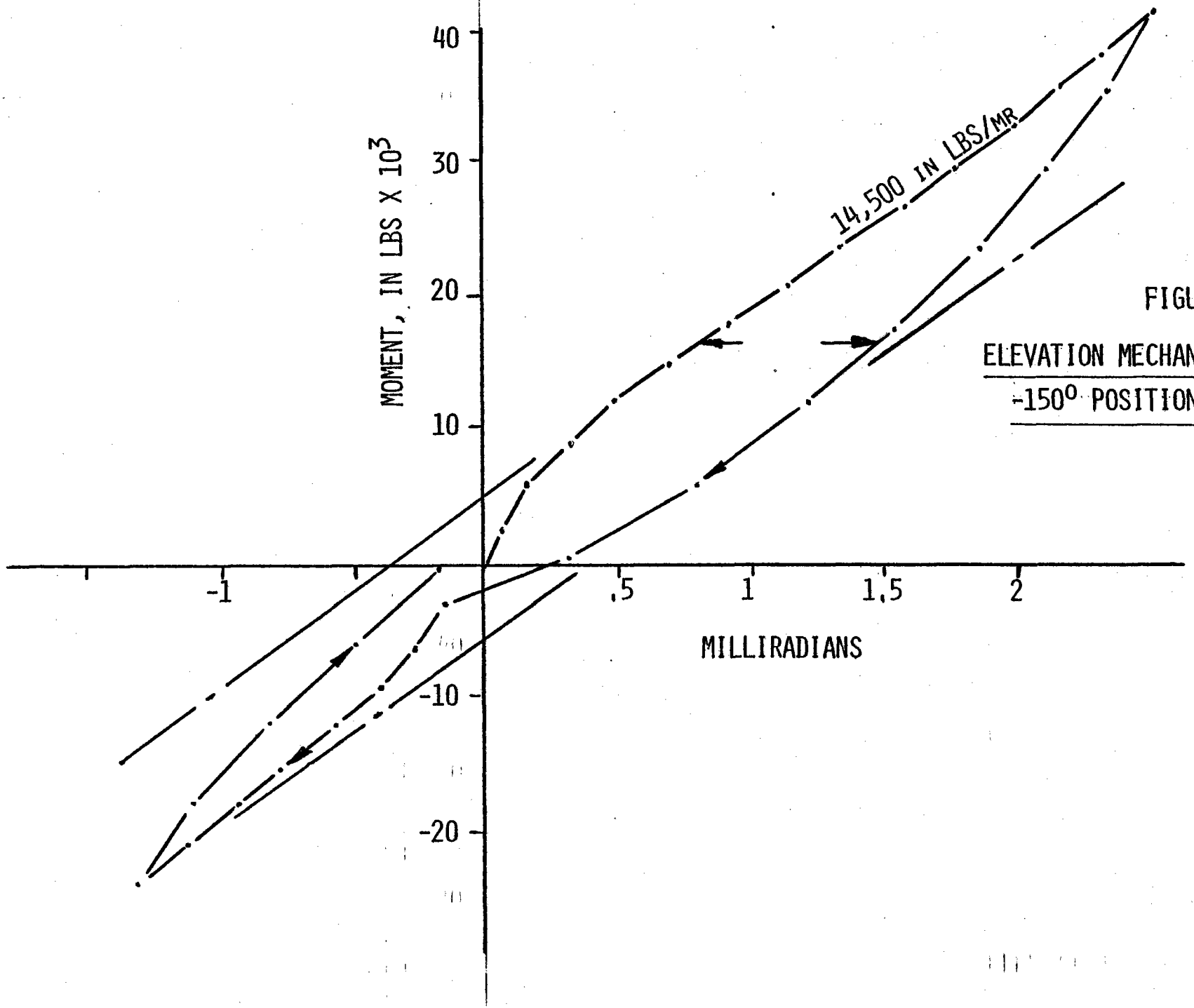

FIGURE: 4.12

ELEVATION MECHANISM

-150° POSITION

FIGURE: 4.13

AZIMUTH MECHANISM
0^0 FACING TOWER

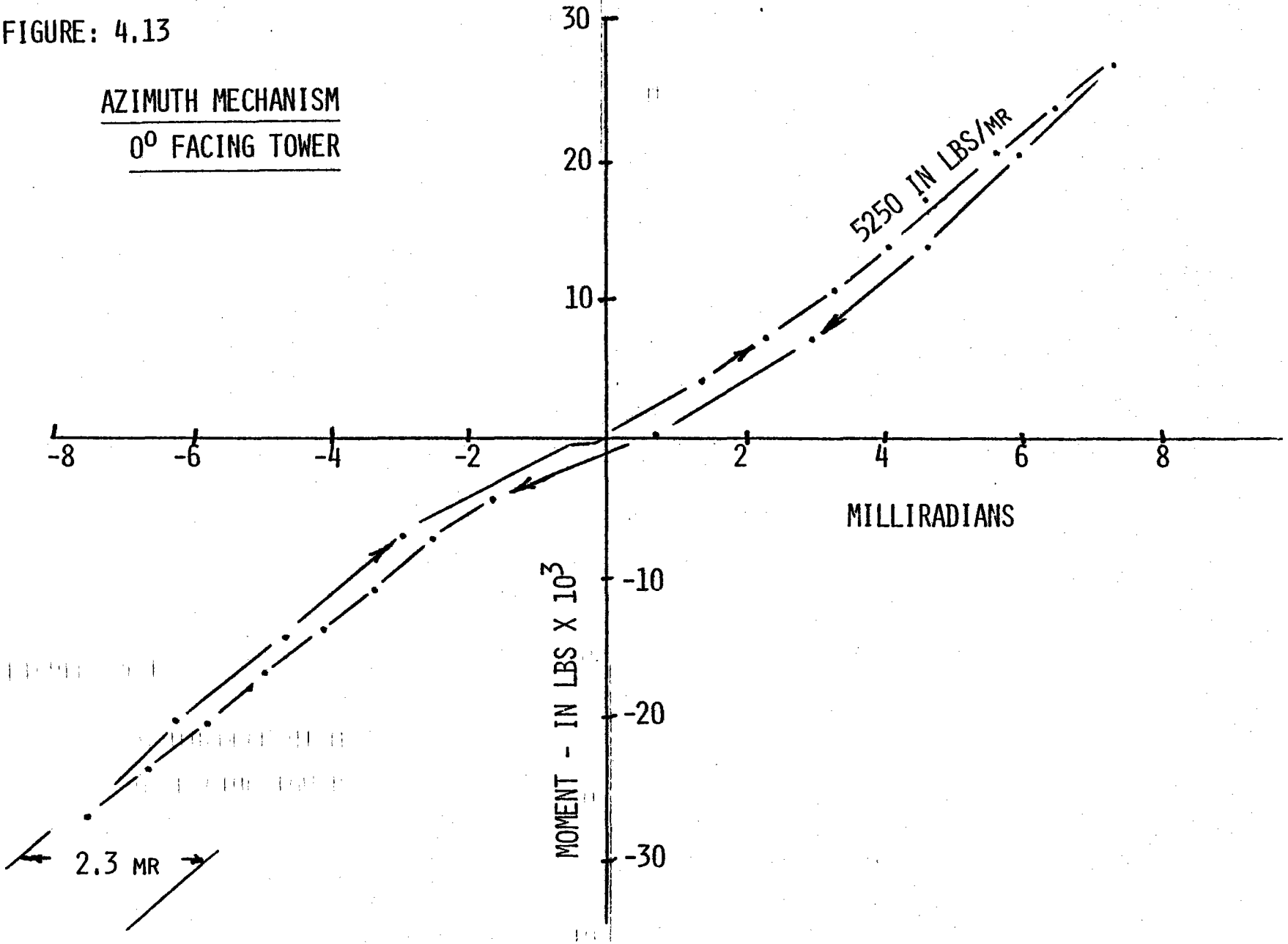

FIGURE: 4.14

AZIMUTH MECHANISM
45° POSITION

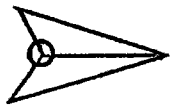

FIGURE: 4.15

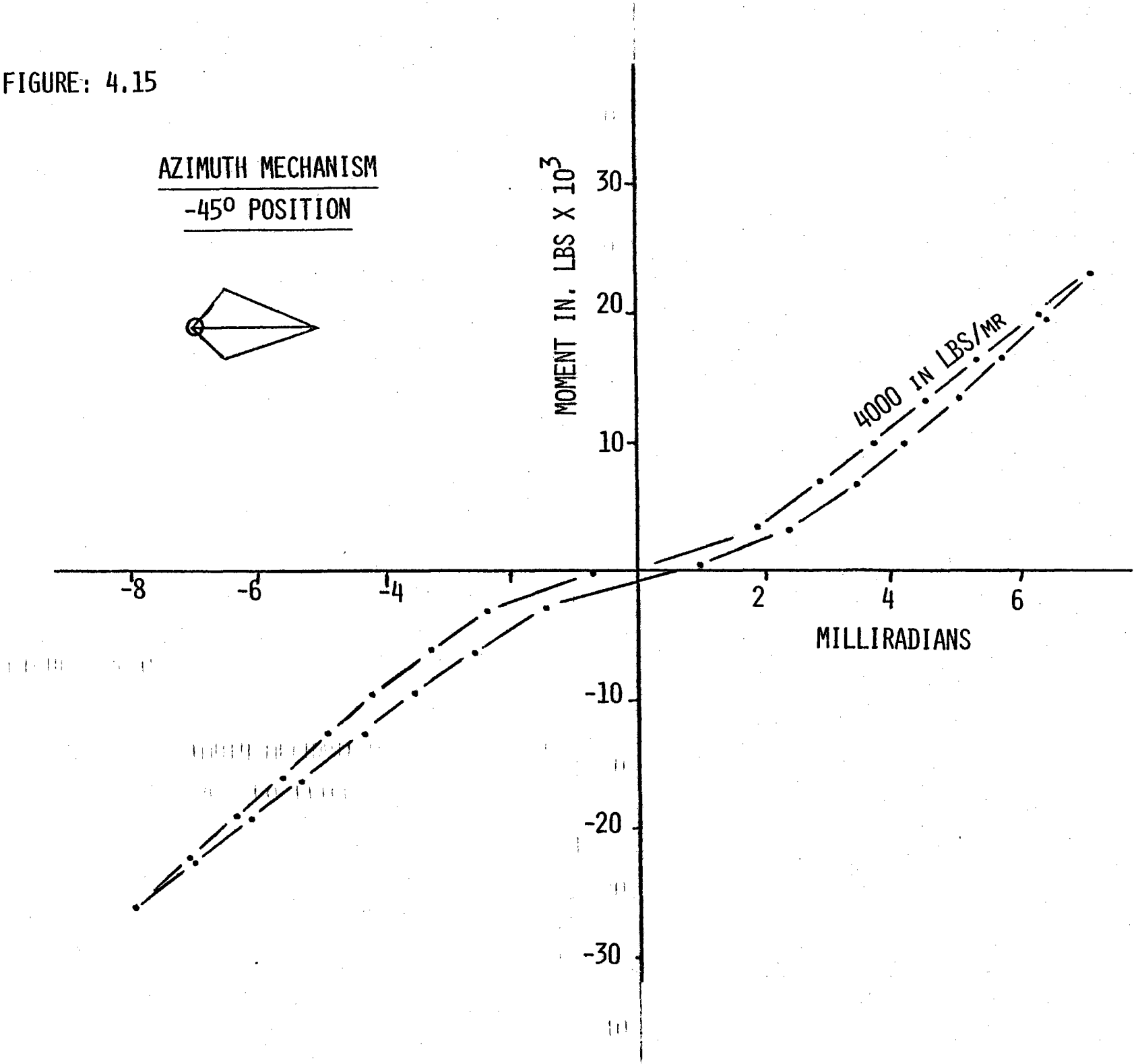

FIGURE: 4.16

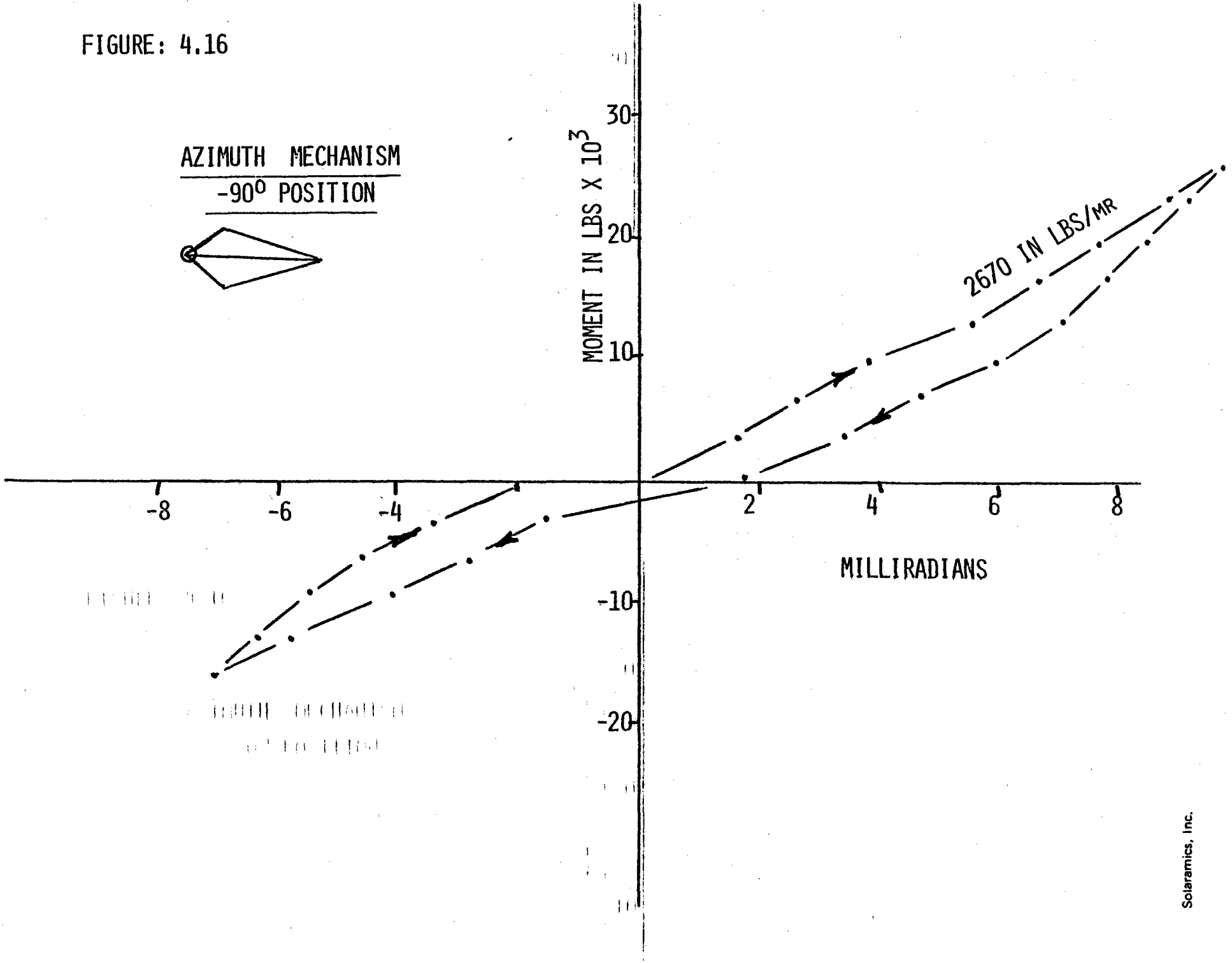

FIGURE: 4-17

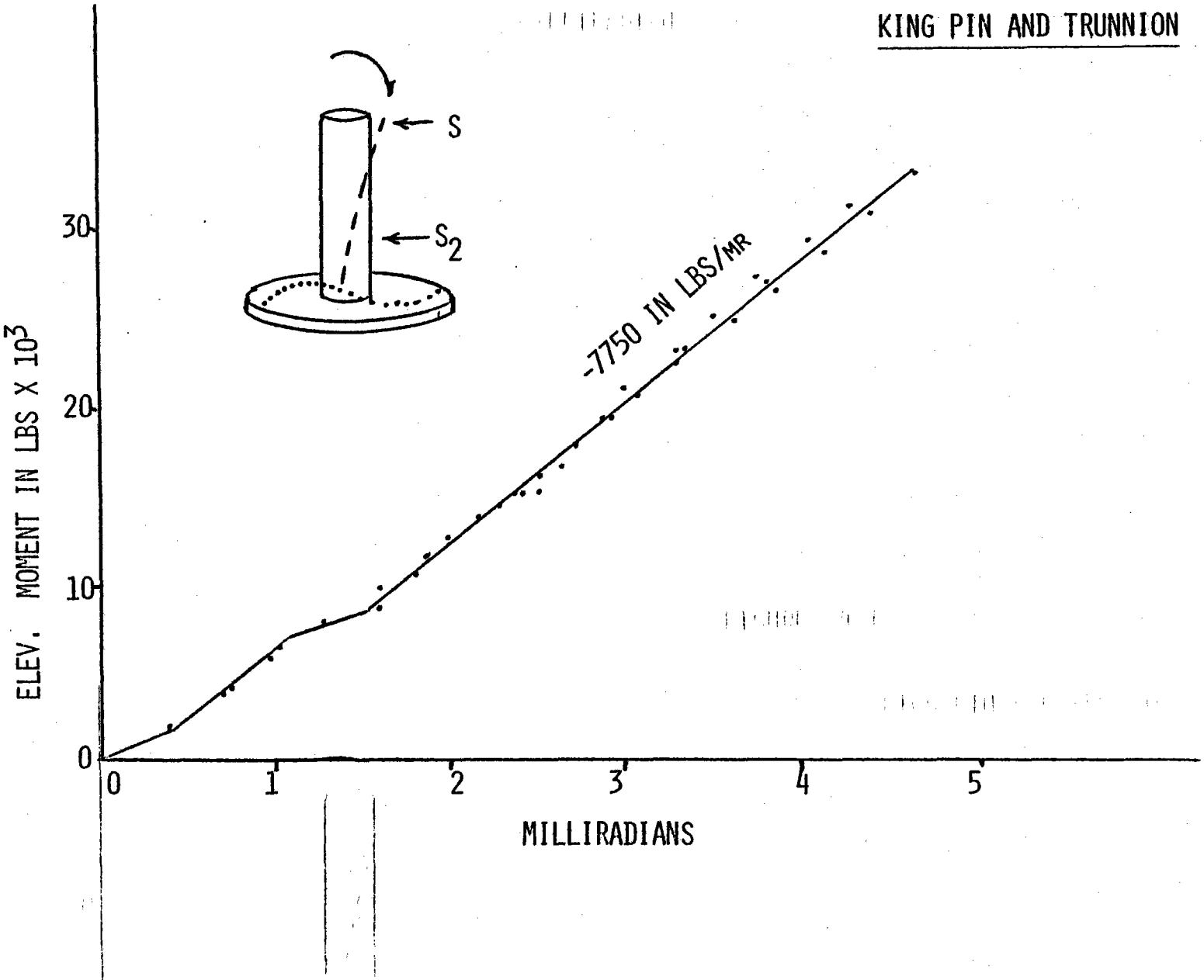

4.0 BENCH TESTS(cont'd)

4.3 Control System Tests

The heliostat will be simulated by assembling actuators, motors, motor controls and welded up simulated support structure. This will be mounted at ground level and a photocell target will be mounted on top of the building. Tests will be accomplished in accordance with the test plan to determine tracking capability and accuracy of the overall system.

The bench test serves to verify the major concepts developed by SOLARAMICS and Energy Control Systems, and determine accuracy of the system. The major concepts listed below were verified in an actual tracking situation:

1) Solaramics tilted heliostat
2) ECS tracking algorithm
3) ECS HAC simulation

The control equipment is divided into two categories:

1. HAC simulation
2. HC simulation

The HAC is simulated by a computer at the ECS offices. Here, tracking data in the form of the ECS algorithm is generated and recorded onto cassette tapes. All factors affecting heliostat tracking (solar ephermis, field location, date, latitude, longitude, etc.) are made at this point.

The tapes are transported to the SOLARAMICS test site where they are read by the HC simulation computer. This data is used to control the heliostat independently for the day. The control configurations were tested for two field locations.

4.3 Control System Tests(cont'd)

These are:

1) 40 meters north, 14 meters east
2) 30 meters south, 9 meters east

The target height was 8 meters above central pivot point for the heliostat. A target array permits determination of pointing accuracy. The target is scanned periodically by the HC and data saved for later analysis by the HAC simulation computer. Tests were carried out over a two week period. During this period several full days of tracking were obtained at both field locations.

The accuracy of tracking we are trying to obtain is on the order of milliradians. The mechanical misalignments including errors in the 23^{o} tilted axis value, leveling errors, azimuthal alignment errors, screw position error, will have an effect on tracking accuracy.

The tracking accuracy for both positions was 4 milliradians in both coordinates. This figure is of the order expected from the aforementioned error sources for the bench test heliostat, and design accuracy can be expected when error sources are eliminated.

The control algorithms have a computed error of .1 milliradian, arising from the least squares fitting technique. We have not seen any errors which can be attributable to the control algorithms, that is, any errors due to tracking algorithm errors are masked by the other error sources and the control errors are thus on the order of magnitude predicted.

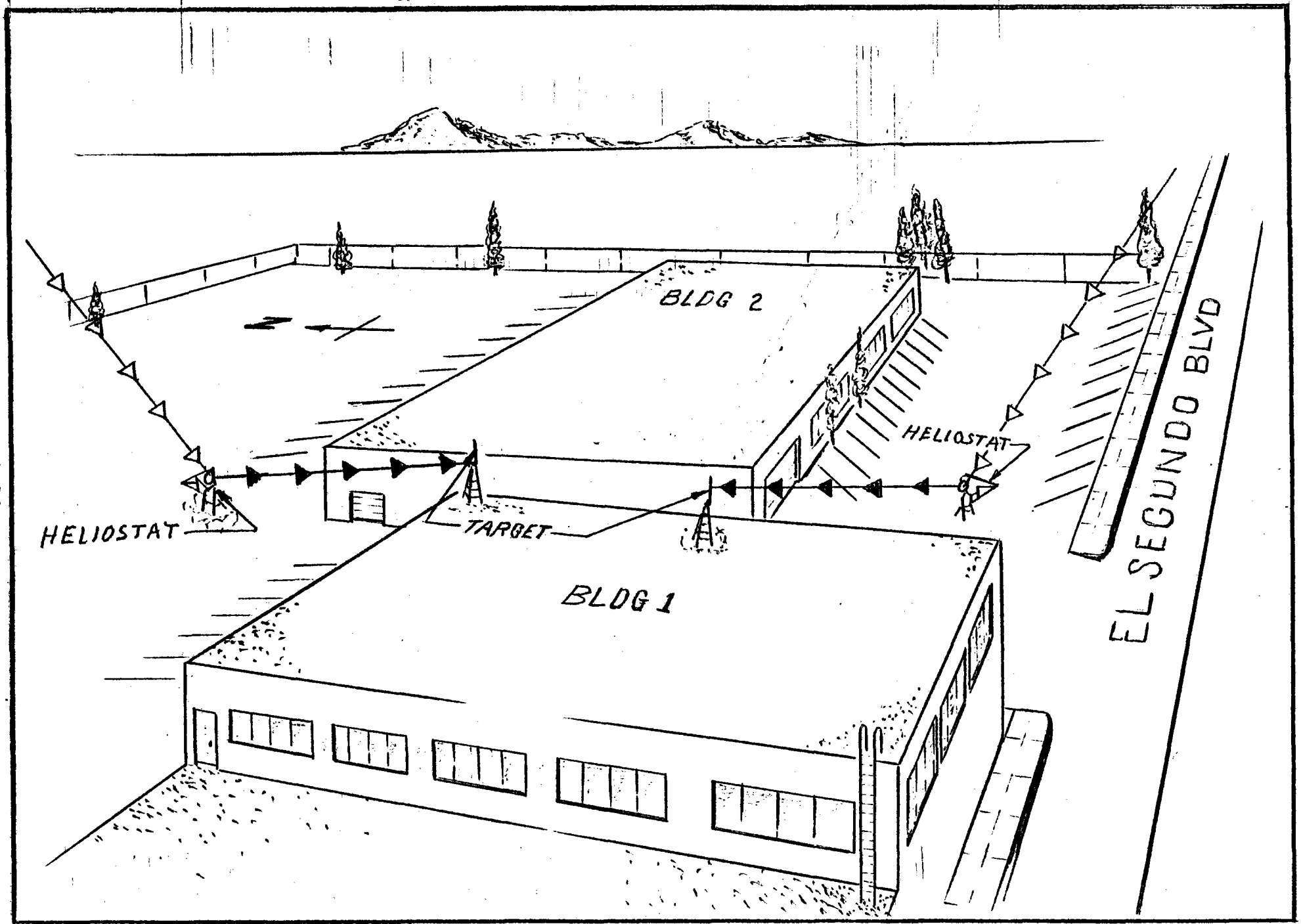

CONTROL SYSTEM TEST
FIGURE 4-18

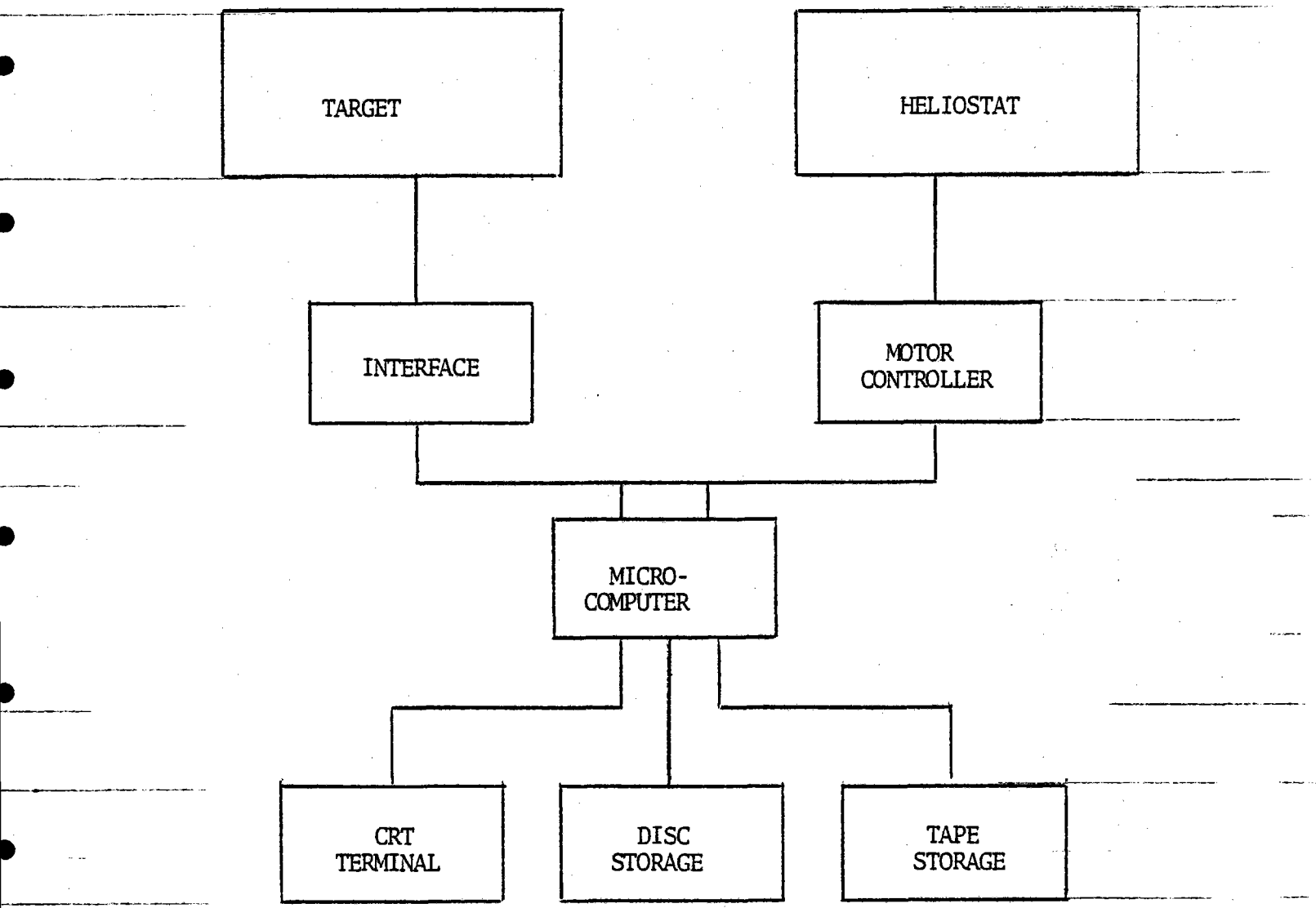

CONTROL SYSTEM

Figure 4-19 Bench Test Block Diagram